Chemical Engineering Journal 505 (2025) 159497

Contents lists available at ScienceDirect

Chemical Engineering Journal

journal homepage: www.elsevier.com/locate/cej

Review

(Deep) eutectic solvents for the separation of platinum group metals and rare earth elements: Characteristics, extraction mechanisms and state of the art

Sahar Gholami [a], María Pérez-Page [a], Carmine D'Agostino [a,b], Jesús Esteban [a,c,*]

[a] Department of Chemical Engineering, School of Engineering, The University of Manchester. Oxford Road. Manchester, M13 9PL, United Kingdom
[b] Dipartimento di Ingegneria Civile, Chimica, Ambientale e dei Materiali (DICAM), Alma Mater Studiorum – Università di Bologna, Via Terracini, 28, 40131 Bologna, Italy
[c] Department of Chemical Engineering and Materials, Faculty of Chemical Sciences, Complutense University of Madrid. Avda. Complutense s/n, 28040 Madrid, Spain

ARTICLE INFO

Keywords:
Critical raw materials
Platinum group metals
Rare earth elements
Deep eutectic solvents
Solvometallurgy
Extraction mechanisms

ABSTRACT

Critical metals, such as platinum group metals (PGMs) and rare earth elements (REEs), are strategically and economically significant due to their widespread use in electronics, clean energy, catalysis, and medical devices. With increasing demand and the continuous depletion of natural reserves, their recovery from metal-bearing waste is gaining attention, aligning with sustainability and circular economy principles. Although hydrometallurgy is a more controllable and energy efficient technique than pyrometallurgy, it employs strong acids with aggressive environmental, health, and safety (EHS) profiles. Therefore, solvometallurgy based on the use of (deep) eutectic solvents ((D)ESs) has gained prominence due to their tunable physicochemical properties, enabling safer and more selective metal separation processes. However, no review has comprehensively investigated the separation of PGMs and REEs utilising (D)ESs. Therefore, this critical review delves into the application of (D)ESs in PGM and REE recovery, focusing on the physicochemical characteristics of these solvents, alongside the phenomenology and mechanisms associated with solid–liquid extraction (SLX) and liquid–liquid extraction (LLX). Proton activity and complexation ability of (D)ESs are the most important factors influencing the dissolution of metal oxides. Furthermore, the LLX mechanism is predominantly governed by metal speciation and the ionic nature of (D)ESs, with ion exchange and neutral ion association being the most prevalent pathways. Additionally, the conducted in-depth evaluation of various operating conditions highlights that acidity and (D)ES composition are key contributors to achieving selective extraction. Finally, this study proposes a strategic framework for circular critical metal recovery, emphasising solvent regeneration and outlining future research directions, particularly concerning process intensification.

1. Introduction

Precious metals and rare earth elements are fundamental to the manufacturing of many products used in our everyday lives, from simple tools to critical technologies such as batteries, wind turbines, and electric cars, which are pivotal for achieving net zero emissions objectives [1,2]. Growing global energy demand and rapid population growth have raised serious concerns over the eventual scarcity of these resources [3]. In light of this, the European Commission (EC) provided a list of critical raw materials (CRMs) [4], which comprises a diverse array of materials of great significance to the economy but with substantial supply risk due to geographic concentration, lack of suitable alternatives, and poor recycling rates [5]. As a consequence of the rise of CRMs demand, the extraction and processing of CRMs will have detrimental effects on the environment and local populations. Hence, it is crucial to discover solutions to mitigate supply risks and ecological damage [6]. The EC approved the "Critical Raw Materials Act," in line with the Green Deal Industrial Plan. This aimed at strengthening the CRM value chain, expanding the import sources, boosting the EU's capacity to monitor and address risks associated with supply interruptions of CRMs while supporting circularity and sustainability [7]. Alongside an updated list of CRMs, the Act delineated a list of strategic raw materials (SRMs) deemed vital to Europe's green and digital transitions, as well as for defence and space-related purposes. The regulation has established precise standards to enhance the EU's supply diversification by 2030, which include

* Corresponding author.
E-mail addresses: jeesteba@ucm.es, jesus.estebanserrano@manchester.ac.uk (J. Esteban).

https://doi.org/10.1016/j.cej.2025.159497
Received 5 September 2024; Received in revised form 24 November 2024; Accepted 10 January 2025
Available online 12 January 2025
1385-8947/© 2025 The Author(s). Published by Elsevier B.V. This is an open access article under the CC BY license (http://creativecommons.org/licenses/by/4.0/).

Nomenclature

Abbreviations

AA(D)ESs Amino acid-based (deep) eutectic solvents
AE Anion exchange
APIs Active pharmaceutical ingredients
BA(D)ESs Brønsted acidic (deep) eutectic solvents
CE Cation exchange
COSMO-RS Conductor-like Screening Model for Real Solvents
CRM Critical raw material
(D)ES Refers to both deep eutectic solvents and eutectic solvents in a generic way
DES Deep eutectic solvent
DME Dispersive microextraction
EC European Commission
EHS Environmental, health and safety
ES Eutectic solvent
ETAAS Electrothermal atomic absorption spectrometry
EXAFS X-ray Absorption Fine Structure
FT-IR Fourier Transform Infrared Spectroscopy
HBA Hydrogen bond acceptor
HBD Hydrogen bond donor
H(D)ES Refers to both hydrophobic deep eutectic solvents and hydrophobic eutectic solvents in a generic way
HREE Heavy rare earth element
HSAB Hard and soft acid and base
IL Ionic liquid
LIBs lithium-ion batteries
LLX Liquid-liquid extraction
LREE Light rare earth element
MC Magnetic constituent
M(D)ESs Magnetic (deep) eutectic solvents
NA(D)ESs Natural (deep) eutectic solvents
NMR Nuclear magnetic resonance
PCB Printed circuit board
PGM Platinum group metal
PLATIRUS PLATInum group metals Recovery Using Secondary raw materials
REE Rare earth element
SAC Spent automotive catalyst
SAXS Small-angle X-ray scattering
SDG Sustainable Development Goal
SLE Solid-liquid equilibria
SLX Solid-liquid extraction
SRM Strategic raw material
SX Solvent extraction
REOs Rare earth oxides
R&D Research and development
TEA Techno-economic analysis
TMs Transition metal ions
TOC Total organic carbon
TSILs Task-specific ionic liquids
TRFS Time-resolved fluorescence spectroscopy
TREE Total rare earth element
TGA Thermogravimetric analysis
THE(D)ESs Therapeutic (deep) eutectic solvents

Chemicals

AGU 1-aminoguanidine hydrochloride
AsA Ascorbic acid
ATPPB Allyltriphenyl phosphonium bromide
[A336][I] Aliquat 336 iodide
But 1-Butanol
CA Citric acid
ChCl Choline chloride
D2EHPA Di-(2-ethylhexyl) phosphoric acid
DecA Decanoic acid
Dec 1-Decanol
Dodec Dodecanol
DEG Diethylene glycol
DNS Dinitrosalicylic acid
DM Diethyldodecanamide
EG Ethylene glycol
FAAS Flame atomic absorption spectroscopy
GA Glycolic acid
Gly Glycerol
GUC Guanidine hydrochloride
[Hbet][Tf_2N] Betainium bis(trifluoromethylsulfonyl)amide
HCl Hydrochloric acid
HexA Hexanoic acid
[HMIM][HSO_4] 1-methylimidazolium hydrogen sulphate
Ibu Ibuprofen
LA Lauric acid
LacA Lactic acid
LevA Levulinic acid
Lid Lidocaine
Lns Lanthanides
MA Maleic acid
Mal Malonic acid
Men Menthol
MSA Methanesulphonic acid
NIA Neutral ion association
[N_{8888}]Br Tetraoctylammonium bromide
[N_{8881}]Cl Trioctylmethylammonium chloride
[N_{7777}]Cl Tetraheptylammonium chloride
[N_{4444}]Cl Tetrabutylammonium chloride
[N_{2222}]Cl Tetraethylammonium chloride
NH_4Cl Ammonium chloride
NH_4NO_3 Ammonium nitrate
OA Oleic acid
*p*TSA *p*-toluene sulphonic acid
[P_{66641}]Cl Trihexyl(tetradecyl)phosphonium chloride
$SC(NH_2)_2$ Thiourea
TCCA Trichloroisocyanuric acid
TEG Triethylene glycol
Thy Thymol
TOPO Trioctylphosphine oxide
Tdec 1-Tridecanol
U Urea

Symbols

α Hydrogen bond acidity (−)
β Solvent's proton acceptance capacity (−)
γ Activity coefficient (−)
π* Dipolarity/polarisability
D Distribution coefficient (−)
EE Extraction efficiency (%)
EI Economic importance (−)
HSP Hansen Solubility Parameter (−)
L Leachability (%)
PF Preconcentration factor (−)
SF Separation factor (−)
S/L Solid-to-liquid ratio ($g.mL^{-1}$ or $g.g^{-1}$)
SR Supply Risk (−)
R_M Recovery efficiency of metal M (%)
R Universal gas constant ($J.mol^{-1}.K^{-1}$)
T Absolute temperature (K)
$T_{m,i}$ Melting temperature of pure substance i (K)
TREE Total REE (%)
TRL Technology readiness level (−)

x	Liquid mole fraction (−)		liquid and solid phases ($J.mol^{-1}.K^{-1}$)
$\Delta_m C_{p,i}$	Difference in molar heat capacity of substance i between	$\Delta_m H_i$	Fusion enthalpy of substance i ($J.mol^{-1}$)

ensuring at least 15 % of the annual consumption of CRMs originating from recycling within the EU itself, hence highlighting the need to devise strategies to achieve this goal [7]. Moreover, this supports the United Nations Sustainable Development Goals (SDGs), specifically SDG12, which emphasises sustainable production and consumption [8].

In its 2023 CRM evaluation, the EC assessed 70 potential raw materials, suggesting 34 components for the updated CRM list, as depicted in Fig. 1, which identifies materials with high supply risk (SR ≥ 1.0) and economic importance (EI ≥ 2.8) [9,10].

Similarly, the Energy Act of 2020 in the United States has defined critical minerals as non-fuel elements essential for infrastructure, economic stability, national security, and the development of renewable energy resources. Reflecting this, the U.S. Geological Survey published a notable list of 50 critical minerals in 2022, which included PGMs and REEs [11]. Similarly, the EU Commission's CRM lists published between 2011 and 2023 have consistently included both PGMs and REEs, further emphasising their crucial importance to the global economy, particularly for low-carbon technologies, and underscoring the challenges posed by disruptions in their supply.

PGMs consist of six elements, namely platinum (Pt), palladium (Pd), rhodium (Rh), ruthenium (Ru), iridium (Ir), and osmium (Os). However, Os is excluded from the CRM list due to a lack of technological significance and the absence of precise data regarding its supply [12]. Owing to the unique characteristics of PGMs, including high resistance to heat, oxidation, and corrosion, as well as their outstanding catalytic properties, these metals are indispensable components in various advanced applications. They play pivotal role in the automotive industry, electronics, hydrogen fuel cells, pharmaceuticals, and as catalysts in chemical and petroleum processes. Specific examples include rhodium-based catalysts for hydroformylation, ruthenium-based catalysts for hydrogenation, and platinum-based catalysts for the hydrogen evolution reaction, which is critical for the generation of renewable chemical fuels [13–16]. Nevertheless, their available natural resources are primarily concentrated in Russia, North America, Canada, and South Africa [17]. The critical importance of PGMs is exacerbated by projected increases in their utilisation over the next two decades, with Pd anticipated to surge by 45 % and Pt by 5 % [18].

REEs are a collection of 17 elements comprising the lanthanide series plus scandium and yttrium. They are typically extracted as co– or by-products of other materials, and their world supply is strongly dependent on a limited number of sources, with China being the main supplier, accounting for 85 % of light rare earth elements (LREEs) and 100 % of heavy rare earth elements (HREEs) [19,20]. The unique optical characteristics of HREEs make them indispensable for high-precision technologies, including laser doping and advanced radiography applications [20]. While HREEs are found in low concentrations, LREEs are more abundant in the Earth's crust [21]. LREEs have broad applications across diverse sectors, with significant contributions to the manufacturing of batteries for hybrid and electric vehicles, solar cells, and advanced permanent magnets, such as NdFeB and SmCO magnets, which are integral to wind turbine technologies [22]. Additionally, they are utilised as catalysts, such as lanthanum-based perovskites for energy-related applications and cerium oxide-based catalysts for processes like fluid catalytic cracking [22–24]. Based on the International Energy Agency's analysis and considering the sustainable development strategy, the demand for REEs for wind turbines is expected to double by 2040, exceeding 10 kt [25], highlighting the need for strategic measures to secure sustainable supply chains and address this growing demand.

The high demand for both PGMs and REEs, coupled with their limited natural reserves, has led to substantial market values (e.g., Pt (973.00 $/troy oz), Pd (1037.00 $/troy oz), Rh (4,600.00 $/troy oz), Ir (4,600.00 $/troy oz), and Ru (480.00 $/troy oz)) [26,27]. Additionally, serious environmental and human health issues arise from primary metal processing and metal-bearing waste [28–30], which highlights the

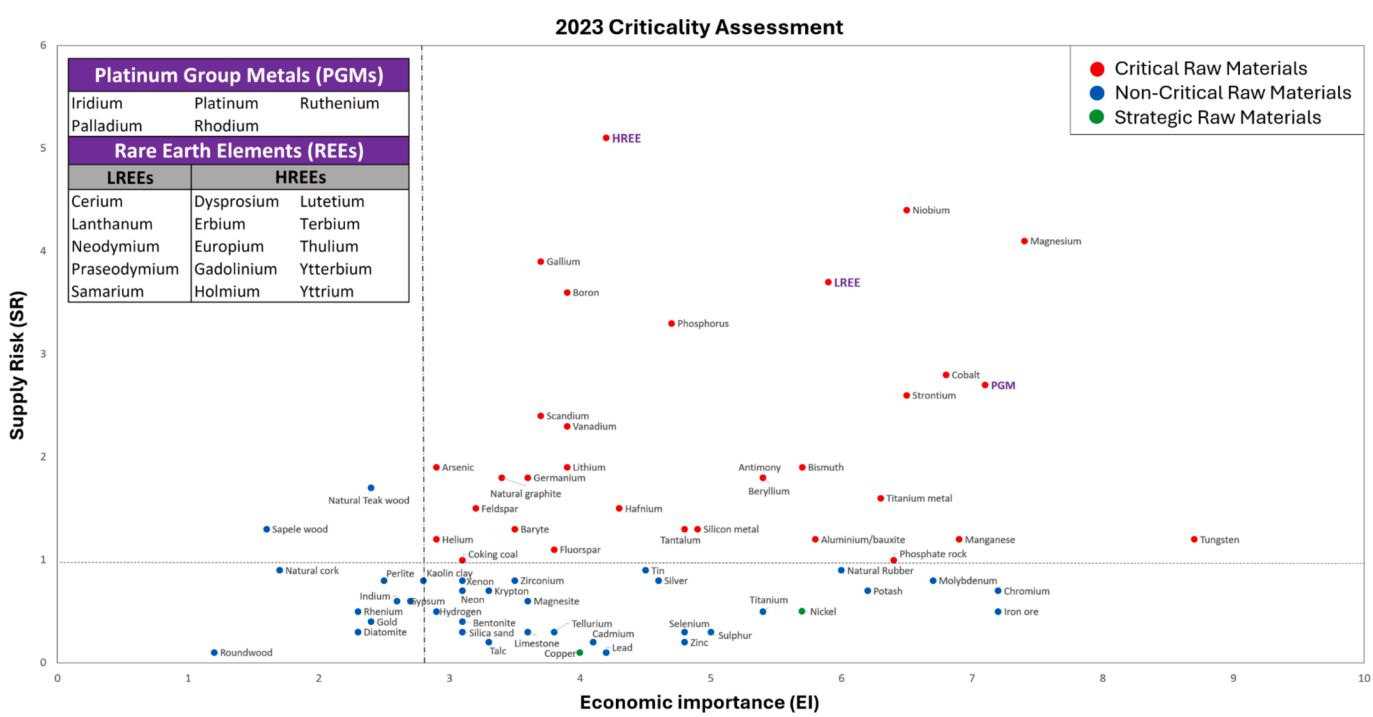

Fig. 1. 2023 criticality assessment results (individual materials and grouped HREEs, LREEs, and PGMs). Adapted from [10].

urgent need for eco-friendly and efficient metal separation processes from secondary resources, such as industrial residues and electronic waste, also referred to as urban mining [31,32].

There are various methods for metal separation and recovery, including pyrometallurgy, hydrometallurgy, biometallurgy, and, more recently, solvometallurgy [33,34]. Given the intricate composition of metal-bearing materials, their recovery typically commences with physical and thermal pre-treatment methods [35]. Subsequently, the pre-treated metallic part is subjected to further processing, primarily using pyrometallurgy and hydrometallurgy [36]. Pyrometallurgy, a long-established high-temperature metal separation technique for eliminating organic and volatile substances, faces challenges including toxic emissions, high energy consumptions, low recovery rates, and substantial capital investment requirements [37]. Biometallurgy, a nascent metallurgical technique, employs naturally existing microbes and their metabolic byproducts to solubilise metals through bioleaching and biosorption. While biometallurgy offers cost and energy savings, it is constrained by slow reaction kinetics and the intricate cultivation of certain bacteria [38].

Hydrometallurgy comprises the dissolution and leaching of metals, followed by subsequent purification steps using solvent extraction (SX), precipitation, cementation, electrodeposition, and/or membrane technologies [39]. This method provides advantages such as reduced energy consumption, higher recovery efficiency, and enhanced capability to handle complex systems with low metal content [40,41]. Leaching, however, usually involves the use of strong acid reagents such as *aqua regia*, hydrochloric acid, nitric acid, or alkaline solutions like cyanides, which can result in EHS risks, as well as industrial equipment corrosion [42,43]. Therefore, there is an urgent need for eco-friendly and efficient leaching reagents.

Solvent extraction, the most widely used purification technique following leaching step, selectively transfers metal ions between two immiscible liquid phases, typically an aqueous acidic solution (leachate) and a hydrophobic organic phase (extractant) [44]. Although SX offers benefits such as high capacity and cost-effectiveness, it may present environmental challenges due to the use of large quantities of acid or base reagents and volatile, flammable organic solvents, thereby making it relevant to seek safer and cleaner solvents [45].

Solvometallurgy employs non-aqueous solvents including ionic liquids (ILs), and, more recently, (deep) eutectic solvents ((D)ESs), to separate metals from primary and secondary resources, although it is still in its early stages (Technology Readiness Level (TRL) = 3–4). Solvometallurgy boasts key advantages, such as achieving greater selectivity compared to conventional acidic aqueous leaching owing to the possibility of tuning ILs and (D)ESs by modifying their composition. This tunability allows for tailored extraction processes with reduced wastewater production, lower chemical consumption, and fewer purification stages [45,46]. Task-specific ionic liquids (TSILs) are advanced ionic liquids modified by adding functional groups (e.g., amines, carboxyls, thiols) to their cation or anion, which gives them targeted reactivity and selectivity for a specific task, such as metal extraction, as exemplified in Table 1. However, they are often associated with high costs and susceptibility to third-phase formation, posing limitations for viability in large-scale applications. Furthermore, environmental concerns arise due to the persistence and toxicity of certain TSILs, such as those containing fluorinated anions, exemplified by betainium bis(trifluoromethylsulfonyl)amide ([Hbet][Tf_2N]), a widely used TSIL in metal separation [47,48]. In contrast, (D)ESs, commonly derived from biobased and more affordable components like choline chloride (ChCl), offering cheaper and greener alternatives with competitive selectivity [33].

(D)ESs are a novel family of green solvents usually formed by combining a hydrogen bond acceptor (HBA) and a hydrogen bond donor (HBD) [53,54]. Their relative amount can vary to modify the solvent for different purposes, such as altering their physicochemical properties or the way they interact with solutes in the case of extraction [55]. (D)ESs could facilitate selective dissolution of certain metal oxides and metal salts under relatively mild conditions, simplifying purification processes and reducing costs. They can also be regenerated and reused for multiple metal separation cycles [56,57]. Additionally, (D)ESs possess other attractive features, including ease of synthesis, low vapour pressure, and low or non-flammability, with generally more favourable EHS profiles [58], making them suitable as cleaner solvents in solvometallurgy [59].

There are a number of extensive review studies within the current body of knowledge that have delved into various critical metal separation techniques, highlighting their strengths, limitations, and recent developments. For instance, Paiva and Nogueira covered the use of ionic liquids in the separation of critical metals, particularly PGMs and REEs, from urban mines, showing high selectivity, recyclability, and efficiency, making them promising candidates for metal extraction technologies [12]. A broader review on PGM recovery with traditional metal separation techniques, including pyro- and hydro-metallurgy, as well as biometallurgy was also presented [35]. Katarzyna and Wieszczycka recently provided a review related to the recovery of metals (e.g., PGMs) from industrial wastewater utilising membrane techniques [60]. Numerous studies focused on reviewing the application of (D)ESs in separation of critical metals including lithium from spent lithium-ion batteries (LIBs) [61]. However, no existing paper has delivered a holistic review concerning the application of (D)ESs in the separation of PGMs and REEs, particularly addressing phenomenological and

Table 1
Some examples of ILs applications in PGM and REE separation.

Metal	IL	Operating conditions: Time	Temperature (°C)	Solvent-to-metal feed ratio	Main results	Ref.
Pt(IV), Pd(II), Rh(III), Ir (IV)	1-hexyl-3-methylimidazole-2-thione (HMImT)	40 min	30	1.2 ($mg.mL^{-1}$)	EE_{Pt}% [a] = 99.8 % EE_{Pd}% = 99.4 % EE_{Rh}% = 99.6 % EE_{Ir}% ≈ 0.1 %	[49]
Pt(IV), Pd(II), Rh (III)	Aliquat 336 iodide ([A336][I])	1 h	25	333 ($mL.mL^{-1}$)	EE_{Pt}% = 100 % EE_{Pd}% = 100 % EE_{Rh}% ≈ 28 %	[50]
Nd(III)	[Hbet][Tf_2N]	24 h	90	400 ($mL.g^{-1}$)	L_{Nd}% [b] = 100 % L_{Co}% = 40 %	[51]
La(III), Ce(III), Nd(III)	1-methylimidazolium hydrogen sulphate ([HMIM][HSO_4])	2 h	80	10 ($mL.g^{-1}$)	L_{RE}% = 15 − 20 %	[52]

[a] Extraction efficiency (%) $= \frac{\text{concentration of metal in extract phase}}{\text{initial concentration of metal in feed}} \times 100$,

[b] Leaching efficiency (%) $= \frac{\text{mass of metal in leachate}}{\text{initial mass of metal in feed}} \times 100$.

mechanistic aspects.

Considering the aforementioned points, this study comprehensively reviews the role of (D)ESs through different steps of the separation of PGMs and REEs. This work comprehensively covers aspects of the extraction mechanisms, the effects of factors influencing metal separation performance, such as the nature of HBAs and HBDs and their composition, as well as operating parameters. Finally, key performance parameters are discussed, including selectivity, extraction and leaching efficiencies in addition to the consideration of potential back-extraction and the regeneration and recyclability of the metal-loaded (D)ESs. Finally, this study suggests avenues for future research regarding the development and application of (D)ESs in PGM and REE separations.

2. Deep eutectic solvents and characteristics in connection with metal separation

2.1. Eutectic and deep eutectic solvents

In 2003, Abbott and his colleagues pioneered the term "deep eutectic solvents" (DESs), referring to the combination of quaternary ammonium salts and amides with notably lower melting temperatures compared to their pure constituents [62]. Later, this concept was broadened by defining DESs as eutectic combinations of Lewis or Brønsted acids and bases, comprising diverse cationic and/or anionic species [55]. Recently, Coutinho recommended a more precise definition for DESs, highlighting the inadequacy of relying solely on the existence of either an eutectic point or a hydrogen bond among precursors of the mixture for its definition [63]. It was emphasised that the descriptor "deep eutectic solvent" should refer to a mixture of at least two pure constituents, typically a HBA and a HBD, where the eutectic point temperature falls below that of an ideal liquid mixture, manifesting considerable negative deviations from thermodynamic ideality. This would be caused by enhanced interactions among the DES precursors compared to those within the individual compounds. Additionally, the eutectic point of DESs cannot be specified by a constant stoichiometric ratio since it arises from the convergence of the melting curves of the individual pure components. Fig. 2 illustrates general examples of these, which are predominantly influenced by the fusion properties of pure components, as described by equation (1) [64].

$$ln(x_i\gamma_i) = \frac{\Delta_m H_i}{R}\left(\frac{1}{T_{m,i}} - \frac{1}{T}\right) + \frac{\Delta_m C_{p,i}}{R}\left(\frac{T_{m,i}}{T} - ln\frac{T_{m,i}}{T} - 1\right) \quad (1)$$

where γ_i denotes the activity coefficient of substance i at a given liquid mole fraction x_i, T and $T_{m,i}$ are the absolute temperature and melting temperature of pure compound i, respectively; $\Delta_m H_i$ and $\Delta_m C_{p,i}$ represent the fusion enthalpy of the pure compound i and the difference in molar heat capacity of substance i between its liquid and solid phases; finally, R denotes the universal gas constant.

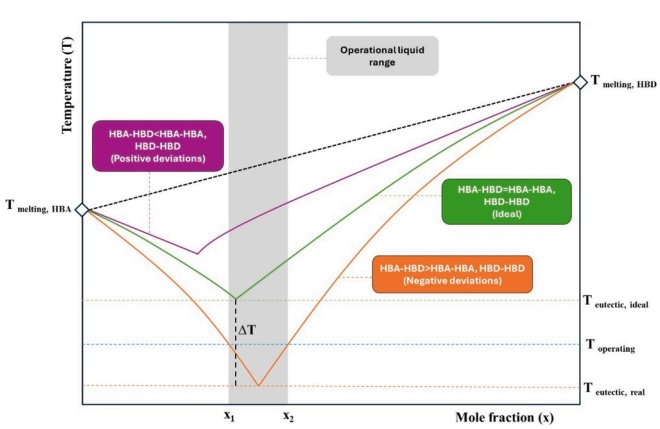

Fig. 2. Generalised solid–liquid equilibrium phase diagrams of a hypothetical binary ideal eutectic solvent (green line) and a deep eutectic mixture (orange line). (For interpretation of the references to colour in this figure legend, the reader is referred to the web version of this article.)
Adapted from [68].

To design novel eutectic or deep eutectic solvents, collectively referred to as (deep) eutectic solvents ((D)ESs) henceforth in this work, it is vital to have a thorough understanding of the solid–liquid equilibria (SLE) to assess the non-ideal behaviour and their functional liquid range [63]. Conventionally, the formulation of (D)ESs has mostly followed a trial-and-error approach; however, the vast number of possible combinations of HBAs and HBDs represents a practical constraint when proposing new (D)ESs. In this sense, the Conductor-like Screening Model for Real Solvents (COSMO-RS), developed by Klamt et al., has proven to be a useful method for predicting SLE phase diagrams and the critical properties of (D)ESs [65,66]. For instance, Abranches et al. applied COSMO-RS to assess the non-ideality of (D)ESs synthesised from phenolic HBDs through the estimation of the SLE diagram. The findings revealed a negative deviation from ideality in the menthol (Men):thymol (Thy) (D)ES, suggesting that the hydrogen bond within this (D)ES is much stronger than those in the pure substances. Experimental results validated the accuracy of these predictions, demonstrating the applicability of COSMO-RS as a robust predictive model in the design of (D)ESs [67].

2.2. Classification of (D)ESs

Taking into account the nature of the initial compounds (i.e., HBA and HBD), five main categories have been defined for (D)ESs [55].

Type I (D)ESs, as described by Abbott et al., are synthesised by combining quaternary onium salts (e.g. ammonium, phosphonium, or sulphonium) with a metal halide, where the metal can be indium (In), zinc (Zn), iron (Fe), gallium (Ga), tin (Sn), or aluminium (Al). Nonetheless, there is a limited availability of non-hydrated metal halides with adequately low melting points leading to the formation of Type I (D)ESs [69].

Type II (D)ESs are prepared from a quaternary onium salt with a hydrated metal halide, with metals such as manganese (Mn), chromium (Cr), nickel (Ni), magnesium (Mg), copper (Cu), cobalt (Co), or Fe, offering no sensitivity to moisture and more possibilities with relatively lower cost [70,71].

Type III (D)ESs consist of a quaternary onium salt combined with HBDs such as amides, alcohols or carboxylic acids. These (D)ESs have garnered a great deal of attention for their attractive features, including straightforward synthesis, with some variants being easily biodegradable, particularly those containing ChCl as HBA. The broad range of available HBDs renders this class of (D)ESs highly tunable for different applications, including metal separation due to their high capacity to dissolve a wide array of metal salts and oxides [62,72,73].

Type IV (D)ESs are prepared from a metal halide combined with a HBD, often with Al or Zn. Due to their high charge density, these mixtures generally do not result in low melting point eutectics [74].

Type V (D)ESs, an emerging category pioneered by Coutinho et al., are highly structured solvents formed solely by non-ionic substances exhibiting robust hydrogen bond interactions and non-ideal behaviour. Lone HBAs and asymmetric HBDs are considered as suitable constituents for the formulation of non-ionic type V (D)ESs. Asymmetric HBDs refer to molecules possessing more pronounced HBD abilities, such as thymol due to its resonance effects that render the hydroxyl group in its structure more positive, enhancing its HBD strength but weakening its HBA site. Lone HBAs refer to substances such as ketones, aldehydes, and tertiary amines, which lack HBD sites [75]. Conversely, regular HBDs, such as aliphatic alcohols and acids, exhibit robust HBA and HBD abilities which usually form ideal solvents with regular HBAs.

Additionally, it is pertinent to acknowledge that there are other (D)ESs reported in the literature that do not exactly align with these five categories. As an example, Chen et al. proposed novel (D)ESs consisting of polyols and carboxylic acids, also referred to as Brønsted acidic (D)ESs

(BA(D)ESs), which have found extensive application in rare earth oxide (REO) leaching [76,77]. Fig. 3 depicts some common HBAs and HBDs used in the synthesis of (D)ESs, where types III and V have commonly been reported for the separation of PGMs and REEs.

(D)ESs can be further divided into several subclasses contingent upon the subclassification of specific precursors used in their formulation into different families of components. Among these, lately the following have attracted attention, such as natural (deep) eutectic solvents (NA(D)ESs), therapeutic (deep) eutectic solvents (THE(D)ESs), amino acid-based (deep) eutectic solvents (AA(D)ESs), and magnetic (deep) eutectic solvents (M(D)ESs) which have also been applied in PGM and REE separation.

NA(D)ESs are formed from primary metabolites, including organic acids, sugars, or choline derivatives, which possess the ability to dissolve natural and synthetic chemicals that exhibit low solubility in water. The combination of two carboxylic acids (e.g., citric acid (CA):malic acid (1:1)), carboxylic acid and sugar (e.g., CA:sucrose (1:1)), or binary/ternary mixtures of carbohydrates (D-(+)-glucose:D-(−)-fructose:sucrose (1:1:1)) fall into this category [53,78].

THE(D)ESs are prepared from active pharmaceutical ingredients (APIs) and developed specifically for pharmaceutical applications to enhance drug solubility, particularly for compounds with limited water solubility [79]. Notably, ChCl and menthol stand out as common HBAs utilised in THE(D)ES formulations, demonstrating compatibility with a diverse array of APIs, including ibuprofen, acetylsalicylic acid, and phenylacetic acid [80].

AA(D)ESs consist of an amino acid as at least one of their precursors, serving either as HBA or HBD. Proline, a secondary amino acid, is commonly employed in formulating AA(D)ESs. These solvents have found application not only in enhancing the solubility of drugs and proteins [81] but also across various fields, such as improving biosynthesis [82], extracting phytochemicals [83], and facilitating the enzymatic hydrolysis of lignocellulose [84].

M(D)ESs, a recent subclass of (D)ESs, incorporate additional magnetic components into their formulation, exhibiting notable response to external magnetic fields. M(D)ESs consist of HBA, HBD, and an extra magnetic constituent (MC), including metal chlorides such as $FeCl_3$, $MnCl_2$, $GdCl_3$, $CoCl_2$, or $NiCl_2$. During the synthesis of M(D)ESs, robust hydrogen bonding and relatively weak electrostatic interactions are established among the components [85]. M(D)ESs are favourable solvents in separation processes due to their straightforward separation with magnetic fields. As an example, they employed in the extraction of thiophene from fuels through microextraction [86].

Another ubiquitous subdivision for (D)ESs, defined relying on affinity to water, comprises hydrophilic and hydrophobic (deep) eutectic solvents (H(D)ESs) [87]. Initially, (D)ESs were characterised by hydrophilic properties and were commonly used in separation processes from solid samples and non-aqueous media [88]. However, their application in liquid–liquid extraction (LLX) proved challenging, prompting the development of H(D)ESs. In response, Van Osch et al. pioneered the introduction of H(D)ESs composed of decanoic acid (DecA) as HBD and various long-chain quaternary ammonium salts as HBAs, aiming to recover volatile fatty acids from aqueous environments. The study illustrated that high hydrophobicity could be ascribed to the utilisation of quaternary ammonium salts with longer carbon chains, which results in greater steric hindrance, thereby reducing water accessibility to the charged core of the salt. This was evidenced by a low water content (approximately 1.8 wt%) and low amount of leached quaternary ammonium salt into the aqueous phase (~1.9 wt%) after extraction [89]. Later, another H(D)ES, comprising lidocaine (Lid):DecA (1:2), was tailored for metal ion extraction (e.g., Co^{2+}) from aquatic media. The results showed a high distribution coefficient (D) (exceeding 0.99), and

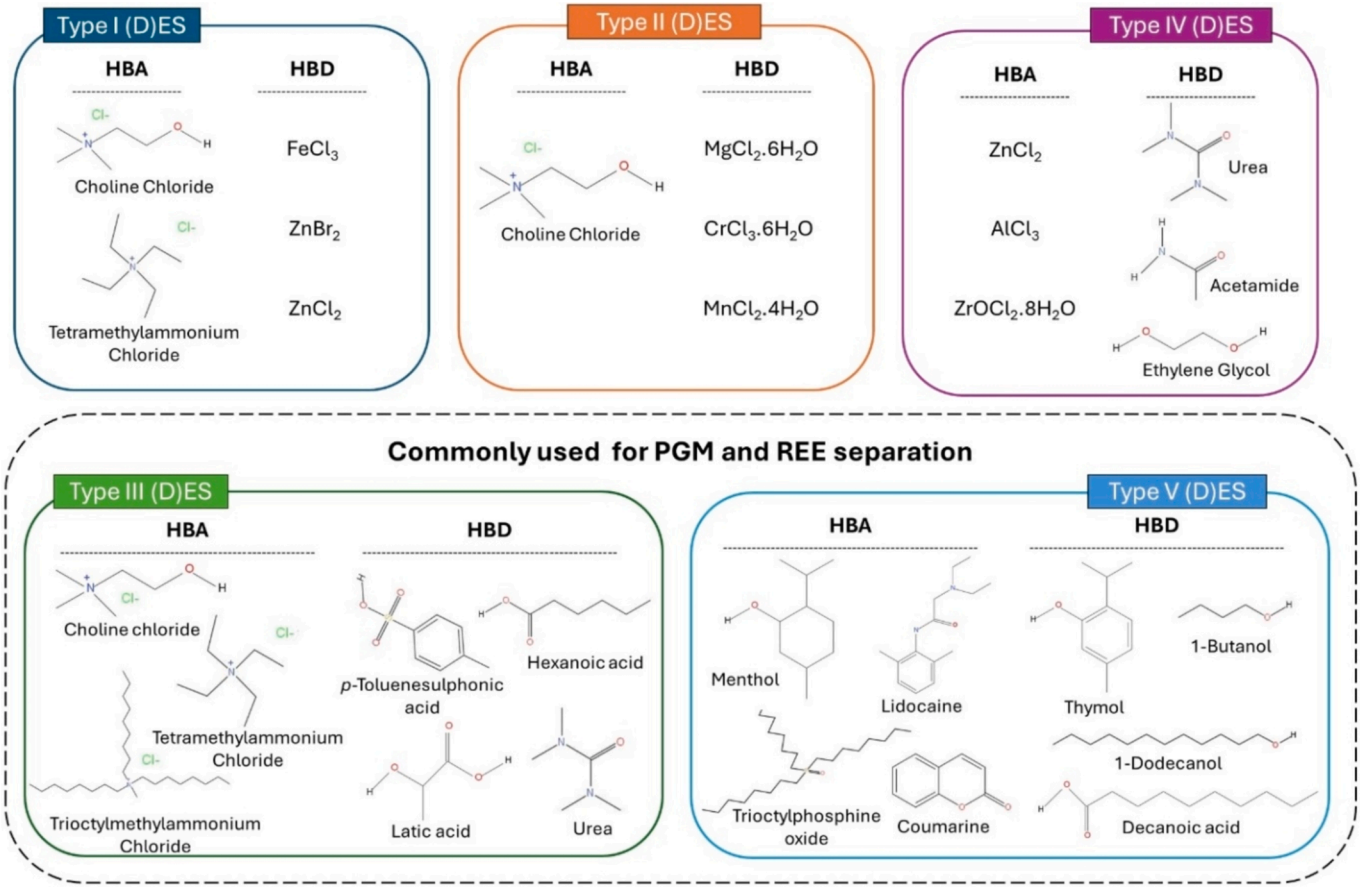

Fig. 3. Common HBAs and HBDs utilised in the synthesis of various types of (D)ESs.

very fast kinetics (about 5 s) [90]. H(D)ESs can be further categorised into ionic and non-ionic H(D)ESs depending on the nature of the HBAs utilised in their composition. For instance, Men:DecA system is classified as non-ionic H(D)ES, while tetrabutylammonium chloride ([N_{4444}]Cl): DecA is an ionic type of H(D)ES [91].

2.3. Physicochemical properties of (D)ESs

(D)ESs are deemed designer solvents due to their adaptable physicochemical properties, which can adjusted with the composition and stoichiometric ratios of their constituents [33,55]. These properties, including thermal and chemical stability, density, interfacial tension, viscosity, polarity, and acidity/alkalinity, play a pivotal role in shaping their applications, including metal separation and recovery. Table 2 presents selected physicochemical data of (D)ESs employed in PGM and REE separation.

2.3.1. Thermal stability

The decomposition temperature is a crucial parameter for the use of solvents in applications under demanding operating conditions. This feature is usually examined using thermogravimetric analysis (TGA) [98]. Within the domain of metal recovery using (D)ESs, comprehending and regulating their decomposition temperature is of foremost significance since this parameter directly affects their stability, performance, and reusability [116]. The thermal stability of various common ChCl-based (D)ESs was assessed using both long-term isothermal and short-term dynamic TGA. It was found that the onset decomposition temperatures of the studied (D)ESs fall between the decomposition temperatures of their individual precursors, with the exception of ChCl:malonic acid (Mal) (1:1) (see Fig. 4), exhibiting a significantly lower onset decomposition temperature of 99.85 °C than that of ChCl (265.85 °C) and Mal (134.85 °C). Furthermore, the results demonstrated that the maximum operating temperatures where (D)ESs remain stable in the liquid state without significant decomposition are substantially lower than those determined by dynamic TGA. As an example, ChCl:Mal (1:1) and ChCl:ethylene glycol (EG) (1:2) showed onset decomposition temperatures of 120.85 °C and 111.55 °C, respectively. In contrast, they

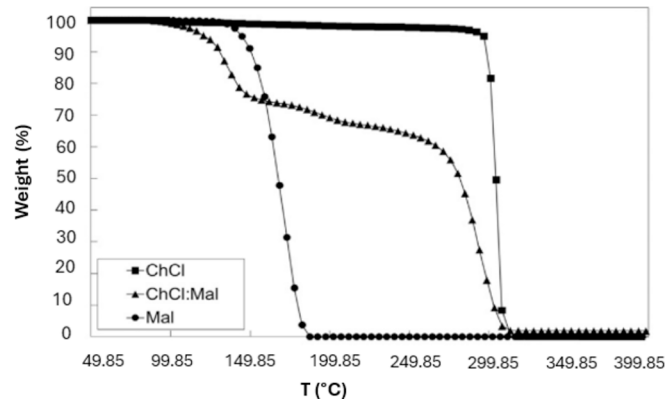

Fig. 4. Dynamic TGA thermogram of the (D)ES composed of ChCl:malonic acid (1:1) and their pure precursors. Reprinted with permission from Elsevier [98].

underwent more than 8 wt% mass loss under isothermal conditions of 50.05 °C over 20 h, underscoring that while (D)ESs may appear thermally stable in short-term dynamic tests, their practical long-term usage temperatures are much lower. Generally, the mass loss could be ascribed to the volatilisation of HBDs; thus, it can be inferred that the thermal stability of (D)ESs depends on the latter to a good extent [98]. In another study, the thermal stability of allyltriphenyl phosphonium bromide (ATPPB)-based (D)ESs combined with HBDs such as glycerol (Gly), EG, diethylene glycol (DEG), and triethylene glycol (TEG), at a 1:4 ratio was also evaluated using TGA. The analysis of the decomposition temperature at 10 % and 90 % weight loss, denoted as $T_{10\%}$ and $T_{90\%}$, respectively, revealed that ATPPB:Gly exhibited the highest thermal stability among the studied (D)ESs, as evidenced by its highest $T_{10\%}$ and $T_{90\%}$ at about 209.13 °C and 361.55 °C, respectively. The thermal stability of the (D)ESs was ranked in the following order: Gly > TEG > DEG > EG [117].

Numerous studies have highlighted the profound influence of the nature and molar ratios of HBAs and HBDs on the thermal stability of (D)ESs [88]. For instance, Pateli et al. reported that increasing the molar ratio of Mal in the ternary (D)ES ChCl:Mal improved its thermal

Table 2
Physicochemical properties of common (D)ESs used in PGM and REE separation and recovery. Data presented at room temperature, unless otherwise stated.

HBA	HBD(s)	HBA: HBD(s) molar ratio	Melting/glass temperature [°C]	Degradation temperature [°C]	Density [kg. m^{-3}]	Viscosity [mPa.s]	Metal
[N_{7777}]Cl	Decanoic acid (DecA)	1:2	− 16.65 [89]	199.22 [89]	890.7 [89]	172.87 [89]	Ir(IV), Rh(III) [92]
[N_{2222}]Cl	Levulinic acid (LevA)	1:2	− 62.2 [93]	132.4 [93]	1047 [93]	149 [93]	Nd(III) [93]
ChCl	Lactic acid (LacA)	1:2	− 77.73 [94]	179.73 [95]	1150 (at 1:1 M ratio) [96]	156 [97]	Nd(III), Dy(III) [97]
ChCl	LevA	1:2	NA	158.35 [98]	1142 [99]	273 [99]	Y(III), Eu(III) [100]
ChCl	*p*-toluenesulphonic acid	1:1	NA	299 [101]	1200 (at 35 °C) [101]	550 [102]	Pt(IV), Pd(II), Rh(III) [103]
Trioctylphosphine oxide (TOPO)	1-dodecanol	1:2	13.99 [104]	NA	849 [104]	27.52 [104]	Sm(III) [104]
TOPO	1-tetradecanol:1-decanol	4:5:5	NA	NA	850 [105]	29.15 [105]	REEs [105]
TOPO	DecA	1:1	− 18 [106]	NA	881.3 [106]	39.03 [106]	Pt(IV), Pd(II) [107]
Lidocaine	Thymol (Thy)	1:2	NA	139.8 [108]	989.08 [108]	122.05 [108]	Pd(II), Pt(IV), Au(III) [109]
Lidocaine	DecA	1:2	NA	NA	983.48 [108]	141.6 [108]	Pd(II), Pt(IV), Au(III) [110]
Coumarin	Thy	1:1	NA	117.7 (at 1:2 M ratio) [111]	1090.24 [108]	25.82 [108]	Pt(IV), Pd(II) [112]
Guanidine hydrochloride (GUC)	LacA	1:2	− 65.7 [113]	112.9 [113]	NA	156.8 [114]	Nd(III) [113]
Ethylene glycol	Maleic acid	4:1	− 98.9 [76]	97.9 [76]	1190 [76]	44.3 [76]	Nd(III) [115]

NA: data not available.

stability. This improvement was ascribed to the development of stronger hydrogen bonds between the components, contributing to a more robust structural framework [118]. Furthermore, research on M(D)ESs has revealed higher thermal decomposition temperatures compared to conventional (D)ESs, pointing at this subset of (D)ESs as interesting alternatives for highly demanding conditions. For instance, (D)ES prepared from tetraoctylammonium bromide ($[N_{8888}]$Br):DecA (1:2) demonstrates a decomposition temperature of 207.66 °C, while those of $[N_{8888}]$Br: DecA:$MnCl_2$ (1:2:1) and $[N_{8888}]$Br: DecA:$CoCl_2$ (1:2:0.5) exhibit 390.6 °C and 443.45 °C, respectively [119].

2.3.2. Chemical stability

Robust chemical stability is a requisite for the safety and applicability of (D)ESs, indicating their ability to withstand alterations stemming from various reactions like oxidation and hydrolysis [88]. Given the generation of water during metal oxide dissolution in (D)ES phase, understanding the impact of water on the physicochemical attributes of (D)ESs is indispensable [97,120]. Studies have revealed that ChCl-based (D)ESs can maintain their hydrogen bonding structure even with a water content up to 42 wt% [121]. At lower levels of water concentration, the hydrogen bonds within the (D)ES are strengthened, increasing stability. However, with increasing water content, hydrogen bond strength diminishes, resulting in behaviour more typical of solutes than solvents [122,123]. Furthermore, the chemical stability of H(D)ESs is a critical factor in LLX from aqueous environments to ensure negligible leaching and subsequent cross-contamination between H(D)ES and the aqueous phase, despite the former typically exhibiting solubilities often below 7 wt% [124]. To mention a couple of studies relevant on this matter, Van Osch et al. demonstrated that after extracting transition metal ions from an aqueous environment using Lid:DecA (1:2) H(D)ES, lidocaine was detected in the water as lidocaine hydrochloric acid, as confirmed by ^{1}H NMR and total organic carbon (TOC) analysis of the aqueous phase. This loss was ascribed to the ion exchange mechanism taking place during the metal extraction process [90]. Additionally, Marrucho et al. tested the water stability of H(D)ESs composed of DL-menthol and a range of organic acids in the extraction of pesticides from aqueous solutions. ^{1}H NMR analysis before and after the operation revealed that the aqueous phase was contaminated with some HBDs including acetic, pyruvic, butyric, hexanoic, and levulinic acids, but no peaks corresponding to DL-menthol were detected in the aqueous phase [125].

Binnemans et al. also emphasised the stability issues associated with certain (D)ESs, particularly those synthesised from ChCl and dicarboxylic acids, which degrade due to the reactivity of choline's alcohol group with carboxylic acids at high temperature, resulting in ester formation [126]. This degradation mechanism underscores the importance of evaluating the stability of (D)ESs under the specific conditions of their intended applications. It is important to note, however, that such side reactions are not universal across all (D)ESs. The stability of (D)ESs is highly dependent on the specific combination of HBA and HBD, as well as the operating conditions. Therefore, characterisation and stability assessments should be conducted on an individual basis to accurately evaluate the potential for side reactions and ensure the reliability of the (D)ES formulation in its intended use.

2.3.3. Density and interfacial tension

Density is an important property of (D)ESs, serving a crucial role in solvent selection and equipment design (e.g. decanters/settlers), particularly in LLX. The densities of (D)ESs are primarily influenced by their composition as well as temperature [88]. In contrast to hydrophilic (D)ESs, their hydrophobic counterparts often demonstrate comparable or slightly lower densities than water, ranging from 889 to 930 kg.m^{-3}, depending on their specific components [91]. Across all H(D)ESs, density inversely correlates with alkyl chain length, irrespective of whether the alkyl chains are attached to the HBA or HBD [87]. The mixture of methyltriphenylphosphonium bromide:EG at various molar ratios from 1:3 to 1:5.5 demonstrated that density notably rises with higher HBD ratios due to strengthened hydrogen bond interactions, which decrease free space [127].

Interfacial tension is another significant element that affects mass transfer and performance of phase separation in biphasic systems. In the case of (D)ES-based systems, there is a general scarcity of work focused on exploring the interfacial tension. Thus far, only a recent study examined the interfacial tension of H(D)ESs and water. The H(D)ESs tested were $[N_{4444}]$Cl: DecA (1:2), Thy:DecA (1:2), and Men:DecA (2:1). The study indicated that the interfacial tensions, and thus the hydrophobicity can be ranked as follows: $[N_{4444}]$Cl:DecA < Thy:DecA < Men:DecA implying that H(D)ESs with greater interfacial tensions often exhibit lower solubility in water [128].

2.3.4. Viscosity

Viscosity profoundly influences mass transfer and dissolution kinetics, which is of great relevance in metal separations [129]. The viscosity of most conventional (D)ESs is relatively high, often exceeding 100 mPa.s at room temperature. For instance, ChCl:urea (U) (1:2) (D)ES has a viscosity of 859.45 mPa.s [130]. This is primarily attributed to the considerable size of ions and the extensive hydrogen bonding, along with van der Waals and/or electrostatic forces, which all contribute to the reduced mobility of free species within the system [55]. In contrast, the new class of (D)ESs, labelled as Type V, displays moderate to low viscosities, facilitating faster mass transfer in metal separation processes [75]. Temperature is also a significant factor influencing the viscosity of (D)ESs. Higher temperatures reduce the internal resistance of molecule, thereby decreasing viscosity and enhancing flowability. Several studies have examined the influence of temperature on viscosity and thus the efficiency of metal separation. For instance, Doche et al. found that the leaching rate of Co(II) in ChCl:EG (1:2) (D)ES was 15 times higher at 80 °C compared to 25 °C, attributed to the reduction in the viscosity of (D)ES [131]. Nevertheless, it is essential to ensure that the optimal temperature for metal separation with (D)ESs is adequately high to enhance mass transfer and separation performance, while remaining below the decomposition thresholds.

2.3.5. Polarity

Polarity is a critical parameter that dictates the solvation properties of solvents, shaping their interactions with themselves and with other substances. Conventionally, the polarity of compounds has been assessed based on solubility parameters. An example of this is the use of the Kamlet–Taft solvatochromic parameters, which consist of three factors: (1) hydrogen bond acidity (α) representing the proton-donating ability of a solvent, (2) hydrogen bond basicity (β) reflecting a solvent's proton acceptance capacity and (3) dipolarity/polarisability (π*) quantifying the dipolarity of a solvent [132,133].

COSMO-RS σ-surface and σ-profile also give comprehensive data on the polarity distribution on the surface of a molecule. The σ-profile graphically and descriptively represents the molecule's electronegativity and electropositivity by displaying the hydrogen bonding cutoff values ($\sigma = \pm 0.0082$ e Å^{-2}) on a normalised graph. Accordingly, a polar molecule has screening charge density (σ) larger than ± 0.0082 e Å^{-2}. A value of $\sigma < -0.0082$ e Å^{-2} represents hydrogen bond donor capacity, whereas the region of $\sigma > 0.0082$ e Å^{-2} depicts hydrogen bond acceptor capacity. The area between the cutoff values (-0.0082 e Å$^{-2} < \sigma < 0.0082$ e Å^{-2}) is also attributed to the non-polar region [134]. It should be also noted that the symmetry of the σ-profile signifies that the molecule has stronger hydrogen bonding and electrostatic interactions with itself [135]. Fig. 5 depicts the σ-surface and σ-profile of some common HBAs and HBDs used in PGM and REE separation. An extension of the Hansen Solubility Parameter (HSP) approach has also been attempted to assess the polarity of thymol-based (D)ESs, focusing on comparing the solubility prediction values with openCOSMO-RS. Their finding revealed that while the model was reasonably effective in predicting the solubility of Men:Thy (1:1) in organic solvents, it exhibited significant deviation for cyclohexanone-based (D)ES, implying that HSP

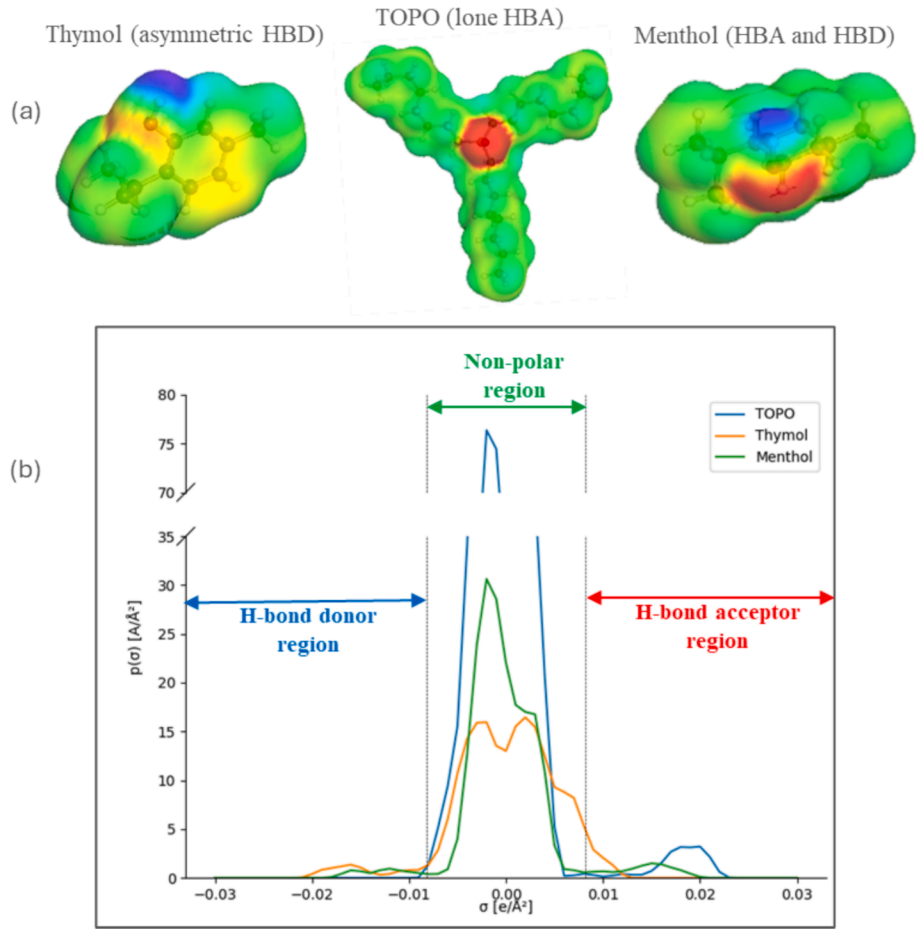

Fig. 5. (a) σ-surface, (b) σ-profile of HBAs and HBDs of H(D)ESs obtained from the COSMO-RS method (COSMOThermX version 18.0.2 using DFT calculation with the BP86 functional level of theory and def-TZVP basis set in TmoleX2021 software package).

approach can facilitate (D)ES pre-screening through identifying potential (D)ES-solute pairs, facilitating the use of more advanced computational methods on fewer number of compounds [136].

2.3.6. Acidity/alkalinity

The efficiency of (D)ESs in metal recovery is largely attributed to their inherent acidic and basic properties. Through careful design of HBA and HBD, the dissociation capacity of (D)ESs can be fine-tuned. The formation of acidic (D)ESs is facilitated using organic acids like carboxylic and sulphonic acids as HBDs. Neutral (D)ESs are synthesised using polyols, sugars, and metal salts as HBDs. For their part, alkaline (D)ESs are not often discussed, but the primary instances are ChCl:U and ChCl:triethanolamine [88]. Research has uncovered that the solubility of different substances in (D)ESs is partially governed by pH. Metal chlorides preferentially dissolve in (D)ESs displaying neutral to slightly basic characteristics. Conversely, metal oxides exhibit greater solubilities in acidic (D)ESs (e.g., ChCl:carboxylic acid) as explained by the metal oxide dissolution mechanisms [72].

By way of some examples, organic acids with robust proton activity, such as glycolic (GA) acid and LacA form (D)ESs that dissolve neodymium oxide (Nd_2O_3) more effectively than glycol (GL) and EG-based (D)ESs, as shown in Fig. 6 [113]. Yang et al. studied the selective leaching of Nd from solid residue of NdFeB carbonyl utilising BA(D)ESs. They found that EG:maleic acid (MA) (2:1), with its suitable acidity and good flowability, resulted in the highest leachability performance [77]. Pateli et al. adjusted the acidity of ChCl:EG (1:2) with trifluoromethanesulphonic acid to explore the impact of proton activity on

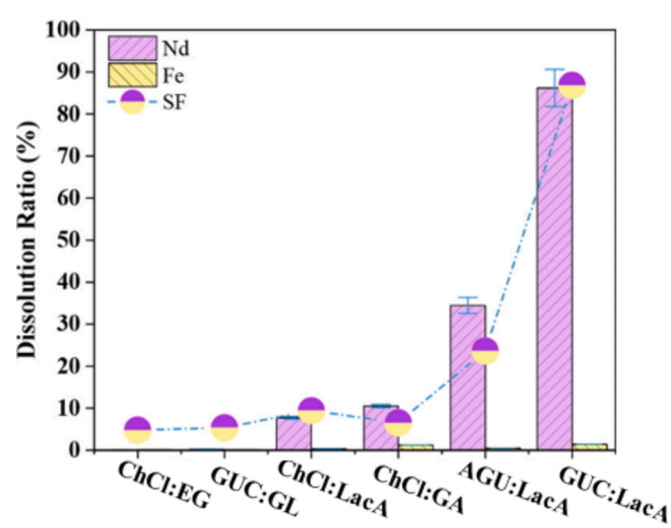

Fig. 6. Comparison of Fe and Nd dissolution ratios across various (D)ESs, highlighting the superior solubility of metal oxides in acidic (D)ES. Reprinted with permission from ACS publishing [113].

dissolving transition metal oxides. Their findings indicated that H^+ activity is crucial for metal oxide dissolution in (D)ESs, especially those with poorly coordinating HBDs [41].

3. The role of (D)ESs in PGM and REE extraction

3.1. Solid-liquid extraction

3.1.1. Dissolution mechanism of PGMs and REEs in (D)ESs

The extraction of most metals, including PGMs and REEs, originates from metal oxides, which are commonly found in natural ores and metal-bearing waste. Therefore, gaining insights into metal oxide dissolution mechanisms and speciation in (D)ESs is of utmost significance for advancing the application of more efficient solvents.

Pateli et al. conducted a comprehensive investigation on the dissolution behaviour of a range of transition metal (d-block) and post-transition metal (p-block) oxides using Type III ChCl-based (D)ESs as leaching reagents [41]. Following metal dissolution, FT-IR and UV–visible spectroscopies were utilised to probe the mechanism involved. It has been proposed that metal oxide dissolution in (D)ESs involves a sequential process.

The initial step involves the adsorption of anionic ligands onto the metal oxide surface, encompassing several phenomena:

(i) ionisation of the HBD as a coordinating ligand (denoted as H_zA) into protons (H^+) and anionic ligands (A^{z-}), as expressed by equation (2):

$$H_zA \rightleftarrows zH^+ + A^{z-} \qquad \text{(Ionisation)} \tag{2}$$

(ii) surface protonation, or the so-called surface hydroxylation, where the metal oxide surface (> M—O, where > indicates the surface of metal oxide) serves as a Lewis base; hence, protonation occurs via protons from HBD functional groups, leading to positive charge at the interface that can act as active sites for the adsorption of anionic ligands. This is shown in equation (3):

$$> M-O + 2H^+ \rightleftarrows \; > M-O\cdots H_2{}^+ \qquad \text{(Surface protonation)} \tag{3}$$

(iii) surface complexation, or anion chemisorption. This involves a competitive reaction between active surface hydroxyl groups and A^{z-}, as described by equation (4):

$$> M-OH_2{}^+ + A^{z-} \rightleftarrows \; > \left[M-OH_2^+\cdots A^{z-}\right] \qquad \text{(Surface complexation)} \tag{4}$$

If the stability of metal–ligand complexes exceeds that of the $M-OH_2^+$ complex, protons disrupt the M–O bonds, hence facilitating the substitution of A^{z-} with hydroxyl active sites to form $> [M-A]^{(z-1)-}$, often observed in an anionic form, particularly for PGMs.

The next step involves the dissolution of the surface-formed complex into the bulk solution of (D)ESs which, in turn, leads to the formation of water within (D)ES phase, as seen in equation (5):

$$> \left[M-OH_2^+\cdots A^{z-}\right] \rightleftarrows [M-A]^{(z-1)-}{}_{(D)ES} + (H_2O)_{(D)ES} \text{(Chemical dissolution)} \tag{5}$$

Based on the UV–vis spectra of the leachate and comparing with solution of identified metal speciation, most dissolved metal ions exist as chloro-complexes [137,138]. This observation suggested that once the surface-formed complex diffused into the bulk solution, as illustrated in equations (2) – (5), the anion of (D)ES (X^-), typically Cl^- replaced the deprotonated HBD ligand anion owing to its significantly higher activity. Consequently, a new complex in the form of $[M-X_n]^{z-}$ was formed, as expressed in equation (6) [33,41,72,139]. The corresponding mechanism is illustrated in Fig. 7 to graphically describe the dissolution mechanism of platinum (IV) oxide, as an example, in (D)ES.

$$[M-A]^{(z-1)-}{}_{(D)ES} + nX^- \rightleftarrows [M-X_n]^{z-}{}_{(D)ES} + A^-_{(D)ES} \qquad \text{(Ligand exchange)} \tag{6}$$

The proposed mechanism was validated for the case of PGM dissolution, particularly Pd and Pt, from spent car catalyst into the (D)ES trihexyl (tetradecyl)phosphonium chloride ($[P_{66641}]Cl$):DecA (1:2). As depicted in Fig. 8, through UV–vis analysis of the leachates and comparing their spectra with identified PGM speciation in standard solution (1 mol.L^{-1} HCl), the presence of Pd and Pt in (D)ES as PGM-chloro complexes, such as $[PtCl_6]^{2-}$ and $[PdCl_4]^{2-}$ [140], confirmed the proposed mechanism.

However, it is important to note that the proposed mechanism, which is based on the dissolution of a series of d- and p-block metal oxides, does not fully account for the dissolution of rare earth elements in (D)ESs.

In a significant study, Riaño et al. examined the leaching of roasted NdFeB magnet waste using ChCl:LacA ($CH_3CHOHCOOH$) in (1:2) molar ratio to elucidate the dissolution mechanism of rare earth oxide (neodymium oxide). Their findings revealed that the dissolution mechanism involves the formation of electrically neutral neodymium-lactate complexes and water within the (D)ES phase, illustrating that, unlike transition metals, REEs do not form anionic REE-chloro complexes [97]. Their proposed mechanism is shown in equation (7).

$$Nd_2O_{3\,(S)} + 6CH_3CHOHCOOH_{(D)ES} \rightleftarrows 2\left[Nd(CH_3CHOCOO)_3\right]_{(D)ES} + 3H_2O_{(D)ES} \tag{7}$$

Later, Amphlett et al. conducted an extensive investigation into the speciation and dissolution behaviour of lanthanides in ChCl:EG (1:2), ChCl:U (1:2), and ChCl:LacA (1:1), utilising multiple spectroscopic techniques, including extended X-ray Absorption Fine Structure (EXAFS) analysis and UV–vis spectroscopy. The role of speciation is

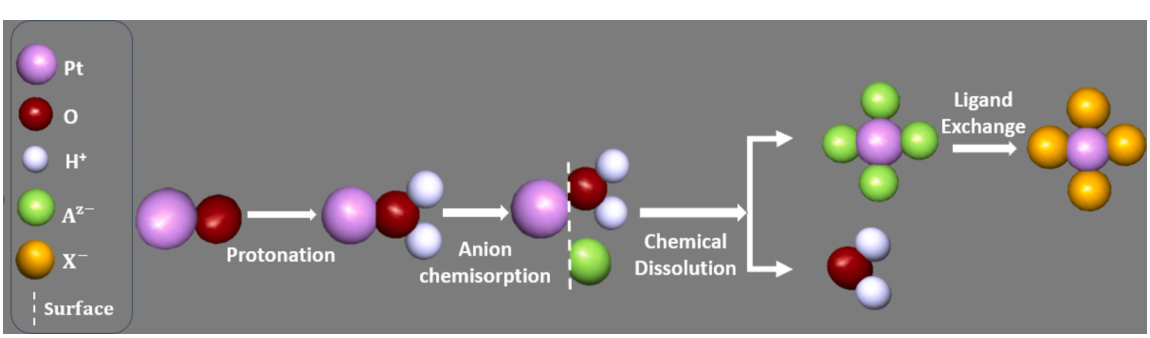

Fig. 7. Schematic representation of the dissolution mechanism of platinum (IV) oxide in (D)ES.

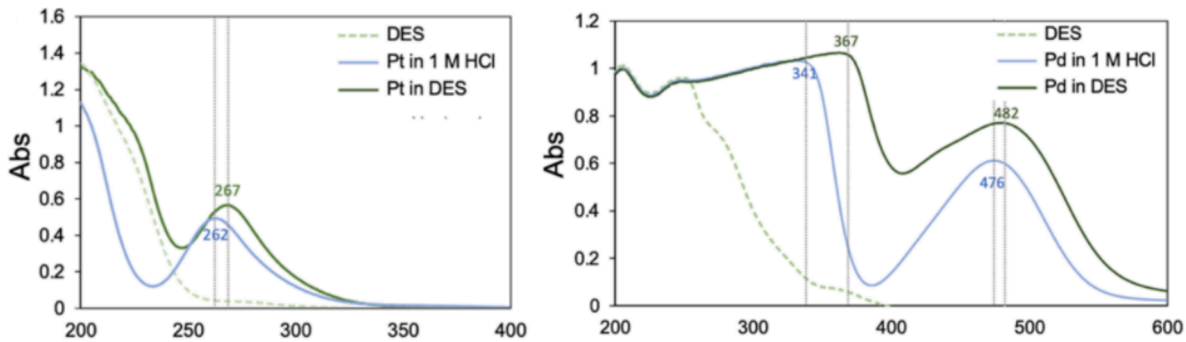

Fig. 8. UV–visible spectral analysis of leachates of Pt (left) and Pd (right) complexes in the (D)ES $[P_{66641}]$Cl:DecA and in HCl solutions. Reprinted with permission from the ACS Publishing [140].

fundamental in dissolution processes as the metal coordination and the lattice energy of the resulting species significantly affect the solubility and stability of the formed species in the lixiviant. Their study uncovered that REE speciation and dissolution significantly relies on the HBD selection within (D)ESs, underscoring the importance of their formulation to optimise metal recovery processes. For instance, in ChCl:EG lanthanides predominantly formed $[Ln(EG)_{4-5}]$ complexes, coordinating mainly with the oxygen atoms of EG, indicating strong Ln-OH interactions. In the case of the ChCl:U, lanthanide speciation revealed a higher coordination number, forming $[Ln(U)_{7-10}]$ complexes, where the carbonyl and amine groups of urea coordinated with the lanthanide ions. Conversely, in ChCl:LacA system, primarily lanthanide-chloro complexes, $[Ln(Cl)_{5-6}]$, were formed, demonstrating weaker Ln −O interactions and stronger Ln −Cl coordination, resulting in the coordination of dissolved metal species with Cl^- rather than LacA as HBD [141]. The discrepancy in the speciation of Nd dissolved in ChCl:LacA (D)ES reported by Riaño et al. [97] compared to that demonstrated in Amphlett's research likely arises from experimental conditions such as Cl^- concentration, and analytical techniques employed. In the study by Amphlett, comprehensive EXAFS analysis on the leachates was directly performed to fully determine the speciation [141].

The potential dissolution mechanism of REOs in (D)ESs is exemplified in a study investigating the roasting-assisted leaching of REEs from monazite using ChCl:*p*TSA monohydrate (2:1) (D)ES. The robust crystalline structure of monazite, characterised by REO^9 polyhedra linked to PO_4 tetrahedra, provides significant chemical and thermal stability, making the separation of individual REEs from monazite challenging [56,142]. Thus, this stable structure requires NaOH roasting before the dissolution step to modify its structure by breaking down the mineral matrix, which enhances its susceptibility to leaching. After that, the REE oxides interact with protons (H^+), supplied by the acidic component in the (D)ES (i.e., *p*TSA). Protonation weakens the REE-oxygen bonds, facilitating the release of REE ions into the solution. The resulting REE^{3+} then undergoes surface complexation, interacting with ions in the (D)ES through coordination bonds, which stabilise them in the solution. This is often accompanied by substitution of ligand with Cl^-, leading to the formation of electrically neutral REE-chloro complexes. The schematic and formula for the proposed mechanism are shown in Fig. 9 and equations (8) – (10), respectively [56].

$$[REE]PO_4 + 3NaOH \rightarrow REE(OH)_3 + Na_3PO_4\, 2REE(OH)_3 \rightarrow REE_2O_3 + 3H_2O \tag{8}$$

$$REE_2O_3 + 6[C_7H_7SO_3]^-{}_{(D)ES} \rightleftarrows 2\left[REE(C_7H_7SO_3)_3\right]_{(D)ES} + 3H_2O_{(D)ES} \tag{9}$$

$$2[REE(C_7H_7SO_3)_3]_{(D)ES} + 6Cl^-_{(D)ES} \rightleftarrows 2[REECl_3]_{(D)ES} + 6(CH_3C_6H_4SO_2O^-)_{(D)ES} \tag{10}$$

Numerous studies have delved into the relationship between the solubilities of metal oxides in (D)ESs and their inherent properties. These properties encompass the oxidation number, charge density, lattice energy, and Gibbs energy of formation of metal oxides, along with the proton activity and complexation capabilities of (D)ESs. Although all the

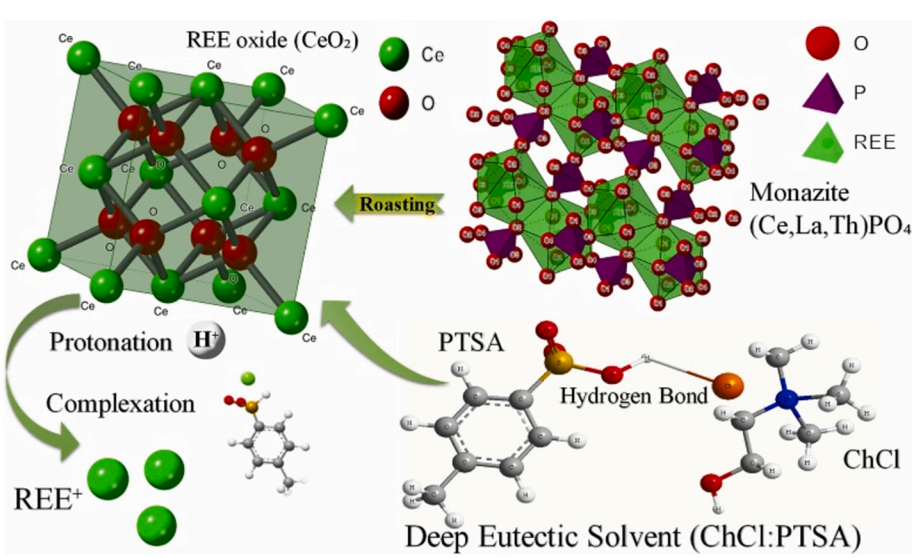

Fig. 9. Depiction of a proposed leaching mechanism of REE from monazite in ChCl:*p*TSA. Reprinted with permission from Elsevier [56].

mentioned factors play an indispensable role in determining solubility performance, proton activity and complexation capabilities of (D)ESs have been identified as primary contributors, which again makes the tunability of (D)ESs relevant [41,72]. This conclusion is supported by Karan et al., which evaluated the recovery of REEs with ChCl:LacA (1:2) and ChCl:*p*TSA (1:1). Their findings demonstrated that *p*TSA significantly enhanced the leaching of REEs, which facilitated the protonation step more effectively than LacA. Consequently, it can be inferred that metal solubility partially relies on the pH value in the medium which is related to the pK_a of the HBDs within (D)ESs employed as leaching reagent [143]. It is pertinent to state that strongly acidic (D)ESs are not desirable as they may act similarly to inorganic acids, thereby losing their selectivity for dissolution of target metals [77]. Additionally, it has been illustrated that the complexation capability exerts a more significant influence on the solubility of metal oxides [41,76].

3.1.2. Survey of studies on PGM and REE dissolution in (D)ESs

The studies on (D)ESs used as leaching agents for the dissolution of PGMs and REEs from both primary and secondary sources are summarised in Table 3 and discussed as follows:

The automotive industry consumes the largest amount of PGMs, primarily for catalytic converters. This has sparked increased interest in PGM recovery (Pt(IV), Pd(II), and Rh(III)) from spent automotive catalyst (SAC) [50]. Recently, research efforts have focused on recycling PGMs from SAC utilising (D)ESs, providing a substitute to traditional leaching reagents such as cyanides, *aqua regia*, and concentrated HCl. Lanaridi et al. studied the effectiveness of ChCl:*p*TSA (1:1.8) with the addition of 0.1 g HNO_3 as an oxidising agent to recover PGMs from SAC [103]. Quantitative dissolution of both Pt and Pd was realised, while Rh exhibited partial dissolution, which could be attributed to its insoluble state (Rh_2O_3) in SAC after being subjected to high operating temperatures. However, the Rh leachability showed an improvement of roughly 25 % once the SAC underwent thermal pre-treatment. To address the high viscosity of the used solvent and improve handling and mixing, water was added to the system with a SAC:(D)ES:H_2O:HNO_3 mass ratio of 1:4:1:1, achieving comparable leaching performance to the case of SAC:(D)ES ratio of 1:5 [103]. Their research on PGM separation and recovery continued to further evaluate the isolation of PGMs from PGM-rich (D)ES phase with $[P_{66614}]Cl$ dissolved in *n*-heptane. Complete extraction of Pt and Pd along with 99 % Rh extraction was observed. Recycling of the (D)ESs was assessed, and whilst no loss in leaching efficiency was observed, there was a pronounced solvent loss, ranging from 50 % to 60 % per cycle. This was attributed to the high viscosity of the (D)ES and handling losses, especially in small-scale experiments [43]. More recently, a selective leaching method utilising a H(D)ES composed of $[P_{66614}]Cl$:DecA (1:2) combined with 1.5 mol.L^{-1} methanesulphonic acid (MSA) serving as a non-oxidising organic acid and 0.05 mol.L^{-1} trichloroisocyanuric acid (TCCA) as a chlorination and oxidation reagent was proposed [140]. The aim of employing H(D)ES was to minimise purification steps, particularly by eliminating SX step, and to ensure a high recovery of all three PGMs through one-step dissolution, as evidenced by achieving leachability rates of 90 %, 100 %, and 89 % for Pt, Pd, and Rh, respectively, while those of other metals such as Al and La were below 5 %. After that, appropriate stripping agents, including 5 mol.L^{-1} ammonium chloride (NH_4Cl) for Rh, 10 mol.L^{-1} ammonium nitrate (NH_4NO_3) for Pt, and 0.005 mol.L^{-1} thiourea ($SC(NH_2)_2$) for Pd, were employed to individually separate them from the leachate. Replenishing the amount of chloride ions into the regenerated H(D)ES before reutilisation enabled its reusability. The performance of the proposed method was compared with the conventional use of *aqua regia*. Unlike *aqua regia*, which leached significant amounts of Fe, La, Al, and Mg, the H(D)ES system with additives effectively suppressed their leaching while enabling highly selective and efficient PGM extraction [140]. Although the limited research discussed above on the application of (D)ESs for the dissolution and separation of PGMs from SACs indicates promising results, further investigation is needed to evaluate their performance under a range of operational conditions and with various formulations. Additionally, due to the widespread applications of PGMs, it is vital to study a wider array of secondary resources including, but not limited to, spent industrial catalysts, e-waste, and end-of-life fuel cells for PGM recycling using (D)ESs.

Compared to the nascent research of PGM dissolution using (D)ESs, the exploration of REE separation with (D)ESs has been more thoroughly investigated. Several studies have focused on the dissolution and separation of REOs from synthetic mixtures, aiming to optimise various operational parameters, including leaching time, temperature, solid-to-liquid (S/L) ratio, and the types and molar ratios of HBA to HBDs. These investigations provide beneficial insights that can be applied to real-life scenarios, enhancing the efficiency and selectivity of REE separation processes using (D)ESs. For instance, Chen et al. developed new BA(D)ESs comprising polyols and carboxylic acids for selective REOs dissolution, leveraging their strong acidity and moderate viscosity [76]. The detailed exploration illustrated that EG:MA (4:1) provided substantial solvation capability for REOs from La_2O_3 to Gd_2O_3, excluding CeO_2 owing to its high valence. Moreover, successful mutual separation of REOs was demonstrated, exemplified by La over Ce, where La was further isolated from the (D)ES phase using a stoichiometric amount of oxalic acid, followed by calcination at 700 °C. The solubility of REOs, specifically Eu_2O_3 and La_2O_3 as representatives of HREO and LREO, respectively, was tested in 3.27 mol.L^{-1} HCl and compared to EG:MA (4:1). The results revealed slightly higher solubilities when using HCl (0.189 g.g^{-1} for Eu_2O_3 and 0.174 g.g^{-1} for La_2O_3) compared to the (D)ES (0.168 g.g^{-1} for Eu_2O_3 and 0.147 g.g^{-1} for La_2O_3), validating the superior solubilising capacity of EG:MA (4:1) and highlighting its potential for application [76]. The selective separation and recovery of REOs, specifically La_2O_3, Eu_2O_3, and Dy_2O_3, was also probed in another investigation using different (D)ESs synthesised from ChCl and guanidine hydrochloride (GUC) as HBAs, and glycolic acid (GA) and LacA as HBDs [114]. While ChCl and GUC share the same Cl^- coordination characteristics in addition to GA and LacA having similar acidity, ChCl:GA showed almost no REO dissolution, while GUC:LacA (1:2) exhibited solubility up to 62000 ppm for La, with extremely high selectivity since solubility for HREOs (i.e., Dy_2O_3) was negligible. The difference was attributed to their structure, where Cl^- is less bound in GUC, making it more available to interact with rare earth cations. Their observations showed higher dissolution ratio for La (about 92.53 %) while those for Eu and Dy were about 7.5 % and < 1 %, respectively, highlighting a relationship between the atomic number of REOs and their leachability into the (D)ES which could be explained by lanthanide contraction and the "hard and soft acid and base" (HSAB) theory. As the atomic number of lanthanides (Lns) increases, their ionic radius decreases due to the lanthanide contraction, making heavier Lns harder acids. Additionally, O^{2-} is a harder base than Cl^-. Therefore, according to HSAB theory, the (D)ES exhibited extremely high solubility for LREOs than for HREOs [114]. Another study aimed to elucidate the selectivity of a novel H(D)ES consisting of TOPO:dinitrosalicylic acid (DNS) (1:1) towards two specific HREOs, including Yb_2O_3 and Lu_2O_3. Their findings demonstrated a higher dissolution of Yb into the studied H(D)ES with a separation factor (SF) of 2.11. This was attributed to the lower lattice energy of Yb_2O_3 (12957.56 kJ.mol^{-1}) compared to that of Lu_2O_3 (12993.59 kJ.mol^{-1}). Metal oxides with lower lattice energy exhibit lower stability, making them more vulnerable to proton attack by the (D)ES. Complete stripping of Yb and Lu from loaded TOPO:DNS was achieved using 4 mol.L^{-1} HCl [144].

Due to the widespread application of NdFeB magnet-based products and their subsequent end-of-life disposal, a substantial volume of this waste is produced, representing a promising secondary resource for the recovery of REEs, particularly Nd(III) [147]. Several studies have delved into the separation of REEs from NdFeB magnet with (D)ESs. Riaño et al. investigated the applicability of different ChCl-based (D)ESs incorporating LacA, U, and EG as HBDs, all in molar ratios of (1:2), for the

Table 3
Compilation and summary of the most relevant studies on the application of (D)ESs for SLX of PGMs and REEs through leaching from primary and secondary sources.

Metal	Metal sample	Pre-treatment	(D)ES HBA:HBD (s) molar ratio	Leaching conditions Temperature (°C)	Time (h)	Solid-to-liquid phase ratio [a]	Main results	Ref.
Pt(IV), Pd (II), Rh (III)	Spent automotive catalyst	Acid pre-treatment with formic acid, grinding and sieving to get particle size < 160 μm	ChCl:*p*TSA (1:1.8)	80	4	0.2 g. g^{-1}	L_{Pt}% [b] = 96 %, L_{Pd} % = 100.3 %, L_{Rh}% = 43 %	[103]
Pt(IV), Pd (II), Rh (III)	Spent automotive catalyst	Acid pre-treatment with formic acid	$[P_{66641}]$Cl: DecA (1:2)	80	24	50 g.L^{-1}	L_{Pt}% = 90 %, L_{Pd}% = 100 %, L_{Rh}% = 89 % S_{Pt}% [c] = 80 %, S_{Rh}%= 80 %, S_{Pd}% = 90 %	[140]
Yb(III), Lu (III)	Rare earth oxides mixture	Ball milling for 4 h	TOPO:DNS (1:1)	90	4	20 g.L^{-1}	L_{Yb}% ≈ 35.91 %, L_{Lu}% ≈ 17.22, $SF_{Yb/Lu}$ [d] = 2.11 S_{Yb}% ≈ 100 %, S_{Lu}% ≈ 100 %.	[144]
REEs except Ce (III)	Rare earth oxides mixture	–	EG:MA (4:1)	60	6	0.05 g. g^{-1}	Maximum solubility for Eu_2O_3 = 0.168 g g^{-1}, La_2O_3 = 0.147 g g^{-1}, Gd_2O_3 = 0.105 g g^{-1}, Nd_2O_3 = 0.063 g g^{-1}, Sm_2O_3 = 0.039 g g^{-1}, Pr_2O_3 = 0.022 g g^{-1}, Y_2O_3 = 0.002 g g^{-1}, CeO_2 = 0.00 g g^{-1} while Tb to Lu oxides were insoluble.	[76]
REEs	Rare earth oxides mixture	–	GUC:LacA (1:2)	50	48	0.02 g. g^{-1}	From single-metal sample: L_{La}% ≈ 92.53 %, L_{Eu}% ≈ 7.5 %, L_{Dy}% < 1 % From binary mixture of Ln_2O_3 – Eu_2O_3: L_{La}% = 81.49 %, L_{Eu}% = 7.4 %, $SF_{La/Eu}$ = 54.38 From binary mixture of Ln_2O_3 – Dy_2O_3: L_{La}% = 89.47 %, L_{Dy}% = 2.95 %, $SF_{La/Dy}$ = 287 From binary mixture of Nd_2O_3 – Dy_2O_3: L_{Nd}% = 45.16 %, L_{Dy}% = 0.5 %, $SF_{Nd/Dy}$ = 16.87	[114]
Nd(III)	NdFeB magnet waste	Crushing and sieving, and oxidative roasting	GUC:LacA (1:2)	40	6	0.1 g. g^{-1}	L_{Nd}% ≈ 84.4 %, L_{Fe}% < 1 %, $SF_{Nd/Fe}$ > 1300 Solubility of Nd = 6.7 × 10^4 ppm S_{Nd}% = 83.1 %, P_{Nd}% [e] = 99.56 %	[113]
Nd(III), Dy (III)	NdFeB magnet waste	Demagnetisation by heating during 5 h at 300 °C in a furnace, ball milling under condition of 30:1 ball-to-powder ratio (g/g) for 2 h at 200 rpm to get particle size < 100 μm, finally oxidative roasting in a muffle furnace at 950 °C for 15 h.	ChCl:LacA (1:2)	70	24	20 g.L^{-1}	L_{Nd}% ≈ 90 %, L_{Dy}% ≈ 82 %, L_B% ≈ 80 %, L_{Fe}% ≈ 95 %, L_{Co}% ≈ 87 % D_{Nd} [e] = 0.14, D_{Dy} = 1.79, $SF_{Dy/Nd}$ = 12.79 P_{Nd}% = 99.87 %, P_{Dy} % = 0.13 %	[97]
Nd(III)	NdFeB carbonylation residue	Grinding and oxidative roasting for 10 h at 1000 °C	EG:MA (2:1)	80	5	8 g.L^{-1}	L_{Nd}% = 28.07 %, L_{Fe}% < 0.01 %, $SF_{Nd/Fe}$ > 3000 EE_{Nd}% [g] = 99.35 %, S_{Nd}% = 98.32 % R_{Nd}% [h] = 85.27 %, P_{Nd}% = 92.58 %	[77]
Nd(III)	NdFeB magnet waste	Oxidative roasting	$[N_{2222}]$Cl: LevA(1:2)	90	9	0.04 g. g^{-1}	L_{Nd}% = 97.63 %, L_{Fe}% < 0.435 %, $SF_{Nd/Fe}$ > 9000 R_{Nd}% ≈ 100 %, P_{Nd}% = 99.65 %	[93]
Nd(III)	NdFeB magnet waste	Grinding to get particle size < 44 μm, followed by NaOH digestion-oxidative roasting	EG:MA (4:1)	70	5	0.1 g. g^{-1}	L_{Nd}% = 97.3 %, L_{Fe}% = 0.84 %	[115]
Y(III), Eu (III)	Lamp phosphor waste	Grinding and sieving to get the fraction < 125 μm	ChCl:LevA (1:2)	80	48	0.1 g. g^{-1}	From individual phosphors: L_{YOX}% > 98 %, L_{HALO}% < 1 % From real lamp phosphor waste: L_{YOX}% ≈ 43.35 %, L_{HALO}% ≈ 26.78 % R_{Eu}% ≈ 86 %, R_Y% ≈ 75 %	[100]
Y(III), La (III), Ce (III), Nd (III), Sm (III)	Basnäsite ore	–	ChCl:U: MAL (1:1:0.5)	50	8 days	1 g.L^{-1}	From single-metal sample: L_{Sm}% ≈ 50 %, L_Y% ≈ 43 %, L_{Nd}% ≈ 40 %, L_{La}% ≈ 8 %, L_{Ce}% ≈ 8 % From multi-component mixture in the presence of dolomite: L_{Sm}% ≈ 90.9 %, L_Y% ≈ 86.5 %, L_{Nd}% ≈ 86.5 %, L_{La}% ≈ 21.3 %,	[129]

(*continued on next page*)

Table 3 (*continued*)

Metal	Metal sample	Pre-treatment	(D)ES HBA:HBD (s) molar ratio	Leaching conditions Temperature (°C)	Time (h)	Solid-to-liquid phase ratio [a]	Main results	Ref.
							L_{Ce}% ≈ 41.7 % From Bastnäsite ore: L_Y% ≈ 86 %, L_{Sm}% ≈ 76.6 %, L_{Nd}% ≈ 61 %, L_{La}% ≈ 23.7 %, L_{Ce}% ≈ 8.6 %	
HREEs (Dy–Lu and Y)	Pure yttrium carbonate salt	Mechanical activation at 1800 rpm for 60 min	ChCl:U: MAL (1:1:0.5)	80	12	1.25×10^{-4} g. g^{-1}	From original sample: L_Y% = 46.5 % From pre-treated sample: L_Y% = 88.37 %	[145]
REE (La (III)-Gd (III))	Monazite concentrate	Milling, NaOH caustic treatment at 500 °C for 2 h, followed by water washing and drying	ChCl:*p*TSA (2:1)	100	72	10 $g.L^{-1}$	From non-roasted sample: L_{REE}% < 5 % From caustic treated sample L_{REE}% > 90 %, L_{Ce}% = 99.8 %, L_{La}% = 99.9 %, L_{Nd}% = 94 %	[56]
REEs	Micro-granite rock deposit	Sulfation roasting, water washing, and grinding to get particle size < 23 μm	ChCl:*p*TSA (1:1)	130	6	0.1 g. g^{-1}	L_{TREE}% = 97 % R_{REE}% = 98.5 %, P_{REE} % = 85 %	[102]
REEs	Us coal by products	Grinding and sieving with an average size of 150 μm	ChCl:U (1:2)	25	1	0.5 g. g^{-1}	L_{REE}% = 89 %	[146]
REEs	Coal fly ash	Grinding and sieving to obtain fraction < 45 μm	ChCl:*p*TSA (1:1)	80	6	0.1 g. g^{-1}	L_{REE}% ≈ 85–95 % S_{REE}% ≈ 100 %	[143]

[f]Distribution ratio,
[a] Metal feed-to-(D)ES phase ratio,
[b] Leaching efficiency %,
[c] Stripping efficiency % $= \frac{\text{Mass of metal in stripping solution}}{\text{Mass of metal in loaded organic phase}} \times 100$,
[d] Separation factor$_{(M1//M2)} = \frac{\text{Mass of metal M1 in leachate}}{\text{Mass of metal M2 in leachate}}$,
[e] Purity of final product % $= \frac{\text{Concentration of metal in final product}}{\text{Concentration of total elements in final product}} \times 100$,
[g] Extraction efficiency %,
[h] Recovery efficiency % $= \frac{\text{Mass of recovered metal in final product}}{\text{Initial mass of metal in feed}} \times 100$.

dissolution and separation of REEs (Nd and Dy) and other precious metals (Fe, Co, B) from roasted NdFeB magnet waste [97]. Their research exhibited high solubility of metal oxides in ChCl:LacA (1:2), while ChCl:U and ChCl:EG exhibited poor solubilities, which was attributed to the high proton activity of LacA. The impact of S/L ratio on leaching efficiency demonstrated that at low S/L ratios, nearly all metals were dissolved non-selectively. In contrast, high S/L ratios limited the solvent's ability to access all metals present in the magnet powder, resulting in reduced leachability. Following the leaching process, a two-step SX procedure was performed to initially extract Fe and Co from Nd and Dy-loaded (D)ES phase employing IL consisting of $[N_{8881}\ Cl][SCN]$ diluted in toluene, and subsequently separate Nd from Dy using Cyanex 923 dissolved in toluene. Nd with 99.87 % purity was ultimately recovered through precipitation-calcination [97]. Another research employed GUC:LacA (1:2), which had previously shown promising results in REO separation, for the selective dissolution of Nd from roasted NdFeB waste [113]. Selective separation of Nd over Fe, with a SF over 1300, was achieved under relatively mild conditions (6 h at 40 °C). The large difference in leachability of Nd than Fe was explained by (i) the higher ionic strength of Nd_2O_3 [72], and (ii) the larger ionic radii of Nd^{3+} (1.12 Å) compared to Fe^{3+} (0.69 Å) leading to lower lattice energy of Nd_2O_3 (U = 13071 $kJ.mol^{-1}$) compared to Fe_2O_3 (U = 15373 $kJ.mol^{-1}$) [148,149]. It was found that Nd_2O_3 with 99.56 % purity could be obtained via precipitation-calcination following a single-step dissolution in (D)ES. Furthermore, and more importantly with a view on the circularity of the process, the solvent displayed proper stability and

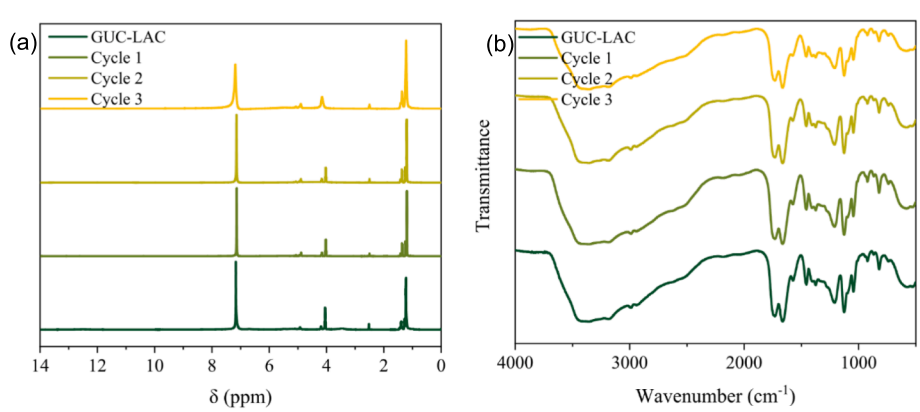

Fig. 10. (a) ^1H NMR and (b) FT-IR spectra of GUC:LAC (1:2) (D)ES before and after leaching processes. Reprinted with permission from ACS Publishing [113].

dissolution capacity after three consecutive cycles, inferred form ^{1}H NMR and FT-IR analysis of (D)ES phase prior and after each separation cycle, as illustrated in Fig. 10 [113].

During the manufacturing process of NdFeB magnets, substantial quantities of REE-enriched waste, are generated, including NdFeB carbonylation slag with REE concentrations ranging from 0.2 % to 2.0 %. However, the selective separation of REEs at ultra-low concentrations presents considerable challenges and necessitates advanced leaching techniques [150]. Yang et al. studied the separation of ultra-low concentrations of REEs from roasted NdFeB carbonylation slag utilising EG:MA (2:1) [77]. This method demonstrated high selectivity for Nd and exhibited minimal interaction with Fe, achieving a selective isolation of Nd with a SF > 3000. The impact of temperature on Nd leaching efficiency was examined, showing that temperatures above 70 °C accelerated Nd_2O_3 dissolution due to enhanced acidity and conductivity of (D)ES. However, very high temperatures turned EG:MA too acidic, resulting in fast Fe_2O_3 dissolution and loss of Nd selectivity. Accordingly, 80 °C was established as the optimum leaching temperature to achieve a balance between selectivity and leaching efficiency. Since stirring speed can affect the uniform dispersion of materials into a solvent, this study investigated the effect of stirring speed on the leachability of Nd into the (D)ES. The results indicated that increasing the stirring speed from 500 to 700 rpm improved the leaching efficiency by 11 %. Since direct precipitation of Nd from leachate was not viable owing to its extremely low concentration, an alternative recovery method was proposed. This method involved initial SX using di-(2-ethylhexyl)phosphoric acid (P204) in sulfonated kerosene, followed by re-extraction with 1.5 mol.L^{-1} HCl, and finally precipitation-calcination utilising 1.2 times the stoichiometric amount of oxalic acid as a precipitating agent. Ultimately, 85.27 % Nd with 92.58 % purity was achieved [77]. Shuping and co-workers identified that previous studies had reported on leaching Nd from NdFeB waste using (D)ESs was incomplete, with a maximum leachability of 90 %, leaving some REEs in the leachate residue. To address this, they developed a novel H(D)ES composed of tetraethylammonium chloride ([N_{2222}]Cl):LevA (1:2), to enhance selectivity toward Nd [93]. Their research demonstrated a leaching efficiency of 97.63 %, with SF of more than 9000, enabling Nd recovery via direct precipitation with high purity (99.65 %). The recyclability and reusability of the H(D)ES was also proved for three consecutive separation cycles, demonstrating its potential for real-life scenarios [93]. Pre-treatment of metal-bearing samples is key to improve leaching efficiency and selectivity for specific metals by altering their state in the sample. For instance, pre-treating NdFeB magnets can lead to the formation of various metal oxides, such as $NdFeO_3$, Nd_2O_3, Fe_3O_4, and Fe_2O_3, based on the conditions and type of pre-treatment [115]. Heo et al. thoroughly evaluated the impact of three pre-treatment techniques, namely oxidative roasting, NaOH digestion, and combination of both (NaOH digestion-oxidative roasting), on the selective leaching of REEs form synthetic NdFeB magnet waste using various (D)ESs, including GUC:LacA (1:2), EG:MA (4:1), and ChCl:LacA (1:2) [115]. The experimental results demonstrated that Nd and Fe could be selectively leached utilising (D)ESs when they exist in the form of Nd_2O_3 and Fe_2O_3, respectively. It was found that applying oxidative roasting alone resulted in the formation of $NdFeO_3$, suppressing REE leachability. On the other hand, employing NaOH digestion yielded $Nd(OH)_3$ and Fe_3O_4, which required oxidative roasting to be converted into Nd_2O_3 and Fe_2O_3, respectively. Consequently, NaOH digestion-oxidative roasting process was recognised as the optimal pre-treatment technique, achieving a maximum selectivity > 4000 and a leaching efficiency of 97.3 % for Nd and 0.8 % for Fe using EG:MA (4:1). This solvent also exhibited reusability for at least two separation cycles with almost negligible change in its leachability and selectivity for Nd [115].

The lamp phosphor waste is recognised as a valuable secondary resource of REEs, notably Eu and Y [24]. In a comprehensive study, the solubility of individual and real lamp phosphor waste in pure LevA and ChCl:LevA (1:2) was explored [100]. Their findings revealed that, under optimal conditions of 48 h, 80 °C, and S/L ratio of 0.1 g.g^{-1}, YOX (Y_2O_3:Eu^{3+}) exhibited more than 98 % solubility, whereas HALO phosphor (Sr, Ca)$_{10}$(PO_4)(Cl,F)$_2$:Sb^{3+},Mn^{2+}) had less than 1 % solubility in both pure LevA and ChCl:LevA (1:2). These results demonstrated that Cl^- from ChCl did not account for the high REE leaching efficiency, underscoring the prominent role of proton activity of LevA in dissolution performance. Additionally, the leaching of real lamp phosphor waste revealed higher leachability and selectivity utilising pure LevA than ChCl:LevA. Besides, LevA offers lower viscosity and corrosiveness, being more environmentally friendly and cheaper, and crucially, unlike carboxylic acid-based (D)ESs, LevA does not undergo decomposition by esterification [100].

(D)ESs have also been applied in the separation of REEs from minerals. For instance, binary and ternary ChCl-based (D)ESs were used to explore the leaching behaviour of REEs, such as Y, La, Ce, Nd, and Sm, from bastnäsite. The research demonstrated that ChCl:U:MAL (1:1:0.5) selectively leached REEs having higher atomic number, such as Sm and Nd, due to the lanthanide contraction. In contrast, the solvent exhibited minimal dissolution of REEs with lower atomic numbers like Ce and La, as well as a slight dissolution of metal impurities (e.g., Ca, Mg and Fe) from dolomite present in the minerals. The exceptional higher dissolution of Y, despite having ionic radii close to La, was attributed to its different valence configuration. Furthermore, the greater leaching percentage observed in multi-component mixtures and/or dolomite-added mixtures, compared to the pure REE carbonate salt, was attributed to the expansion of the carbonate surface, serving as new active bicarbonate ligands in the (D)ES, as well as the evolution of more CO_2 gas, thereby facilitating further REE dissolution and complexation [111]. Following the successful use of ChCl:U:MAL (1:1:0.5) in REE separation from carbonate salts, another attempt was made to elucidate the impact of mechanical activation on Y carbonate dissolution. Their findings revealed that subjecting the Y carbonate salt to mechanical activation resulted in a considerable enhancement in Y dissolution at elevated leaching temperatures. For instance, at 80 °C, the leaching efficiency of inactivated Y was 48.61 %, whereas that of activated Y increased to 88.37 %, which could be ascribed to the reduction in particle size and the augmentation of the contact area during the reaction. However, mechanical activation exhibited negligible effectiveness when subjected to lower leaching temperatures [145]. Monazite, a vital mineral for extracting REEs particularly La, Ce, and Nd, is typically processed using conventional hydrometallurgical methods [151]. Accordingly, various binary and ternary (D)ESs, including ChCl:*p*TSA (2:1), ChCl:*p*TSA:EG (2:1:1), and PEG-400:*p*TSA (1:1) were tested to separate REEs from monazite concentrate [56]. Leaching of non-roasted monazite showed insufficient separation of REE from La to Gd, with leaching percentage below 5 %. This inefficiency was attributed to its robust crystal structure featuring REO^9 polyhedra linked to PO_4 tetrahedra [142,152]. In contrast, NaOH roasting of monazite at 500 °C for 2 h led to rare earth hydroxides, which were then effectively leached using (D)ESs. It was shown that ChCl:*p*TSA (2:1) exhibited the greatest REE dissolution efficiency (> 90 %), but with slow kinetics (after 72 h). Additionally, leachability was highly contingent upon temperature, as increasing the temperature reduces solvent viscosity, thereby enhancing mass transfer [56]. In the search for new REE-rich deposits, Indian exploration agencies discovered the micro-granites of Bhatikhera [153]. The recovery of REE from this resource utilising ChCl:*p*TSA (1:1) achieved around 95 % REE leachability at 130 °C. [102]. The study examined the influence of sample particle size on REE leaching efficiency, revealing that finer materials (< 23 μm) resulted in higher recovery rates due to their increased surface area and the enhanced REE phase liberation through grinding. A comparison of the solvation potential of ChCl:*p*TSA with 3 mol.L^{-1} H_2SO_4 demonstrated superior selectivity and REE dissolution. To further illustrate, ChCl:*p*TSA achieved a total REE (TREE) recovery of 97 %, with 99.2 % leachability for LREEs and 94 % for HREEs. In contrast, H_2SO_4 achieved 85 % TREE recovery, with 90 % leachability for LREEs and 75 % for HREEs. This demonstrated that even

with employing strong mineral acids, higher LREE dissolution could be achieved compared to HREE, likely due to the integration of HREEs with refractory zircon and other minerals in the studied sample [102]. The investigation on ChCl:*p*TSA for REE separation was extended to coal flyash (CFA) [143], a secondary resource containing about 0.22 % REEs [154]. In this study, the REE leachability of the (D)ES was compared with that of individual *p*TSA and ChCl, as well as with 1.5 mol.L^{-1} H_2SO_4. The results showed that (D)ES yielded TREE recovery of 94.8 %, with 96.8 % recovery for LREEs and 89.6 % for HREEs. This performance was about 5 % to 8 % higher than that obtained with *p*TSA and ChCl alone, and about 35 % higher than with H_2SO_4. The relatively higher leachability of LREEs compared to HREEs was attributed to the higher basicity of LREEs, indicating higher tendency to accept protons from the functional groups of HBD, thereby facilitating leaching with the (D)ES. Additionally, the investigation into the molar composition of the HBD demonstrated that an increase led to higher viscosity of the (D)ES. This hindered the diffusion of REEs into the solvent, thereby diminishing their solubility. Besides, Cl^- in ChCl played a pivotal role as ligand in the mechanism; thus, a decrease in Cl^- concentration lowered the leachability with the corresponding (D)ES [143].

The reviewed studies indicate that (D)ESs with favourable attributes, such as low viscosity, high thermal stability, effective proton activity, robust complexation ability, and good regeneration and reutilisation, show promising potential for leaching PGMs and REEs. Additionally, their tunability by altering the nature and molar composition of HBA to HBDs enhances their versatility, enabling selective metal separation based on the distinct solubility profiles of various metals. However, (D)ESs are not yet suitable for replacing mineral acids in industrial leaching applications, likely due to challenges such as relatively high viscosity and slow leaching kinetics. Therefore, more research is essential to further elucidate the mechanisms and kinetics of leaching with (D)ESs, which could also facilitate the optimal selection of HBAs and HBDs for effective (D)ES formulations in real-life applications.

3.2. Liquid-liquid extraction

3.2.1. Solvent extraction mechanisms for PGMs and REEs using H(D)ESs

The extraction of PGMs and REEs from aqueous systems with conventional extractants has been discussed extensively in the literature, where solvents like TOPO, di-(2-ethylhexyl) phosphoric acid (D2EHPA), Alamine 336, and Cyanex 923 have profusely been used [155,156]. However, the mechanism of the extraction of critical metals from acidic aqueous solutions using H(D)ESs is not yet fully understood. To elucidate this, various techniques have been employed, such as slope analysis from the distribution coefficients calculated from ICP measurements, as well as ^{31}P NMR ^{1}H NMR, UV–vis, EXAFS, and FT-IR spectroscopies. In general, the mechanism of metal extraction into H(D)ES phase is affected by the type of metal ions, source composition, and predominantly metal speciation and nature of the employed H(D)ES.

Table 4
List of identified PGM speciation in aqueous chloride solutions.

Metal	PGM-chloro complex
Platinum	Pt(II) $[PtCl_4]^{2-}$*
	Pt(IV)$[PtCl_6]^{2-}$*
Palladium	Pd(II) $[PdCl_4]^{2-}$*
	Pd(IV)$[PdCl_6]^{2-}$*
Rhodium	Rh(III)$[RhCl_6]^{3-}$*, $[RhCl_4]^-$, $[RhCl_5]^{2-}$, $[RhCl_5(H_2O)]^{2-}$*, $[RhCl_4(H_2O)_2]^-$
	Rh(IV)$[RhCl_6]^{2-}$
Ruthenium	Ru(III)$[RuCl_6]^{3-}$*, $[RuCl_5(H_2O)]^{2-}$, $[RuCl_4(H_2O)_2]^-$, $[RuCl_3(H_2O)_3]$
	Ru(IV)$[RuCl_6]^{2-}$, $[Ru_2OCl_{10}]^{4-}$, $[Ru_2OCl_8(H_2O)_2]^{2-}$
Iridium	Ir(III)$[IrCl_6]^{3-}$, $[IrCl_5(H_2O)]^{2-}$, $[IrCl_4(H_2O)_2]^-$
	Ir(IV)$[IrCl_6]^{2-}$*, $[IrCl_5]^-$, $[IrCl_4(H_2O)_2]$

*indicates the predominant speciation.

PGMs form a range of complexes with a variety of different ligands. PGM-chloro complexes have been extensively studied owing to the cost-effectiveness and widespread use of aqueous chloride solution as leaching agent, which effectively dissolve and concentrate all PGMs. PGM-chloro complex speciation can be modulated by varying the chloride ion concentration or pH level of the solution. The major PGM species encountered in chloride media are shown in Table 4 [43,92,157,158].

Concerning REE, the predominant oxidation state in aqueous solution is + 3, classified as hard acids according to the HSAB theory [159]. This indicates a tendency to primarily form complexes with hard ligands, which are characterised by highly electronegative donor atoms such as O and F. Therefore, REE complexes containing chloride and nitrate ligands, considered as intermediate ligands, exhibit moderately weak stability in most low-temperature natural aqueous environments and constitutes a negligible portion of REE in solution. However, at high temperatures, the stability of the REE-chloro complexes may intensify and potentially become significant [160,161].

Treshatov et al. conducted a pioneering study on the transfer of metallic species from aqueous solutions into H(D)ESs, shedding light on the metal extraction mechanism. The investigation identified several extraction mechanisms associated in the process, including ion exchange, ion pair formation in aqueous phase, and neutral ion association [162]. Although the metal studied was not a PGM or REE, the discovered mechanisms are applicable to both.

Ion exchange mechanism.

Ion exchange as one of the predominant mechanisms of extracting metals into H(D)ESs involves the substitution of either the anionic or cationic components of H(D)ESs, contingent upon the ionic characteristics of target metals and the inherent features of anions or cations integrated into the structure of H(D)ESs. In general, due to the anionic nature of PGM-chloro complexes, as illustrated in Table 4, the anion exchange (AE) mechanism explains PGM extraction using ionic H(D)ESs [163].

In the process of AE, the negatively charged metal–ligand complex present in the aqueous phase interacts electrostatically with the cations of HBA, typically quaternary ammonium cations. This interaction facilitates the transfer of metal complex into the H(D)ES phase, replacing the anion of bulk solution (e.g., chloride anion), and establishing an ion pair with the cation. This mechanism relies on the nature of anions included in the ionic H(D)ESs; for instance, nitrates and halides, which display high hydrophilicity, are easily replaced by anionic metal-chloro complexes. In contrast, anions such as fluoride (e.g.,NTf_2^-) are highly hydrophobic and exhibit resistance to transfer to the aqueous phase [164]. The general reaction for AE mechanism is demonstrated in equation (11).

$$zA^-_{org} + [MX_n]^{z-}_{aq} \rightleftarrows [MX_n]^{z-}_{org} + zA^-_{aq} \tag{11}$$

where A^-_{org} and A^-_{aq} represent the anion of H(D)ES in the organic and aqueous phases, respectively, while $[MX_n]^{z-}_{aq}$ and $[MX_n]^{z-}_{org}$ denote the anionic metal–ligand complexes in the aqueous and H(D)ES phases, respectively.

By way of an example, using trioctylmethylammonium chloride ($[N_{8881}]Cl$):1-hexanol (1:1), the AE mechanism for extraction of Pd(II) relies on the nitrogen atom of HBA ($[[N_{8881}]Cl$) due to its strong positive charge, which allows the adsorption of $[PdCl_4]^{2-}_{aq}$ via electrostatic interaction. This process leads to the formation of ion pairs with $[N^+_{8881}]$ in the organic phase, as described in equation (12) [163].

$$2\left(C_6H_{13}OH\cdots Cl^-.N^+_{8881}\right)_{org} + [PdCl_4]^{2-}_{aq} \rightleftarrows \left[2C_6H_{13}OH\cdots PdCl_4^{\ 2-}.2N^+_{8881}\right]_{org} + 2Cl^-_{aq} \tag{12}$$

Another example of AE mechanism was observed in the extraction of Pt

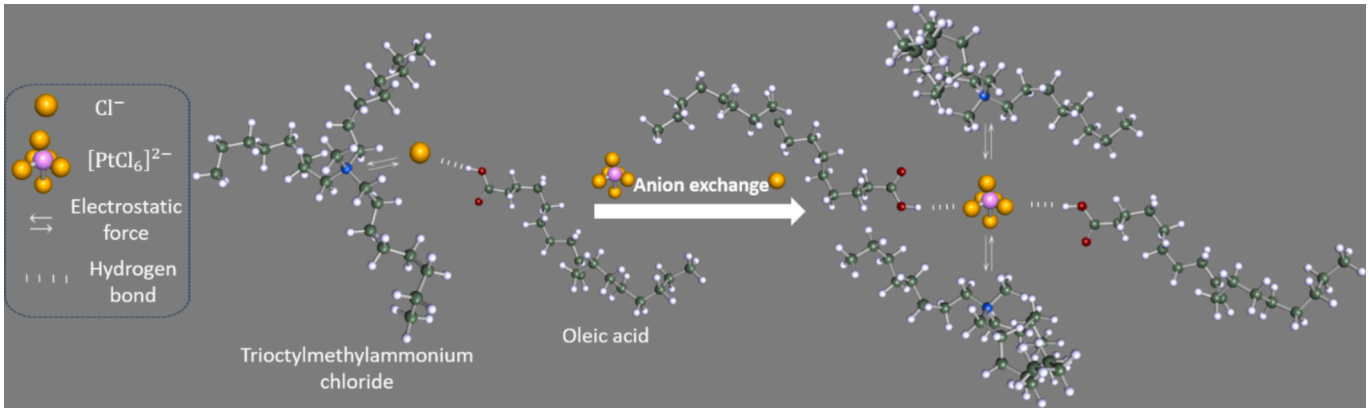

Fig. 11. Anion exchange mechanism of $[PtCl_6]^{2-}$ with $[N_{8881}]$Cl:OA ionic H(D)ES. Interpreted and adapted from Wang et al. [165].

(IV) using the ionic $[N_{8881}]$Cl:oleic acid (OA) (1:1), as detailed in equation (13). The corresponding reaction is illustrated in Fig. 11 [165].

$$2\left(C_{17}H_{33}COOH\cdots Cl^{-}.N^{+}_{8881}\right)_{org} + [PtCl_6]^{2-}_{aq} \rightleftarrows \left[2C_{17}H_{33}COOH\cdots PtCl_6^{2-}.2N^{+}_{8881}\right]_{org} + 2Cl^{-}_{aq} \quad (13)$$

As previously discussed, REEs typically do not form anionic chloro complexes like PGMs; therefore, the AE is not a viable extraction pathway for REEs using ionic H(D)ES. Despite the potential for AE, cation exchange (CE) mechanism is less common in metal extraction using H(D)ESs. This could be attributed to the strong hydrogen bond and/or electrostatic interaction within the components of H(D)ES. CE entails the exchange of the cationic part of H(D)ES phase with metal cation, while simultaneously forming ion pairs between metal cation and the anionic part of H(D)ES, typically deprotonated HBDs, in the H(D)ES phase. The utilisation of Lid:DecA(1:2) for extracting Pd(II) from acidic aqueous media through CE serves as a compelling demonstration [110]. This H(D)ES undergoes partial ionisation (approximately 25 % at around 22 °C) due to proton transfer from the functional group of DecA to Lid, resulting in the formation of $LidH^{+}$ and deprotonated DecA $(C_9H_{19}COO^{-})$ [166]. It was shown that upon Pd extraction into the H(D)ES phase, $LidH^{+}$ could interact with the chloride anion, forming $LidH^{+}Cl^{-}$ and being released to the aqueous phase due to its superior water solubility (50 mg.mL^{-1}) compared to Lid alone (0.41 mg.mL^{-1}) [90,110]. The proposed CE extraction mechanism was further validated using slope analysis, a common approach in the field of solvent extraction for estimating the number of extractant molecules or protons involved in the reaction. This method requires the conversion of metal extraction efficiency (EE) into metal distribution ratio (D), as defined in equations (14) – (16), and subsequently examining the correlation between log D and equilibrium pH and logarithmic concentration of H(D)ES. As shown in Fig. 12, the slope of log D *vs.* log [H(D)ES] was obtained at 1.8584, suggesting that approximately 2 molecules of H(D)ES were required for Pd extraction with the corresponding H(D)ES. Furthermore, the positive correlation between D and equilibrium pH after extraction suggests that the extraction reaction involved the CE between the Pd cations and protons, leading to the release of protons into the aqueous phase. Consequently, the CE mechanism of Pd(II) extraction with Lid:DecA can be described in equations (17) and (18) [110].

$$D = \frac{\text{concentration of metal in extract phase}}{\text{concentration of metal in raffinate phase}} \quad (14)$$

$$EE\,(\%) = \frac{\text{concentration of metal in extract phase}}{\text{concentration of metal in initial source}} \times 100\% \quad (15)$$

$$EE(\%) = \frac{D}{D+1} \times 100\% \quad (16)$$

$$(C_9H_{19}COOH)_{org} + Lid_{org} \rightleftarrows LidH^{+}_{org} + (C_9H_{19}COO^{-})_{org} \text{ (partial ionisation)} \quad (17)$$

$$\left((C_9H_{19}COOH)_2\cdots Lid\right)_{(D)ES} + 2LidH^{+}_{(D)ES} + 2(C_9H_{19}COO^{-})_{(D)ES} + [PdCl_4]^{2-}_{aq} \rightleftarrows \left[Pd(C_9H_{19}COO)_2(C_9H_{19}COOH)_2\cdots Lid\right]_{(D)ES} + 2(LidH^{+}Cl^{-})_{aq} + 2Cl^{-}_{aq} \quad (18)$$

The CE mechanism has also been evidenced in rare earth $\left(Gd^{3+}\right)$ extraction using non-ionic H(D)ES composed of diethyldodecanamide (DM):ibuprofen (Ibu) (3:1) through FT-IR analysis. The spectra showed a carboxylate (C = O) stretching vibration peak in the H(D)ES phase after REE extraction (vibration peak at 1731 cm^{-1} before extraction and 1573 cm^{-1} after extraction), highlighting the dominant role of Ibu as a carboxylic acid extractant for REE extraction [167]. On the other hand, research has shown that metal extraction using carboxylic acid

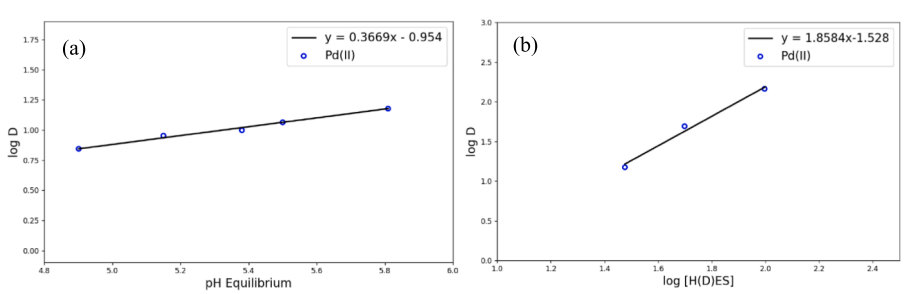

Fig. 12. Slope analysis (a) between log D and equilibrium pH, (b) between log D and H(D)ES concentration for Pd(II) extraction, adapted from Ola and Matsumoto [110].

extractants, referred to as $(HA)_2$ in equation (19), typically follows a CE mechanism [168]. The general reaction formula for rare earth extraction via CE corresponds to [167]:

$$RE^{3+}_{aq} + m\left((HA)_2\right)_{org} \rightleftarrows \left[REA_3(HA)_{2m-3}\right]_{org} + 3H^+_{aq} \quad (19)$$

Ion pair formation in aqueous phase mechanism

Ion pair (IP) formation in aqueous phase is another viable mechanism in metal extractions, particularly for anionic PGM-ligand species $\left([MX_n]^{z-}_{aq}\right)$, using ionic H(D)ES based on quaternary ammonium salts as HBA. A key characteristic of this mechanism is that ion pairing between $[MX_n]^{z-}_{aq}$ and the cation of ionic H(D)ES dissolved in the aqueous phase $\left(Cat^+_{aq}\right)$ occurs in the aqueous phase, after which the formed neutral complexes transition to the H(D)ES-rich phase, as described in equation (20) [92].

$$zCat^+_{aq} + [MX_n]^{z-}_{aq} \rightleftarrows \left[(Cat^+)_z.MX_n^{z-}\right]_{(D)ES} \quad (20)$$

In some cases, the combination of both AE and IP formation in the aqueous phase plays a role in extraction process. For instance, Zakusilova et al., proposed two mechanisms for extracting Ir(IV) from hydrochloric acid media using tetraheptylammonium chloride ($[N_{7777}]Cl$): DecA in (1:2) molar ratio. They developed a mathematical model to assess the extraction constants of both mechanisms, namely K_{IP} and K_{AE}. Their findings demonstrated that the predominant mechanism was IP formation in aqueous phase with $K_{IP} = (1.1 \pm 0.4) \times 10^8$, whereas AE was found to be negligible with $K_{AE} = (1.8 \pm 0.4) \times 10^{-5}$. As a result of IP formation in aqueous phase, a $[N_{7777}]_2[IrCl_6]_{(D)ES}$ complex was formed, as seen in equation (21) [92].

$$2\left[N^+_{7777}\right]_{aq} + [IrCl_6]^{2-}_{aq} \rightleftarrows [N_{7777}]_2[IrCl_6]_{(D)ES} \quad (21)$$

Nevertheless, this mechanism may not be applicable for REE extraction using ionic H(D)ESs, as explained earlier in the ion exchange mechanism subsection.

Neutral ion association mechanism

Neutral ion association (NIA) represents a fundamental mechanism for metal extraction using non-ionic H(D)ESs, wherein the target metal transfers into the H(D)ES phase to form a chemical entity. Vargas et al. tackled the elucidation of this mechanism for extraction of anionic PGM-chloro complexes using TOPO:DecA non-ionic H(D)ES [107]. Their research uncovered an interplay between the extraction mechanism and the hydrogen bond interactions among H(D)ES precursors. The extraction proceeded through NIA accompanied by the co-extraction of protons from HCl, resulting in the protonation of TOPO, as evidenced by a positive $\Delta\delta^{31}P$ shift in ^{31}P NMR spectra of TOPO:DecA when mixed with HCl. Accordingly, the hydrogen bond interaction between TOPO and DecA required some disruption to enable the formation of TOPO···H^+ adduct with an ionic hydrogen bond. This underscores the structural reorganisation of H(D)ES phase caused by acid co-extraction, leading to alteration of the eutectic composition towards lower TOPO concentrations since the number of available TOPO molecules to interact with DecA diminished. It was also suggested that while there is ongoing interest in discovering "deep" eutectic solvents, this deepness appears to limit the extraction mechanism if it is facilitated by hydrogen bond, owing to the higher energy barrier between HBA and HBD within deep eutectic solvents compared to eutectic solvents [107].

The extraction of Pt(IV) with Lid:Thy (1:1) is another example where the NIA mechanism was corroborated through UV–vis and FT-IR characterisation of H(D)ES and $[PtCl_6]^{2-}$ before and after operation, as shown in Fig. 13 (a) and (b). The UV–vis results indicate that the Pt speciation did not change due to the overlapping of its absorption wavelengths before and after extraction. Furthermore, the FT-IR analysis of Lid:Thy demonstrated a notable shift in the C –N stretching vibration peaks highlighting the dominant role of Lid in Pt extraction. The extraction mechanism is schematically described in Fig. 14 and formulated in equation (22) [109].

$$[C_{14}H_{22}N_2O\cdots HOC_{10}H_{13}]_{(D)ES} + [PtCl_6]^{2-}_{aq} + 2H^+_{aq} \rightleftarrows [C_{14}H_{24}N_2O][PtCl_6]_{(D)ES} + [C_{10}H_{13}OH]_{(D)ES} \quad (22)$$

Metal extraction in some cases may also encompass a combination of mechanisms at equilibrium. By way of an example, the extraction of anionic PGM-chloro complexes using TOPO:DecA at different molar ratios and concentrations of HCl was studied. This highlights the adaptability of the non-ionic H(D)ES, where each precursor played a pivotal role in selectively extracting PGM from acidic media depending on acid concentration, type of metal complex, and the composition of H(D)ES. Based on UV–vis analysis of the extract phase, two extraction mechanisms were identified. At low acid concentrations, extraction was facilitated by CE with DecA, emphasising the role of acidic extractant. Conversely, under highly acidic conditions, extraction proceeded through NIA, where TOPO functioned as a solvating extractant for PGM extraction into H(D)ES phase [112].

The NIA mechanism was also identified in REE extraction using non-ionic H(D)ES. The extraction mechanism was analysed from aqueous solutions of HCl using ternary non-ionic H(D)ES composed of Bis(2-ethylhexyl) amine (BEA):OA:1-decanol (Dec) (5:1:9). Although the studied H(D)ES is non-ionic in nature, it is partially ionised to $BEAH^+$ and deprotonated OA ($C_{17}H_{33}COO^-$), as illustrated in equation (23), due to the proton transfer from the carboxylic functional group of OA to the amino group of BEA, similar to the case of Lid:DecA described earlier [169,170].

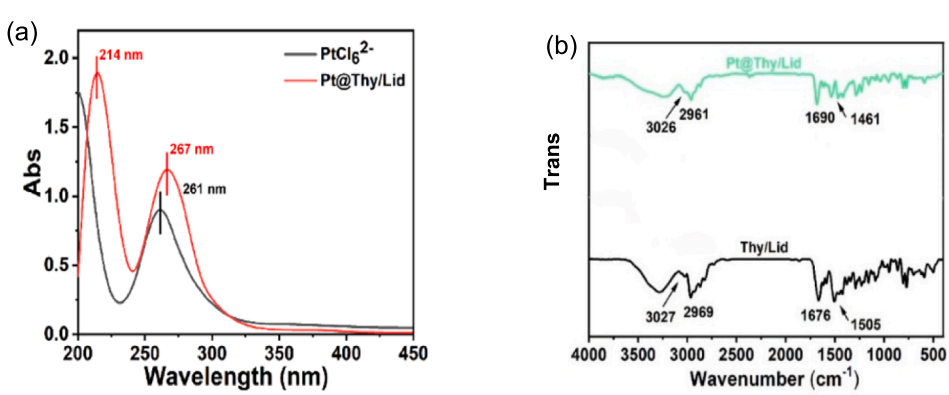

Fig. 13. (a) UV–vis absorption spectra of $[PtCl_6]^{2-}$ before and after extraction using Lid:Thy H(D)ES. Reprint with permission from [109], (b) FT-IR analysis of Lid:Thy H(D)ES before and after Pt extraction. Reprinted with permission from Elsevier [109].

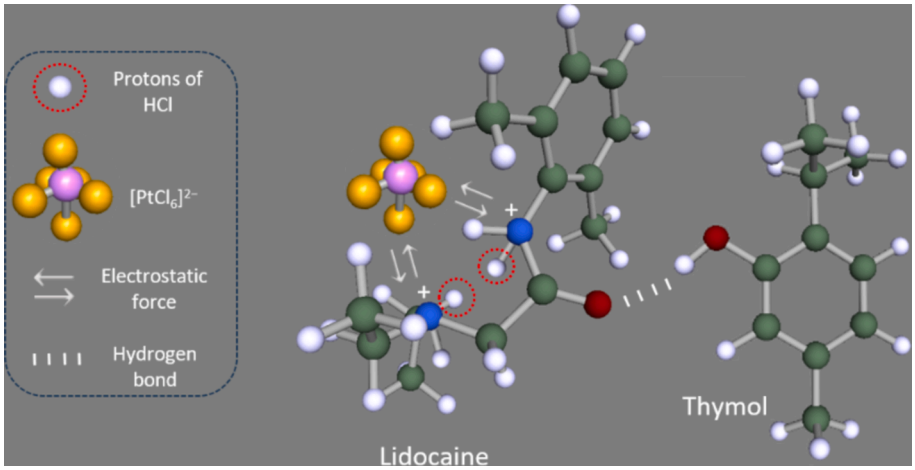

Fig. 14. Schematic representation of the NIA mechanism of $[PtCl_6]^{2-}$ with non-ionic H(D)ES Lid:Thy as interpreted from the findings and discussion of Liu et al. [109].

$$(C_{17}H_{33}COOH) + BEA + C_{10}OH \rightleftarrows [C_{10}OH\cdots BEAH^{+}\cdots C_{17}H_{33}COO^{-}]_{(D)ES} \quad (23)$$

Slope analysis was employed to determine the stoichiometric ratio of RE^{3+} and Cl^{-} loaded into the H(D)ES phase. The results of slope analysis for Dy^{3+} and Ho^{3+}, as representatives for REEs, were 2.14 and 2.63, respectively, suggesting the occurrence of more than one mechanism for REE extraction using the studied H(D)ES. Based on the nature of employed H(D)ES and the principal of electrical neutrality, when stoichiometric ratio was 3, the mechanism followed NIA, while at a stoichiometric ratio of 2, extraction proceeded through CE as evidenced by monitoring total nitrogen (TN) and total organic carbon (TOC) levels in the raffinate phase in proportion to the concentration of REEs extracted into the H(D)ES phase. Hence, it was inferred that NIA and partial CE reactions proceeded concomitantly during the extraction of RE^{3+} with the studied H(D)ES, as depicted in equations (24) and (25), respectively [170].

It is noteworthy that REE extraction using non-ionic H(D)ESs through NIA does not involve acid co-extraction due to the following reasons: (i) REEs do not exist in anionic speciation in the aqueous phase, (ii) REEs remain in their cationic form in the presence of soft or intermediate ligands like chloride or nitrate anions at low temperature and solvent extraction typically operate at room temperature [105,160].

$$RE^{3+}_{aq} + 3Cl^{-}_{aq} + [C_{10}OH\cdots BEAH^{+}\cdots C_{17}H_{33}COO^{-}]_{(D)ES} \rightleftarrows [C_{10}OH\cdots BEA\cdots HCl\cdots RECl_2C_{17}H_{33}COO^{-}]_{(D)ES} \quad (24)$$

$$RE^{3+}_{aq} + 2Cl^{-}_{aq} + [C_{10}OH\cdots BEAH^{+}\cdots C_{17}H_{33}COO^{-}]_{(D)ES} \rightleftarrows [C_{10}OH\cdots RECl_2C_{17}H_{33}COOH]_{(D)ES} + (BEAH^{+})_{aq} \quad (25)$$

Despite the identification of several extraction mechanisms, including AE, CE, IP formation in aqueous phases, and NIA, the extraction process using H(D)ES systems remains intricate and require further research. An in-depth comprehension of the SX mechanisms of PGMs and REEs utilising H(D)ESs can lay the foundation for designing novel (H)DESs, aiming at more improvement in the performance and sustainability of the separation processes, making them suitable for industrial applications.

3.2.2. Survey of studies on PGM and REE extraction using (D)ESs

(D)ESs are employed not only in leaching step but also in solvent extraction processes of PGMs and REEs and it is important to analyse the techniques, operational conditions, separation efficiencies, selectivity, solvent recyclability and reusability.

Accurate determination of metal elements in environmental samples is essential for assessing their environmental impact and economic viability for separation. However, direct detection is challenging due to ultra-low concentrations and intricate sample compositions with competing ions. Consequently, selective extraction and preconcentration are often necessary before quantification via techniques like flame atomic absorption spectroscopy (FAAS) [171]. Several studies have examined the potential of (D)ESs for the microextraction and determination of Pd, as summarised in Table 5, confirming the effectiveness of the proposed procedures by achieving a high preconcentration factor (PF) and recovery efficiency under slightly acid conditions within a very short period of time.

H(D)ESs have been applied in SX processes to recover PGMs and REEs from single-element and multi-component acidic leaching solution of secondary resources. As previously noted, HCl solutions are commonly used leaching agents in metallurgy. Consequently, metal extraction from HCl solution serves as a practical model [175]. Several studies investigated PGM extraction from model solution using ionic and non-ionic H(D)ESs. For instance, ionic H(D)ESs consisting of $[N_{8881}]Cl$ and saturated carboxylic acids/alcohols, including hexanoic acid (HexA) and 1-hexanol, was utilised to extract Pd(II) from a model HCl solution containing low concentrations of metal impurities such as Cr, Fe, Ni, and Cu [163]. The study considered the effect of pH since it determines the type of Pd speciation in the aqueous phase and, thus; affects its EE [176]. It was demonstrated that under basic conditions, $[PdCl_3(OH)]^{2-}$ was the predominant speciation for Pd, exhibiting high hydrophilicity. In contrast, at lower pH (pH = 1), it commonly exists in the form of $[PdCl_4]^{2-}$, which results in a higher Pd distribution into the H(D)ES phase. It was also found that with an increase in initial Pd concentration, the EE experienced an upward trend, which could be attributed to the proposed AE mechanism within this system. Furthermore, employing 0.5 mL of hydrazine hydrate (80 wt%) facilitated over 99 % Pd recovery from the loaded H(D)ES. The study also underscored the high reusability of the H(D)ES, maintaining extractions above 96 % even after five cycles

Table 5
Summary of studies on the use of (D)ESs for microextraction in environmental sample analysis.

Metal	(D)ES HBA:HBD(s) molar ratio	Extraction Conditions Initial metal concentration ($\mu g.L^{-1}$)	Time (min)	Organic-to-aqueous phase ratio [a] ($mL.mL^{-1}$)	pH	Main results	Ref.
Pd(II)	ChCl:phenol (1:4)	10	7	1:70	5	PF [b] = 70 LOD [c] = 4.0 $\mu g.L^{-1}$ LOQ [d] = 1.2 $\mu g.L^{-1}$ RSD [e] = 3.6 %R% ≥ 98 %	[172]
Pd(II)	Hydroxyl ammonium chloride:phenol:disodium 4,5-dihydroxy-1,3-benzenedisulfonate:$FeCl_3$ (1:1:1:2)	30	1	1:350	6	PF = 116 LOD = 1.18 $\mu g.L^{-1}$ LOQ = 3.45 $\mu g.L^{-1}$ RSD = 2.3 %R% ≥ 92 %	[173]
Pd(II)	Menthol:phenyl salicylate (1:1)	1	3	1:166.67	4	PF = 191 LOD = 0.03 $\mu g{\cdot}L^{-1}$ LOQ = 0.10 $\mu g{\cdot}L^{-1}$ RSD = 4.6 % R% > 95.1 %	[174]

[a] (D)ES-to-metal solution volumetric phase ratio,
[b] Preconcentration Factor,
[c] Limit of Detection,
[d] Limit of Quantification,
[e] Relative Standard Deviation.

[163]. In another study, the effectiveness of non-ionic H(D)ESs based on TOPO combined with 1-hexanol, 1-butanol, and L-menthol for Pt(IV) extraction from model HCl solution was assessed [177]. The findings revealed a positive correlation between HCl concentration and Pt EE, attributed to the proposed NIA mechanism, where protonated TOPO interacted with $[PtCl_6]^{2-}$. The influence of salinity on Pt EE was also investigated, showing that increasing NaCl concentration mirrored the trend observed with HCl concentration. This was primarily due to the common-ion effect [178,179], which promoted the formation of $[PtCl_6]^{2-}$, and the salting-out effect [180], which reduced Pt hydration and enhanced its interaction with the H(D)ES. Further corroboration came from examining the impact of increasing NaBr concentration, demonstrating a slight increase in Pt EE compared to NaCl. This was ascribed to the absence of the common-ion effect, highlighting the sole contribution of the salting-out effect. Under optimised experimental conditions of high acidity (pH = 0) and salinity ([NaCl] = 3 $mol.L^{-1}$), the highest Pt EE of 98.7 % was achieved with TOPO:1-butanol (But) (1:1). Moreover, it was established that Pt could be completely re-extracted from the loaded H(D)ES using 0.5 $mol{\cdot}L^{-1}$ NaOH, and the recycled H(D)ES was successfully reutilised across 4 separation cycles [177]. Schaeffer et al. carried out a significant study on the selective extraction of Pt(IV) and Pd(II) from HCl model solution containing transition metal ions (TMs), such as Fe, Cu, Co, Ni, and Cr, using TOPO:Thy (1:1) non-ionic H(D)ES [112]. A compromise between distribution ratio and selectivity was observed. Although the highest distribution ratios were obtained at high HCl concentrations (≥ 2 $mol.L^{-1}$), the highest selectivity for Pt and Pd over TMs was achieved at low HCl concentration ([HCl] < 1 $mol.L^{-1}$), facilitating the selective recovery of PGMs from complex matrices with very fast kinetics (5-min mixing time). Furthermore, a separation factor ($SF_{Pt/Pd}$) of approximately 5 indicated the potential for separating Pt from Pd. The versatility of TOPO-based H(D)ESs was also highlighted by their successful application as a template for the valorisation of Pd nanoparticles through the addition of 0.1 $mol.L^{-1}$ sodium acetate [112]. The study on TOPO-based H(D)ESs for Pt(IV) and Pd(II) extraction from model solution was continued by Vargas et al., where they specifically focused on the selective separation of Pt from Pd [107]. It was found that EE and selectivity exhibited considerable variation, influenced by the nature and stoichiometry of H(D)ES precursors and HCl concentration. To illustrate this further, at a low HCl concentration of 2 $mol.L^{-1}$ in TOPO:DecA, a decrease in EE of both Pt and Pd was observed when the TOPO molar ratio (x_{TOPO}) was reduced from 0.5 to 0.3. However, at a high HCl concentration of 8 $mol.L^{-1}$, the degree of reduction varied, with EE_{Pt}% remaining nearly constant, while EE_{Pd}% dramatically decreased from 82.1 % at x_{TOPO} = 0.5 to 34.2 % at x_{TOPO} = 0.3, facilitating the selective extraction of Pt from Pd. On the other hand, in TOPO:Thy, a different extraction behaviour was observed since the highest selectivity for Pt over Pd ($SF_{Pt/Pd}$ = 38.4) was obtained at a low HCl concentration of 2 $mol.L^{-1}$ and x_{TOPO} = 0.4. These results highlight the non-linear and highly complex extraction behaviour of non-ionic type V H(D)ESs, which remain poorly understood and necessitates further research and exploration [107].

The research on Pt and Pd extraction was extended to encompass THE(D)ES including Lid:Thy (1:1) H(D)ES [109]. It was demonstrated that selective extraction could be achieved by tuning the acidity of the aqueous solution as increasing the HCl concentration led to the varying levels of reduction in EE. This reduction was attributed to the competition between chloride anions and anionic Pt-chloro complexes. At HCl concentration ranging from 2 to 3 $mol.L^{-1}$, the EE for Au remained high at 98.5 %, while those for Pt and Pd sharply declined to 6.2 % and 0.3 %, respectively, allowing the selective separation of Au from the model solution. Subsequently, the selective extraction of Pt and Pd from the remaining solution was obtained by lowering the HCl concentration ranging from 0.25 to 0.5 $mol.L^{-1}$, achieving EE of 99.9 % for Pt and 89.5 % for Pd. It was also shown that controlling the acidity would be beneficial for the selective re-extraction of the metals loaded into the H(D)ES phase using KSCN as stripping reagent. The regenerated H(D)ES maintained its stability and EE for Pt and Pd but experienced a loss in efficiency for Au due to its high acidity operating conditions [109]. The effectiveness of Lid-based H(D)ES for the separation of Pd (II), Pt(IV) and Au(III) from an acidic model leaching solution was extended by Ola and Matsumoto [110]. Their findings agreed with previous study, illustrating that under high acidity (pH = 1), Au was selectively extracted with an efficiency of 98.2 % using Lid:DecA (1:2), while Pd was completely separated at low acidity (pH = 4.4) with negligible EE for Pt (< 9 %). The analysis of EE *vs.* mixing time demonstrated that a relatively long stirring duration of 180 min (three times longer than the process with Lid:Thy) was required to achieve equilibrium. The extraction behaviour of Lid:DecA for Pd was explained by CE mechanism in which distribution ratio has a positive correlation with pH. Therefore, it can be concluded that for metal extraction with H(D)ESs via CE mechanism, higher pH levels are advantageous [90,110]. However, a substantial rise in pH may cause metal hydroxide precipitation, leading

to a reduction in EE [172,181]. Therefore, an optimum pH value should be found for metal extraction using H(D)ESs.

In further studies with other PGMs, the extraction of Ir(IV) and Rh (III) was assessed from model solutions of HCl with the ionic H(D)ES composed of tetraheptylammonium chloride ($[N_{7777}]Cl$):DecA (1:1) [92]. Selective extraction of Ir over Rh with the highest SF of approximately 20 was reached at 0.4 mol.L^{-1} HCl concentration within only 1 min, indicating a very quick and efficient extraction potential of the H (D)ES for Ir. The selective Ir extraction was attributed to the lower charge density and weaker hydration of $[IrCl_6]^{2-}$ compared to $[RhCl_6]^{3-}$ [182,183]. The influence of HCl concentration revealed that an increased concentration of chloride ions led to a reduction in the solubility of $[N_{7777}]Cl$ in the aqueous phase, aligning with Le Chatelier's principle [184]. Since the solubility of $[N_{7777}]Cl$ is crucial for the IP mechanism, this reduction consequently decreased the EE [92]. The use of quaternary ammonium-based H(D)ESs was further extended to Pt (IV), Ir(IV), Ru(III), and Rh(III) extraction using $[N_{8881}]Cl$:oleic acid (OA) (1:1) from industrial wastewater under highly acidic conditions (pH = 1) [165]. The low EE of Rh(III) was attributed to its speciation and structure, primarily existing in the form of octahedral $RhCl_6^{3-}$ and $RhCl_5(H_2O)^{2-}$ [183]. The H(D)ES confirmed outstanding reusability and stability over five extraction-stripping cycles, maintaining EE higher than 90 % for Ru, Ir, and Pt. For Rh, an increasing trend in extraction percentage was observed, likely due to the residual ascorbic acid (AsA) from previous stripping procedures, as demonstrated in Fig. 15. AsA played a dual role as a component of stripping agent for Pt(IV) re-extraction and as a reducing agent for Rh(III) to convert it into a more soluble form of Rh(I) [165,185].

The only study addressing the extraction of all critical PGMs employed H(D)ESs composed of tetrabutylammonium bromide ($[N_{4444}]Br$) and tetraoctylammonium bromide ($[N_{8888}]Br$) as HBA and hexanoic, octanoic, nonanoic acids as HBDs in 1:2 stoichiometric ratios from HCl model solution [175]. They found that longer alkyl chains in HBA increased hydrophobicity and stability, thereby enhancing metal recovery. Conversely, HBDs with shorter alkyl chains exhibited more efficiency, particularly for inert PGMs like Ir and Rh. Therefore,$[N_{8888}]Br$:HexA (1:2) was identified as the optimum solvent.. Although excellent re-extraction of PGMs was achieved using 1 mol.L^{-1} thiourea in 0.5 mol.L^{-1} HCl, with high recovery efficiencies, individual separation of PGMs was not feasible. The developed method was applied for PGM extraction from refinery wastewater but under different operational conditions since only Pt and Pd were targeted metals for extraction. The method achieved quantitative extraction of Pt and Pd (> 99 %) while exhibiting very low EE for metal impurities (< 10 %) and inert PGMs (< 5 %), highlighting the potential of H(D)ESs for Pt and Pd extraction [175].

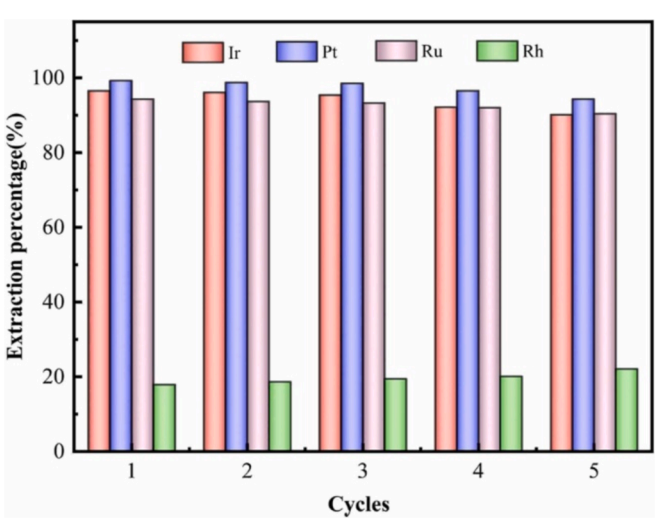

Fig. 15. Reutilisation of $[N_{8881}]Cl$:oleic acid (1:1) H(D)ES for Pt(IV), Ir(IV), Ru (III), and Rh(III) extraction across 5 cycles. Reprinted with permission from Elsevier [165].

Several studies have demonstrated the effective application of H(D) ESs in the extraction of REEs. A comprehensive study was conducted on the REE extraction from model solution of spent magnets leachate utilising $[N_{8881}]Cl$:Gly (1:2) diluted in kerosene [186]. This study focused on the operating conditions to assess the extraction of various rare earth ions by adjusting mixing time, O/A volumetric ratio, and $NaNO_3$ concentration as a salting-out agent. To further illustrate, the selective extraction of Nd(III) with an EE of 93.8 % and $SF_{Nd/Fe}$ of 381.29 was achieved from a simulated solution of spent NdFeB magnet in nitrate medium under the operational conditions of pH = 2, O/A ratio = 2:1, time = 5 min, and $[NaNO_3]$ = 3.5 mol.L^{-1}. In another case, the selective extraction of Sm(III) with 93.6 % efficiency and nearly zero efficiency for Co was realised under pH = 2, O/A = 4:1, time = 15 min, and [NaNO3] = 2 mol.L^{-1}. This further highlights the higher selectivity of the studied H(D)ES for Lns over TMs. Furthermore, the complete re-extraction of REEs from loaded H(D)ES phase using 0.6 mol.L^{-1} HCl solution was obtained [186]. The selective extraction of Sm(III) from a synthetic solution of SmCo magnet leachate using a non-ionic H(D)ES consisting of TOPO:doedecanol (Dodec) (1:2) was investigated. The extraction process achieved over 99 % efficiency for both Sm and Fe, with minimal co-extraction of Co and Cu from the magnet waste leachate. It is worth noting that another H(D)ES composed of DecA: lauric acid (LA) (2:1) was proposed for the selective extraction of Cu from Co in the raffinate, highlighting that adjusting the compositions of H(D)ESs can successfully tune the selectivity towards various target metals [104]. Yu et al. continued the research on the extraction of REEs, including Nd(III), Dy(III), and Pr(III), from a nitrate solution of spent NdFeB magnet by utilising a ternary H(D)ES composed of TOPO:1-tridecanol (Tdec):Dec in a 4:5:5 ratio It was also demonstrated that increasing the HNO_3 concentration adversely affects the REE EE due to the competition between protons (H^+) and RE^{3+}, as the NIA mechanism for REEs is not mediated by the protonation of TOPO, unlike in the NIA mechanism for PGMs [105].

The similar chemical characteristics of REEs lead to slight variations in the ligand binding energies of adjacent Ln^{3+} ions (below 6.5 kJ.mol^{-1}), making their mutual separation challenging [187]. A detailed study on Ln extraction from nitrate solution using non-ionic TOPO:DecA (1:1) was conducted [188]. They observed a similar trade-off between D and SF as noted in the previously referenced study [107]. The TOPO: DecA (1:1) system exhibited the greatest D_{Ln} under low acidic conditions ($[HNO_3]$ = 0.5 − 1.0 mol.L^{-1}), with a notable selectivity for Eu over its adjacent Gd ($SF_{Eu/Gd}$ = 1.8), as depicted in Fig. 16. However, as acidity increased and x_{TOPO} decreased, the D_{Ln} in different levels dropped. A notable reduction was observed for light and middle Lns, resulting in a shift in selectivity towards heavy Lns, as evidenced by $SF_{Lu/La}$ = 115 under HNO_3 concentration of 4.0 mol.L^{-1}. To elucidate the extraction behaviour of the H(D)ES for Lns, time-resolved fluorescence spectroscopy (TRFS), Raman spectroscopy, and small-angle X-ray scattering (SAXS) were employed. The changes observed were attributed to the H (D)ES phase structuration and reorganisation, though this mechanism remains unclear. Therefore, an in-depth investigation in this context is necessary. Moreover, the stripping procedure to selectively recover Lns from the loaded H(D)ES phase was not addressed. Comprehensive experimental investigations are required to establish suitable conditions that will enable the mutual separation of heavy Lns with high efficiency and purity [188].

The separation of Y(III) from HREEs co-existing in ion-adsorbed rare earth minerals presents significant challenges owing to their similar chemical properties and ionic radii [189,190]. To address this, ternary H (D)ESs composed of bis(2-ethylhexyl) amine (BEA):OA:DL, as well as their pure precursors, were employed as extractants [170]. The results demonstrated nearly zero EE with the sole HBA and HBD, indicating synergistic effects between H(D)ES components. Furthermore, the

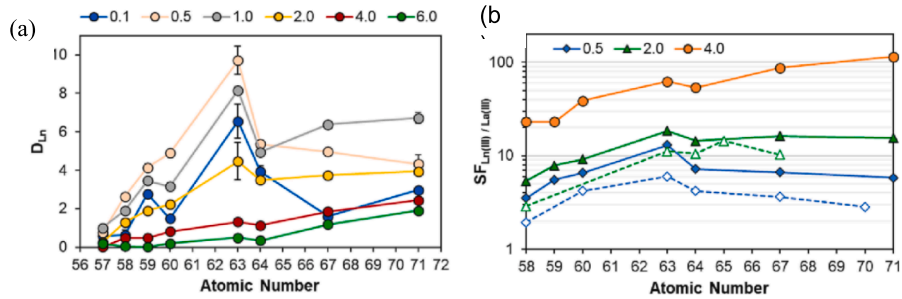

Fig. 16. (a) Lanthanide distribution ratios (D_{Ln}) as a function of atomic number and HNO_3 concentration, (b) separation factors of lanthanides over La ($SF_{Ln(III)/La(III)}$) as a function of atomic number and HNO_3 concentration (full lines) and compared with conventional extraction utilising TOPO alone (dashed lines). Reprinted with permission from Elsevier [188].

inclusion of Dec as a third component significantly influenced EE and selectivity. It was found that increasing the molar composition of DL resulted in varying degrees of decline in EE; however, it remained above 35 % for HREEs, thereby enhancing selectivity toward HREEs. To assess the applicability of the developed method for industrial applications, the extraction of HREEs (Dy-Lu) and Y from a Y-concentrated industrial solution was tested. The results demonstrated promising performance of the ternary H(D)ES, indicating a trend of increasing EE% and SF with the atomic number [170].

A summary of the previously described studies on the application of H(D)ESs in PGM and REE in LLX is presented in Table 6.

As per the studies summarised above, H(D)ESs offer high extraction loading and capacity, exceptional selectivity for target metals, and promising recyclability and reusability. Additionally, H(D)ESs eliminate the need for complexing agents and, in most cases, organic solvents, as well as prevent the formation of a third phase during extraction. However, most studies have been conducted on model solutions, and the application of H(D)ESs on PGM and REE separation and recovery from real samples is notably scarce. While studying model solutions is crucial for understanding the complex behaviour of H(D)ESs and optimising extraction conditions, further investigation in real samples is needed.

3.3. An overall framework for the circularity of metal separation and recovery

Based on the mechanisms and practical methodologies discussed in Sections 3.1 and 3.2 regarding the application of (D)ESs in the leaching and solvent extraction of PGMs and REEs, here we propose a circular (D)ES-based solvometallurgical flowsheet, illustrated in Fig. 17. Given the complex composition of PGM/REE-bearing samples, separation and recovery typically starts with pre-treatment processes designed to remove unwanted components and enhance leachability. Following pre-treatment, the sample undergoes solvometallurgical processing, which consists of three main steps. The first step is leaching, where hydrophilic (D)ESs serve as leaching reagents, often in combination with additives such as oxidising agents or reducing agents, to selectively dissolve metal ions from metal substrate. This step enables the efficient extraction of target metals into the leachate. The second step is purification via solvent extraction processes, wherein hydrophobic (D)ESs are employed as extractants to selectively separate target metal ions from the metal-loaded leachate. In cases where the solvent exhibits high viscosity, diluents such as kerosene, toluene, or *n*-heptane are often added to enhance mass transfer and improve the overall extraction efficiency of PGMs and REEs. The final step is metal recovery, achieved through sequential approaches tailored to the composition of the extract phase and the desired metal purity. These include scrubbing of impurities using reagents such as calcium chloride, water, or ethanol, followed by stripping with acidic or alkaline solutions. The stripping process achieves two objectives: (i) the separation of target metals from the extract phase and (ii) the regeneration of the (D)ES for subsequent separation cycles. Depending on the extraction mechanism, the used H(D)ES typically requires a replenishment or makeup stream owing to losses along the process. For instance, in the case of an anion exchange (AE) mechanism utilising quaternary ammonium chloride-based H(D)ES, chloride ions may need to be added. Similarly, for Lid-based H(D)ESs, the addition of HBA may be necessary to maintain the extraction system's efficiency [90,165]. The metal-rich strip phase is then subjected to precipitation, commonly using complexing agents like oxalic acid to form metal oxalates, which are subsequently calcined at high temperature to yield high-purity PGM or REE oxides. However, it is pertinent to state that there is evidence suggesting that applying H(D)ESs as lixiviants in direct non-aqueous leaching of PGMs and REEs could be economically and environmentally beneficial as it reduces the number of purification steps, particularly the SX step [93,140].

3.4. Process intensification strategies for metal separation and recovery

In response to the growing focus on green process intensification, there is an emphasis on the enhancement of traditional separation methods with more energy efficient alternatives, such as applying ultrasound and microwave-assisted methods [194]. Both have been reported in metal separation [195,196]. For instance, the influence of ultrasound on the leaching of Ni and Cu from a printed circuit board (PCB) utilising hydrophilic $CaCl_2{\cdot}6H_2O$:EG (1:1) was explored. The research demonstrated that, despite the high viscosity of solvent, the application of high-power ultrasound enabled the rapid separation of metals from PCB [197]. The application of ultrasound was also studied in solvent extraction of Ni with Lix 65 N and Lix 70 as extractants, revealing a four- to seven-fold increase in the EE with respect to conventional LLX. This enhancement could be attributed to increased interfacial area and, thus, mass transfer resulting from ultrasonication [198]. Microwave heating facilitates rapid and uniform heating, improving the separation efficiency [199]. The application of microwave heating in the leaching of PGMs from SAC using *aqua regia* as a lixiviant was studied, demonstrating a significant enhancement in the leachability, achieving a yield of 98.3 % within only 5 min, while the conventional acid leaching process required approximately 2.5 h to attain a leaching efficiency of 96.5 % [200]. Microwave irradiation was also utilised for inert PGM extraction from HNO_3 leachate using [Hbet][Tf_2N]. The study demonstrated that SX with the aid of microwave irradiation at 200 W for 80 s resulted in EE of 97.2 % for Ru(III) and 91.5 % for Rh(III). In contrast, conventional SX approach achieved lower efficiencies of 79.4 % for Ru(III) and 77.4 % for Rh(III) over an extended period of 52 h [47]. Considering the previously stated premises, there is a clear gap within the existing body of knowledge regarding the application of ultrasound and microwave for PGM and REE separation from secondary resources using (D)ESs, suggesting several pathways for future investigation.

Table 6
Compilation and summary of the most relevant studies on the application of H(D)ESs for LLX of PGMs and REEs from leachates and model solutions.

Metal	H(D)ES HBA:HBD(s) Molar ratio	Extraction Conditions Initial metal concentration (mmol. L^{-1})	Time (min)	Organic-to-aqueous phase ratio	pH	Main results	Ref.
Pd(II)	1,10-phenanthroline: Thy (1:4)	20.00	1	1:2 $mL.mL^{-1}$	1.30[a]	$EE_{Pd}\%^{+}$ = 99.92 %, D_{Pd}^{+} = 2502.5	[191]
Pd(II)	$[N_{8881}]$Cl:HexA (1:2)	0.94 $^{+}$ 0.20 *	20	1:100 $g.mL^{-1}$	1.00[a]	$EE_{Pd}\%^{+}$ = 99.96 % $EE_{Pd}\%^{*}$ = 99.34 % $S_{Pd}\%$ > 99 %	[163]
Pt(IV)	TOPO:But (1:1)	5.60 $^{+}$ 3.00 *	60	1:71.43 $g.mL^{-1}$	0.00[a]	$EE_{Pt}\%^{+}$ = 98.9 %, $EE_{Pt}\%^{*}$ = 95.6 %, EE % of other metal impurities* < 13 %	[177]
Pt(IV), Pd(II)	TOPO:Thy (1:1)	2.00 each	5	1:2 $mL.mL^{-1}$	≤ − 0.30[a] for maximum D ≥ 0.00[a] for maximum SF	D_{Pt}^{+} = 327, D_{Pd}^{+} = 18.2 D_{Pt}^{*}= 16.62, D_{Pd}^{*}= 3.4, D_{TMs}^{*} < 0.01, $SF_{Pd/Pt}^{*}$ = 0.2 $S_{Pd}\%^{*}$ = 96 %	[112]
Pt(IV), Pd(II)	TOPO:Thy (2:3)	2.00 each	1	1:2 $mL.mL^{-1}$	− 0.30[a]	$EE_{Pt}\%^{*}$ = 63.10 %, D_{Pt}^{*} = 1.7, $EE_{Pd}\%^{*}$ = 4.26 %, D_{Pd}^{*} = 0.04, $SF_{Pt/Pd}^{*}$ = 38.41 S_{Pt} = 100 %, $S_{Pd}\%$ = 100 %	[107]
Pd(II), Pt(IV), Au (III)	Lid:Thy (1:1)	1.00 each	60	1:30 $g.mL^{-1}$	− 0.48 to − 0.30[a] for Au 0.60 to 0.30[a] for Pt and Pd	D_{Pt}^{+} = 327, D_{Pd}^{+} = 18.2 D_{Pt}^{*} = 16.62, D_{Pd}^{*} = 3.4, D_{TMs}^{*} < 0.01, $SF_{Pd/Pt}^{*}$ = 0.2 $S_{Pd}\%^{*}$ = 96 %	[109]
Pd(II), Pt(IV), Au (III)	Lid:DecA (1:2)	10.00 *	180	1:1 $mL.mL^{-1}$	1.00[a] for Au 4.40[a] for Pd(II)	$EE_{Au}\%^{*}$= 98.2 %, DAu = 55.7, $EE_{Pt}\%^{*}$ < 9 %, $EE_{Pd}\%^{*}$ = 100 % D_{Pd}^{*} = ∞ due to the equilibrium concentration of metal in aqueous phase was not detectable through ICP-AES analysis.	[110]
Ir(IV), Rh(III)	$[N_{7777}]$Cl:DecA (1:2)	0.01 for Rh,0.05 for Ir	1	1:13.4 $mL.mL^{-1}$	0.40[a]	D_{Ir}^{*} ≈ 63, D_{Rh}^{*} ≈ 11, $SF_{Ir/Rh}^{*}$= 20	[92]
Ir (IV), Pt(IV), Ru (III), Rh(III)	$[N_{8881}]$Cl:OA (1:1)	2.36 for Pt(IV), 2.95 for Ir (IV),5.25 for Ru(III), and 2.11 for Rh (III)	5	1:1 $mL.mL^{-1}$	1.00[a]	$EE_{Ir}\%^{*}$ = 97.57 %, $EE_{Pt}\%^{*}$ = 99.55 %, $EE_{Ru}\%^{*}$ = 94.26 %, $EE_{Rh}\%^{*}$ = 15.10 % $S_{Pt}\%^{*}$ = 99.8 %, $S_{Ir}\%^{*}$ = 97.3 %, $S_{Ru}\%^{*}$ = 98.9 %, $S_{Rh}\%^{*}$ = 96.3 %	[165]
PGMs	$[N_{8888}]$Br:HexA (1:2) $[N_{8888}]$Br: octanoic acid(1:2) for wastewater	0.05 for Pt(IV), 0.09 for Pd(II), 0.05 for Ir (IV),0.10 for Rh(III), 0.10 for Ru (III)	30 10 for wastewater	1:100 $g.mL^{-1}$ 1:1000 $g.mL^{-1}$ for wastewater	1.00[a] − 0.48[a] for wastewater	From model solution: $EE_{Pt}\%^{*}$ > 99.7 %, $EE_{Pd}\%^{*}$ > 99.7 %, $EE_{Ru}\%^{*}$ = 87.3 %, $EE_{Ir}\%^{*}$ = 45.1 %, $EE_{Rh}\%^{*}$ = 28.5 % $S_{Pt}\%^{*}$ = 79.5 %, $S_{Pd}\%^{*}$ = 99.4 %, $S_{Ru}\%^{*}$ = 98.7 %, $S_{Ir}\%^{*}$ = 54.7 %, $S_{Rh}\%^{*}$ = 92.2 % From platinum refinery wastewater: $EE_{Pd}\%^{*}$ = 99.7 %, $EE_{Pt}\%^{*}$ = 99.9 %. $S_{Pd}\%^{*}$ = 99.9 %, $S_{Pt}\%^{*}$ = 99.5 %, $P_{Pd}\%$ and $P_{Pt}\%$ = 99.9 %	[175]
Nd(III)	$[N_{8881}]$Cl:Gly (1:2)	60.45	5	1:0.50 $mL.mL^{-1}$	2.00[b]	$EE_{Nd}\%^{*}$ = 93.8 %, D_{Nd}^{*} =5.172 $S_{Nd}\%^{*}$ = 100 %	[186]
Sm(III)	$[N_{8881}]$Cl:Gly (1:2)	202.18	15	1:0.25 $mL.mL^{-1}$	2.00[b]	$EE_{Sm}\%^{*}$ = 93.6 % $S_{Sm}\%^{*}$ = 100 %	[186]
Sm(III)	TOPO:Dodec (1:2)	49.68	20	1:0.25 $mL.mL^{-1}$	1.60[b]	$EE_{Sm}\%^{*}$ > 90 % $S_{Sm}\%^{*}$ = 99 %, $P_{Sm}\%$ ≥ 98.50 %	[104]
Cerium (III)	TOPO:propanol (1:1)	30.00	15	1:1 $mL.mL^{-1}$	NA	$EE_{Ce}\%^{+}$ = 93.8 %	[192]
Nd(III), Dy(III), Pr (III)	TOPO:Tdec:Dec (4:5:5)	10.00 each	10	1:0.50 $mL.mL^{-1}$	− 0.20[b]	$EE_{Dy}\%^{*}$ ≈ 95.07 %, $EE_{Nd}\%^{*}$ ≈ 81.90 %, $EE_{Pr}\%^{*}$ ≈79.01 % for each S%* > 99 %, P % > 99 %	[105]
Sc(III) and Y(III)	TOPO:isostearic acid (1:2)	1.00 each	180	1:1 $mL.mL^{-1}$[c]	1.00 for Sc > 5.00 for Y	At high acidic conditions: $EE_{Sc}\%$ = 100 %, $S_{Sc}\%$ = 100 % At low acidic conditions: E_{Y} % = 100 %	[193]
La(III), Ce(III), Ce (IV), Pr(III), Nd (III), Eu(III), Gd (III), Y(III), Lu (III)	TOPO:DecA (1:1)	7.50 each	1	1:2 $g.g^{-1}$	0.00 to 0.30[b] for maximum distribution ratios − 0.60[b]for maximum selectivity	At low acidic conditions: D_{La}^{*} = 1, D_{Ce}^{*} = 2.64, D_{Pr}^{*} = 4.15, D_{Nd}^{*} = 4.90, D_{Eu}^{*}= 9.72, D_{Gd}^{*} = 5.37, D_{Y}^{*} = 6.38, D_{Lu}^{*} = 6.72, $SF_{Eu/Gd}^{*}$ = 1.8 At high acidic conditions: D_{La}^{*} = 0.02, D_{Ce}^{*} = 0.49, D_{Pr}^{*} = 0.49, D_{Nd}^{*} = 0.82, D_{Eu}^{*} = 1.33, D_{Gd}^{*} = 1.14, D_{Y}^{*} = 1.86, D_{Lu}^{*} = 2.44	[188]
HREEs (Dy–Lu), Y (III)	BEA:OA:Dec (5:1:9)	2.00 each	30	1:1 $mL.mL^{-1}$ for model solution	3.00[a]	From model solution: $SF_{Dy/Y}^{*}$ = 2.86, $SF_{Ho/Y}^{*}$ = 2.92,	[170]

(continued on next page)

Table 6 (*continued*)

Metal	H(D)ES HBA:HBD(s) Molar ratio	Extraction Conditions Initial metal concentration (mmol. L^{-1})	Time (min)	Organic-to-aqueous phase ratio	pH	Main results	Ref.
				1:0.2 mL.mL^{-1} for industrial Y-enriched		$SF_{Er/Y}$* = 3.65, $SF_{Tm/Y}$* = 6.06, $SF_{Yb/Y}$* = 10.30, $SF_{Lu/Y}$* = 9.87 From Y-concentrated industrial solution: $SF_{Dy/Y}$* ≥ 3.05, $SF_{Ho/Y}$* ≥ 3.37, $SF_{Er/Y}$* ≥ 4.29, $SF_{Tm/Y}$* ≥ 6.00, $SF_{Yb/Y}$* ≥ 10.80, and $SF_{Lu/Y}$* ≥ 11.20 S_{HREEs} %* = 96.70 %	
Gd(III), Al(III)	DM:Ibu (3:1)	30.00 for Gd 90.00 for Al	30	1:1 mL.mL^{-1}	2.00[a]	EE_{Al}%* > 98.80 %, EE_{Gd}%* = 2.43 % $SF_{Al/Gd}$* > 400, P_{GdCl3} in the raffinate = 99.90 %	[167]

[a] pH according to the HCl concentration in the aqueous metal sample,
[b] pH according to the HNO_3 concentration in the aqueous metal sample,
[c] aqueous sample is formed with 1 mol.L^{-1} aqueous ammonium nitrate solution,
* in multi-metal solution,
+ in single-metal solution.

3.5. Transitioning (D)ESs toward industrial applications: Barriers and solutions

Although substantial academic research over the past decade has highlighted the potential of (D)ESs for metal recovery, particularly from secondary resources such as spent LIBs [33,48], these innovative solvents remain confined largely to lab-scale experiments. In 2020, collaborative efforts across the EU culminated in the PLATInum group metals Recovery Using Secondary raw materials (PLATIRUS) project. This initiative aimed to strengthen the security of PGM supply chains through the development of greener recycling processes. As part of this project, researchers investigated the use of (D)ES composed of ChCl and oxalic acid as a lixiviant for leaching and reducing PGMs from SAC. While this study demonstrated the potential of (D)ESs as green solvents

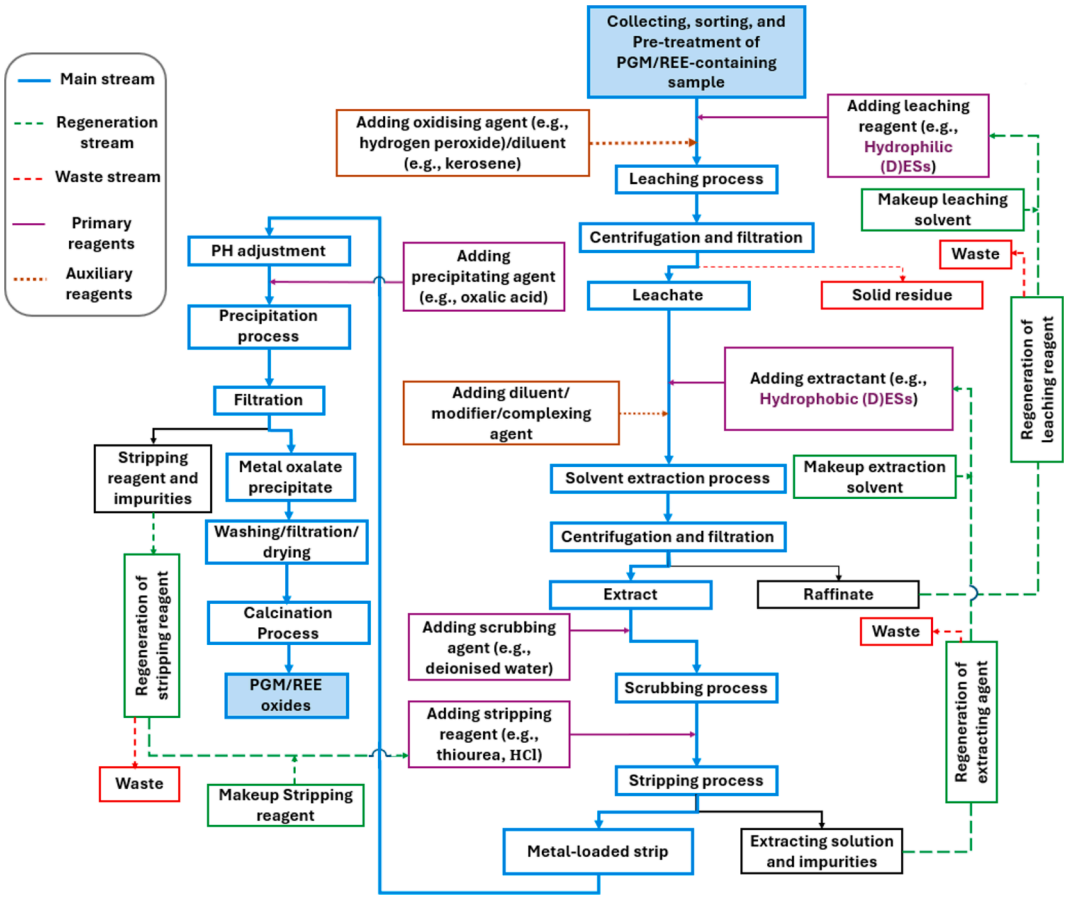

Fig. 17. Proposed overall flowsheet concept for the solvometallurgical separation and recovery of PGMs and REEs using (D)ESs.

for PGM recovery, it also highlighted the need for improvements in recovery efficiency and cost-effectiveness to enable their widespread adoption in the recycling industry in full large-scale processes [199].

Critical factors determining the economic viability of (D)ESs include their intended application, market demand, pricing of final product, expenses associated with production (e.g., formulation and raw material costs), scale of production, and cost savings or benefits they offer compared to conventional solvents or processes [201–203]. However, there is a notable lack of dedicated techno-economic analysis (TEA) studies to systematically evaluate these factors. While generally (D)ESs are recognised for their superior EHS benefits, existing studies indicate that their application in metallurgy is more expensive than traditional solvents [48,204]. Interestingly, the addition of water to (D)ESs in certain processes, such as biogas upgrading, has proven to reduce the total annual cost (TAC), primarily due to a decrease in viscosity, which in turn lowers energy consumption associated with pumping and handling [205].

Another major barrier that currently impedes the large-scale application of (D)ESs is their limited chemical and thermal stability, especially in ion exchange-based metal extraction pathways. This leads to the leaching of (D)ES components into the aqueous phase, thereby reducing recovery efficiency and solvent recyclability. Overcoming these barriers necessitates a holistic approach that integrates techno-economic analysis (TEA) and sustainability metrics to systematically evaluate and optimise (D)ES-based processes for industrial applications. Achieving this will require advancements in TRL implementation through scale-up [204].

4. Conclusions and outlook

PGMs and REEs are two subsets of identified CRMs of crucial relevance to the future of catalysis, electronic goods, and the development of clean technologies to reach net zero emissions and resource utilisation. Considering their relative scarcity and with a view on circularity and the environment, it is crucial to develop solvometallurgical processes using less energy-intensive conditions and cleaner solvents than traditional metallurgy processes. In this sense, (D)ESs have emerged as promising designer solvents to selectively separate PGMs and REEs from various sources. The findings of this critical review, along with potential directions for future research, are outlined as follows:

The properties of (D)ESs can be precisely tuned through different HBAs, HBDs, and their molar ratios. Key physicochemical traits, such as acidity, viscosity, and thermal and chemical stability, directly impact their application in metal separation performance. Acidity facilitates metal oxide dissolution in SLX via protonation, viscosity affects mass transfer and separation rates, thermal stability is crucial for high-temperature SLX, and chemical stability is vital in LLX when exposed to highly acidic solutions. Additionally, density and interfacial tension support effective phase separation;

Spectroscopic analyses using FT-IR, NMR, and UV–visible techniques provide critical insights into the dissolution mechanisms of metal oxides in (D)ESs. This primarily entails two sequential steps: The initial adsorption of anionic ligands onto the metal oxide surface, followed by subsequent chemical dissolution within the (D)ES matrix. Notably, in the case of PGM oxides, an additional ligand exchange step is observed, resulting in the formation of anionic chloro-complexes, a phenomenon that may absent in REO dissolution. These findings emphasise the distinct dissolution behaviours of PGMs and REOs in (D)ESs;

Effective pre-treatment of metal-bearing samples is crucial to improve leaching efficiency and selectivity of metal recovery, especially in samples with highly stable crystalline structures. In this regard, techniques such as NaOH digestion and oxidative roasting modify the chemical states of metals within samples, establishing optimal conditions for targeted metal extraction

A thorough understanding of SX mechanisms for PGM and REE extraction using H(D)ESs allow the design of new (D)ESs and optimising operating parameters, particularly aqueous medium acidity, to enhance process performance. The primary mechanisms identified are ion exchange (AE/CE), ion pairing in aqueous phase (IP), and neutral ion association (NIA), with metal types, speciation, and H(D)ES composition as major influencing factors. PGMs can be extracted through all identified pathways, while REEs are mainly restricted to the NIA and CE mechanisms. Additionally, ionic (D)ESs favour AE and IP pathways, whereas non-ionic types proceed through CE and NIA. Importantly, in NIA with acid co-extraction, a trade-off between separation efficiency and solvent stability suggests challenges due to the high energy barrier in hydrogen-bonding within DESs compared to ESs. This insight directs future work toward tailored (D)ES formulations to overcome these limitations and further advance the industrial application of sustainable separation processes. Whilst notable efforts have been made to investigate various extraction mechanisms, kinetic studies on these processes are still scarce;

In light of the need for circular processes and findings from recent studies, this work proposes a conceptual flowsheet for the separation and recovery of PGMs and REEs using (D)ESs. The primary steps include leaching, solvent extraction, and final metal recovery, which involves scrubbing, stripping, precipitation, and calcination to produce PGM/REE oxides ready for practical applications. A crucial aspect is solvent regeneration and reutilisation, which has shown promising results in the literature, with H(D)ES demonstrating recyclability;

Finally, the integration of process intensification techniques, such as ultrasound and microwave-assisted methods, demonstrated a promising approach to enhance the efficiency of metal separation processes while reducing mixing time and energy demands. Comparative studies on mechanical versus ultrasonic agitation and conductive versus microwave heating highlight the potential for improved mass and energy transfer. However, there remains a significant research gap in applying these methods for PGM and REE recovery from secondary resources using (D)ESs, indicating valuable directions for future investigation.

CRediT authorship contribution statement

Sahar Gholami: Writing – review & editing, Writing – original draft, Methodology, Investigation, Formal analysis, Data curation, Conceptualization. **María Pérez-Page:** Writing – review & editing, Supervision, Resources. **Carmine D'Agostino:** Writing – review & editing, Supervision, Resources. **Jesús Esteban:** Writing – review & editing, Writing – original draft, Supervision, Resources, Project administration, Methodology, Investigation, Formal analysis, Conceptualization.

Declaration of competing interest

The corresponding author is currently part of the Early Career Board of Chemical Engineering Journal. The authors declare that they have no known competing financial interests or personal relationships that could have appeared to influence the work reported in this paper..

Acknowledgements

The University of Manchester is acknowledged for a PhD scholarship for SG. JE gratefully acknowledges grant RYC2022-035654-I funded by MICIU/AEI/10.13039/501100011033 and by ESF + .

Data availability

This is a review article. The data are available in the original sources referenced

References

[1] Euelectric, Raw materials: A journey from mine to everyday goods, (2023). https://www.eurelectric.org/in-detail/rawmaterials (accessed May 20, 2024).

[2] R. Jaggers, Decarbonisation: Materials and circularity challenges for clean technologies, (2021).
[3] P. Christmann, Mineral resource governance in the 21st century and a sustainable European Union, Miner. Econ. 34 (2021) 187–208, https://doi.org/10.1007/s13563-021-00265-4.
[4] E. Commission, Study on the EU's List of Critical Raw Materials (2020), https://doi.org/10.2873/587825.
[5] European Commission, Critical raw materials resilience: Charting a path towards greater security and sustainability, Brussels, (2020). https://eur-lex.europa.eu/legal-content/EN/TXT/PDF/?uri=CELEX:52020DC0474.
[6] V. Forti, C.P. Baldé, R. Kuehr, G. Bel, L. Jinhui, D.S. Khetriwal, J. Linnell, F. Magalini, I.C. Nnororm, P. Onianwa, D. Ott, A. Ramola, U. Silva, R. Stillhart, D. Tillekeratne, V. Van Straalen, M. Wagner, Yamamoto, The Global e-Waste Monitor 2020 (2020). https://ewastemonitor.info/gem-2020/.
[7] European Commission, Critical raw materials: Ensuring secure and sustainable supply chains for EU's green and digital future, (2023). https://ireland.representation.ec.europa.eu/news-and-events/news/critical-raw-materials-ensuring-secure-and-sustainable-supply-chains-eus-green-and-digital-future-2023-03-16_en (accessed May 26, 2024).
[8] M.E. Mondejar, R. Avtar, H.L.B. Diaz, R.K. Dubey, J. Esteban, A. Gómez-Morales, B. Hallam, N.T. Mbungu, C.C. Okolo, K.A. Prasad, Q. She, S. Garcia-Segura, Digitalization to achieve sustainable development goals: Steps towards a Smart Green Planet, Sci. Total Environ. 794 (2021) 148539, https://doi.org/10.1016/j.scitotenv.2021.148539.
[9] E. Commission, Methodology for Establishing the EU List of Critical Raw Materials (2017), https://doi.org/10.2873/769526.
[10] K.B. Syariah, G. Ilmu, Study on the Critical Raw Materials for the EU 2023 (2023), https://doi.org/10.2873/725585.
[11] USGS, U.S. geological survey releases 2022 list of critical minerals, (2022). https://www.usgs.gov/news/national-news-release/us-geological-survey-releases-2022-list-critical-minerals (accessed May 26, 2024).
[12] A.P. Paiva, C.A. Nogueira, Ionic liquids in the extraction and recycling of critical metals from urban mines, Waste and Biomass Valorization 12 (2021) 1725–1747, https://doi.org/10.1007/s12649-020-01115-0.
[13] A.E. Hughes, N. Haque, S.A. Northey, S. Giddey, Platinum group metals: A review of resources, production and usage with a focus on catalysts, Resources 10 (2021) 1–40, https://doi.org/10.3390/resources10090093.
[14] Z. Huang, T. Cheng, A.H. Shah, G. Zhong, C. Wan, P. Wang, M. Ding, J. Huang, Z. Wan, S. Wang, J. Cai, B. Peng, H. Liu, Y. Huang, W.A. Goddard, X. Duan, Edge sites dominate the hydrogen evolution reaction on platinum nanocatalysts, Nat. Catal. 7 (2024) 678–688, https://doi.org/10.1038/s41929-024-01156-x.
[15] R. Franke, D. Selent, A. Börner, Applied hydroformylation, Chem. Rev. 112 (2012) 5675–5732, https://doi.org/10.1021/cr3001803.
[16] A. Seretis, P. Diamantopoulou, I. Thanou, P. Tzevelekidis, C. Fakas, P. Lilas, G. Papadogianakis, Recent advances in ruthenium-catalyzed hydrogenation reactions of renewable biomass-derived levulinic acid in aqueous media, Front. Chem. 8 (2020) 1–22, https://doi.org/10.3389/fchem.2020.00221.
[17] G.M. Mudd, S.M. Jowitt, T.T. Werner, Global platinum group element resources, reserves and mining – A critical assessment, Sci. Total Environ. 622–623 (2018) 614–625, https://doi.org/10.1016/j.scitotenv.2017.11.350.
[18] J. Zhang, M.P. Everson, T.J. Wallington, F.R. Field, R. Roth, R.E. Kirchain, Assessing economic modulation of future critical materials use: The case of automotive-related platinum group metals, Environ. Sci. Technol. 50 (2016) 7687–7695, https://doi.org/10.1021/acs.est.5b04654.
[19] M. Alipanah, D.M. Park, A. Middleton, Z. Dong, H. Hsu-Kim, Y. Jiao, H. Jin, Techno-economic and life cycle assessments for sustainable rare earth recovery from coal byproducts using biosorption, ACS Sustain. Chem. Eng. 8 (2020) 17914–17922, https://doi.org/10.1021/acssuschemeng.0c04415.
[20] W.L. Leal Filho, R. Kotter, P.G. Özuyar, I.R. Abubakar, J.H.P.P. Eustachio, N. R. Matandirotya, Understanding rare earth elements as critical raw materials, Sustainability 15 (2023), https://doi.org/10.3390/su15031919.
[21] Y. Kanazawa, M. Kamitani, Rare earth minerals and resources in the world, J. Alloys Compd. 408–412 (2006) 1339–1343, https://doi.org/10.1016/j.jallcom.2005.04.033.
[22] V. Balaram, Rare earth elements: A review of applications, occurrence, exploration, analysis, recycling, and environmental impact, Geosci. Front. 10 (2019) 1285–1303, https://doi.org/10.1016/j.gsf.2018.12.005.
[23] H. Khan, S.E. Lofland, J. Ahmed, K.V. Ramanujachary, T. Ahmad, Emerging rare earth perovskite nanostructures for efficient electrochemical energy conversion and storage, Int. J. Hydrogen Energy 58 (2024) 954–963, https://doi.org/10.1016/j.ijhydene.2024.01.286.
[24] K. Binnemans, P.T. Jones, B. Blanpain, T. Van Gerven, Y. Yang, A. Walton, M. Buchert, Recycling of rare earths: a critical review, J. Clean. Prod. 51 (2013) 1–22, https://doi.org/10.1016/j.jclepro.2012.12.037.
[25] Iea50, The Role of Critical Minerals in Clean Energy Transitions, (2021). https://www.iea.org/reports/the-role-of-critical-minerals-in-clean-energy-transitions (accessed May 20, 2024).
[26] Johnson Mathhey, PGM management. https://matthey.com/products-and-markets/pgms-and-circularity/pgm-management (accessed November 20, 2024).
[27] S. Brown, L. Cole, A. Cowley, J. Dickson, M. Fujita, N. Girardot, S. Grant, J. Jiang, R. Raithatha, M. Ryan, M. Underwood, A. Wang, PGM market report, 2024. https://matthey.com/documents/161599/509428/PGM-Market-Report-24.pdf.
[28] A. Islam, T. Ahmed, M.R. Awual, A. Rahman, M. Sultana, A.A. Aziz, M.U. Monir, S.H. Teo, M. Hasan, Advances in sustainable approaches to recover metals from e-waste-A review, J. Clean. Prod. 244 (2020) 118815, https://doi.org/10.1016/j.jclepro.2019.118815.
[29] W. Li, V. Achal, Environmental and health impacts due to e-waste disposal in China – A review, Sci. Total Environ. 737 (2020) 139745, https://doi.org/10.1016/j.scitotenv.2020.139745.
[30] A. Balali, S. Gholami, M. Javanmardi, A. Valipour, A. Yunusa-Kaltungo, Assessment of heavy metal pollution in the soil of a construction and demolition waste landfill, Environ. Nanotechnology, Monit. Manag. 20 (2023) 100856, https://doi.org/10.1016/j.enmm.2023.100856.
[31] Q. Guo, E. Wang, Y. Nie, J. Shen, Profit or environment? A system dynamic model analysis of waste electrical and electronic equipment management system in China, J. Clean. Prod. 194 (2018) 34–42, https://doi.org/10.1016/j.jclepro.2018.05.112.
[32] Y. Ding, S. Zhang, B. Liu, H. Zheng, C. chi Chang, C. Ekberg, Recovery of precious metals from electronic waste and spent catalysts: A review, Resour. Conserv. Recycl. 141 (2019) 284–298. 10.1016/j.resconrec.2018.10.041.
[33] Z. Yuan, H. Liu, W.F. Yong, Q. She, J. Esteban, Status and advances of deep eutectic solvents for metal separation and recovery, Green Chem. 24 (2022) 1895–1929, https://doi.org/10.1039/D1GC03851F.
[34] Y.K. Taninouchi, T.H. Okabe, Trends of technological development of platinum group metal recycling: Solubilization and physical concentration processes, Mater. Trans. 64 (2023) 627–637, https://doi.org/10.2320/matertrans.MT-M2022150.
[35] S. Karim, Y. Ting, Recycling pathways for platinum group metals from spent automotive catalyst: A review on conventional approaches and bio-processes, Resour. Conserv. Recycl. 170 (2021) 105588, https://doi.org/10.1016/j.resconrec.2021.105588.
[36] O. Lanaridi, M. Schnürch, A. Limbeck, K. Schröder, Liquid- and solid-based separations employing ionic liquids for the recovery of platinum group metals typically encountered in catalytic converters: A review, ChemSusChem 15 (2022) e202102262.
[37] R. Nithya, C. Sivasankari, A. Thirunavukkarasu, A. Silver, Electronic waste generation, regulation and metal recovery: a review, Environ. Chem. Lett. 19 (2021) 1347–1368, https://doi.org/10.1007/s10311-020-01111-9.
[38] W. Zhuang, J.P. Fitts, C.M. Ajo-franklin, S. Maes, L. Alvarez-cohen, T. Hennebel, Recovery of critical metals using biometallurgy, Curr. Opin. Biotechnol. 33 (2015) 327–335, https://doi.org/10.1016/j.copbio.2015.03.019.
[39] M.K. Jha, J.C. Lee, M.S. Kim, J. Jeong, B.S. Kim, V. Kumar, Hydrometallurgical recovery/recycling of platinum by the leaching of spent catalysts: A review, Hydrometallurgy 133 (2012) 23–32, https://doi.org/10.1016/j.hydromet.2012.11.012.
[40] A. Zupanc, J. Install, M. Jereb, T. Repo, Sustainable and selective modern methods of noble metal recycling, Angew. Chemie Int. Ed. 62 (2023) e202214453.
[41] I.M. Pateli, D. Thompson, S.S.M. Alabdullah, A.P. Abbott, G.R.T. Jenkin, J. M. Hartley, The effect of pH and hydrogen bond donor on the dissolution of metal oxides in deep eutectic solvents, Green Chem. 22 (2020) 5476–5486, https://doi.org/10.1039/D0GC02023K.
[42] B. Ghosh, M.K. Ghosh, P. Parhi, P.S. Mukherjee, B.K. Mishra, Waste printed circuit boards recycling: An extensive assessment of current status, J. Clean. Prod. 94 (2015) 5–19, https://doi.org/10.1016/j.jclepro.2015.02.024.
[43] O. Lanaridi, S. Platzer, W. Nischkauer, A. Limbeck, M. Schnürch, K. Bica-Schröder, A combined deep eutectic solvent–ionic liquid process for the extraction and separation of platinum group metals (Pt, Pd, Rh), Molecules 26 (2021) 7204, https://doi.org/10.3390/molecules26237204.
[44] K. Pianowska, J. Kluczka, G. Benke, K. Goc, J. Malarz, M. Ochmański, K. Leszczyńska-Sejda, Solvent extraction as a method of recovery and separation of platinum group metals, Materials (basel). 16 (2023) 4681, https://doi.org/10.3390/ma16134681.
[45] K. Binnemans, P.T. Jones, Solvometallurgy: An emerging branch of extractive metallurgy, J. Sustain. Metall. 3 (2017) 570–600, https://doi.org/10.1007/s40831-017-0128-2.
[46] A.P. Abbott, G. Frisch, S.J. Gurman, A.R. Hillman, J. Hartley, F. Holyoak, K. S. Ryder, Ionometallurgy: Designer redox properties for metal processing, Chem. Commun. 47 (2011) 10031–10033, https://doi.org/10.1039/c1cc13616j.
[47] S. Ikeda, T. Mori, Y. Ikeda, K. Takao, Microwave-assisted solvent extraction of inert platinum group metals from HNO3 (aq) to betainium-based thermomorphic ionic liquid, ACS Sustain. Chem. Eng. 4 (2016) 2459–2463, https://doi.org/10.1021/acssuschemeng.6b00186.
[48] A. Kovačević, M. Tolazzi, M. Sanadar, A. Melchior, Hydrometallurgical recovery of metals from spent lithium-ion batteries with ionic liquids and deep eutectic solvents, J. Environ. Chem. Eng. 12 (2024) 113248, https://doi.org/10.1016/j.jece.2024.113248.
[49] X. Yin, H. Yi, Q. Wang, Y. Wang, X. Sun, C. Lv, J. Guo, Y. Yang, Extraction and separation of multiple platinum group metals from hydrochloric acid solution with sole 1-hexyl-3-methylimidazole-2-thione using microextraction method, Hydrometallurgy 174 (2017) 167–174, https://doi.org/10.1016/j.hydromet.2017.10.009.
[50] V.T. Nguyen, K. Binnemans, S. Riaño, Refining of palladium, platinum, and rhodium from a pregnant leach solution of spent automotive catalysts by continuous counter-current solvent extraction with ionic liquids in mixer-settlers, Ind. Eng. Chem. Res. 62 (2023) 9549–9562, https://doi.org/10.1021/acs.iecr.3c00851.
[51] D. Dupont, K. Binnemans, Recycling of rare earths from NdFeB magnets using a combined leaching/extraction system based on the acidity and thermomorphism of the ionic liquid [Hbet][Tf_2N], Green Chem. 17 (2015) 2150–2163, https://doi.org/10.1039/C5GC00155B.

[52] A.K. Sahin, D. Voßenkaul, N. Stoltz, S. Stopic, M.N. Saridede, B. Friedrich, Selectivity potential of ionic liquids for metal extraction from slags containing rare earth elements, Hydrometallurgy 169 (2017) 59–67, https://doi.org/10.1016/j.hydromet.2016.12.002.
[53] S. Gholami, A. Roosta, Bubble point of aqueous mixtures of sugar-based deep eutectic solvents and their individual components: Experimental study and modeling, J. Mol. Liq. 296 (2019) 111876, https://doi.org/10.1016/j.molliq.2019.111876.
[54] S. Gholami, A. Roosta, Experimental study and modeling of bubble point of aqueous mixtures of deep eutectic solvents based on dicarboxylic acids and choline chloride, J. Chem. Eng. Data 65 (2020) 2743–2750, https://doi.org/10.1021/acs.jced.0c00070.
[55] E.L. Smith, A.P. Abbott, K.S. Ryder, Deep eutectic solvents (DESs) and their applications, Chem. Rev. 114 (2014) 11060–11082, https://doi.org/10.1021/cr300162p.
[56] G. Shakiba, R. Saneie, H. Abdollahi, E. Ebrahimi, A. Rezaei, M. Mohammadkhani, Application of deep eutectic solvents (DESs) as a green lixiviant for extraction of rare earth elements from caustic-treated monazite concentrate, J. Environ. Chem. Eng. 11 (2023) 110777, https://doi.org/10.1016/j.jece.2023.110777.
[57] G. Zante, M. Boltoeva, Review on hydrometallurgical recovery of metals with deep eutectic solvents, Sustain. Chem. 1 (2020) 238–255, https://doi.org/10.3390/suschem1030016.
[58] Q. Zhang, K. De Oliveira Vigier, S. Royer, F. Jérôme, Deep eutectic solvents: Syntheses, properties and applications, Chem. Soc. Rev. 41 (2012) 7108–7146, https://doi.org/10.1039/c2cs35178a.
[59] M.K. Tran, M.T.F. Rodrigues, K. Kato, G. Babu, P.M. Ajayan, Deep eutectic solvents for cathode recycling of Li-ion batteries, Nat. Energy 4 (2019) 339–345, https://doi.org/10.1038/s41560-019-0368-4.
[60] K. Staszak, K. Wieszczycka, Recovery of metals from wastewater—state-of-the-art solutions with the support of membrane technology, Membranes (basel). 13 (2023) 114, https://doi.org/10.3390/membranes13010114.
[61] A. Zhu, X. Bian, W. Han, D. Cao, Y. Wen, K. Zhu, S. Wang, The application of deep eutectic solvents in lithium-ion battery recycling: A comprehensive review, Resour. Conserv. Recycl. 188 (2023) 106690, https://doi.org/10.1016/j.resconrec.2022.106690.
[62] A.P. Abbott, G. Capper, D.L. Davies, R.K. Rasheed, V. Tambyrajah, Novel solvent properties of choline chloride/urea mixtures, Chem. Commun. (2003) 70–71, https://doi.org/10.1039/b210714g.
[63] M.A.R. Martins, S.P. Pinho, J.A.P. Coutinho, Insights into the nature of eutectic and deep eutectic mixtures, J. Solution Chem. 48 (2019) 962–982, https://doi.org/10.1007/s10953-018-0793-1.
[64] J. Rowlinson, Molecular thermodynamics of fluid-phase equilibria, J. Chem. Thermodyn. 2 (1970) 158–159, https://doi.org/10.1016/0021-9614(70)90078-9.
[65] A. Klamt, M. Diedenhofen, A refined cavity construction algorithm for the conductor-like screening model, J. Comput. Chem. 39 (2018) 1648–1655, https://doi.org/10.1002/jcc.25342.
[66] A.K. Lavrinenko, I.Y. Chernyshov, E.A. Pidko, Machine learning approach for the prediction of eutectic temperatures for metal-free deep eutectic solvents, ACS Sustain. Chem. Eng. 11 (2023) 15492–15502, https://doi.org/10.1021/acssuschemeng.3c05207.
[67] D.O. Abranches, M.A.R. Martins, L.P. Silva, N. Schaeffer, S.P. Pinho, J.A. P. Coutinho, Phenolic hydrogen bond donors in the formation of non-ionic deep eutectic solvents: The quest for type V DES, Chem. Commun. 55 (2019) 10253–10256, https://doi.org/10.1039/c9cc04846d.
[68] D.O. Abranches, J.A.P. Coutinho, Everything you wanted to know about deep eutectic solvents but were afraid to be told, Annu. Rev. Chem. Biomol. Eng. 14 (2023) 141–163, https://doi.org/10.1146/annurev-chembioeng-101121-085323.
[69] A.P. Abbott, G. Capper, D.L. Davies, R. Rasheed, Ionic liquids based upon metal halide/substituted quaternary ammonium salt mixtures, Inorg. Chem. 43 (2004) 3447–3452, https://doi.org/10.1021/ic049931s.
[70] A.P. Abbott, G. Capper, D.L. Davies, R.K. Rasheed, Ionic liquid analogues formed from hydrated metal salts, Chem. – A Eur. J. 10 (2004) 3769–3774, https://doi.org/10.1002/chem.200400127.
[71] J. Cao, B. Qi, J. Liu, Y. Shang, H. Liu, W. Wang, J. Lv, Z. Chen, H. Zhang, X. Zhou, Deep eutectic solvent choline chloride·2CrCl3·6H2O: An efficient catalyst for esterification of formic and acetic acid at room temperature, RSC Adv. 6 (2016) 21612–21616, https://doi.org/10.1039/c6ra01029f.
[72] A.P. Abbott, G. Capper, D.L. Davies, K.J. McKenzie, S.U. Obi, Solubility of metal oxides in deep eutectic solvents based on choline chloride, J. Chem. Eng. Data 51 (2006) 1280–1282, https://doi.org/10.1021/je060038c.
[73] A.P. Abbott, D. Boothby, G. Capper, D.L. Davies, R.K. Rasheed, Deep eutectic solvents formed between choline chloride and carboxylic acids: Versatile alternatives to ionic liquids, J. Am. Chem. Soc. 126 (2004) 9142–9147, https://doi.org/10.1021/ja048266j.
[74] A.P. Abbott, G. Capper, D.L. Davies, H.L. Munro, R.K. Rasheed, V. Tambyrajah, Preparation of novel, moisture-stable, Lewis-acidic ionic liquids containing quaternary ammonium salts with functional side chains, Chem. Commun. 1 (2001) 2010–2011, https://doi.org/10.1039/b106357j.
[75] D.O. Abranches, J.A.P. Coutinho, Type V deep eutectic solvents: Design and applications, Curr. Opin. Green Sustain. Chem. 35 (2022) 100612, https://doi.org/10.1016/j.cogsc.2022.100612.
[76] W. Chen, J. Jiang, X. Lan, X. Zhao, H. Mou, T. Mu, A strategy for the dissolution and separation of rare earth oxides by novel Brønsted acidic deep eutectic solvents, Green Chem. 21 (2019) 4748–4756, https://doi.org/10.1039/C9GC00944B.
[77] Q. Yang, Y. Li, B. Li, P. Duan, Z. Ren, Z. Zhou, Selective leaching and recovery of neodymium from NdFeB carbonyl residues, Sep. Purif. Technol. 329 (2024) 125137, https://doi.org/10.1016/j.seppur.2023.125137.
[78] Y. Dai, J. van Spronsen, G.J. Witkamp, R. Verpoorte, Y.H. Choi, Natural deep eutectic solvents as new potential media for green technology, Anal. Chim. Acta 766 (2013) 61–68, https://doi.org/10.1016/j.aca.2012.12.019.
[79] M.M. Abdelquader, S. Li, G.P. Andrews, D.S. Jones, Therapeutic deep eutectic solvents: A comprehensive review of their thermodynamics, microstructure and drug delivery applications, Eur. J. Pharm. Biopharm. 186 (2023) 85–104, https://doi.org/10.1016/j.ejpb.2023.03.002.
[80] I.M. Aroso, J.C. Silva, F. Mano, A.S.D. Ferreira, M. Dionísio, I. Sá-Nogueira, S. Barreiros, R.L. Reis, A. Paiva, A.R.C. Duarte, Dissolution enhancement of active pharmaceutical ingredients by therapeutic deep eutectic systems, Eur. J. Pharm. Biopharm. 98 (2016) 57–66, https://doi.org/10.1016/j.ejpb.2015.11.002.
[81] A.P. Golovanov, G.M. Hautbergue, S.A. Wilson, L.Y. Lian, A simple method for improving protein solubility and long-term stability, J. Am. Chem. Soc. 126 (2004) 8933–8939, https://doi.org/10.1021/ja049297h.
[82] Y.-C. He, D.-P. Zhang, Z.-C. Tao, Y. Lu, Y. Ding, F. Liu, Z.-Z. Zhu, H. Rui, G.-W. Zheng, X. Zhang, Improved biosynthesis of ethyl (S)-4-chloro-3-hydroxybutanoate by adding l-glutamine plus glycine instead of NAD+ in β-cyclodextrin–water system, Bioresour. Technol. 182 (2015) 98–102, https://doi.org/10.1016/j.biortech.2015.01.111.
[83] L. Duan, L.L. Dou, L. Guo, P. Li, E.H. Liu, Comprehensive evaluation of deep eutectic solvents in extraction of bioactive natural products, ACS Sustain. Chem. Eng. 4 (2016) 2405–2411, https://doi.org/10.1021/acssuschemeng.6b00091.
[84] Y. Liang, W. Duan, X. An, Y. Qiao, Y. Tian, H. Zhou, Novel betaine-amino acid based natural deep eutectic solvents for enhancing the enzymatic hydrolysis of corncob, Bioresour. Technol. 310 (2020) 123389, https://doi.org/10.1016/j.biortech.2020.123389.
[85] P. Makoś-Chełstowska, M. Kaykhaii, J. Płotka-Wasylka, M. de la Guardia, Magnetic deep eutectic solvents – Fundamentals and applications, J. Mol. Liq. 365 (2022) 120158, https://doi.org/10.1016/j.molliq.2022.120158.
[86] T. Khezeli, A. Daneshfar, Synthesis and application of magnetic deep eutectic solvents: Novel solvents for ultrasound assisted liquid-liquid microextraction of thiophene, Ultrason. Sonochem. 38 (2017) 590–597, https://doi.org/10.1016/j.ultsonch.2016.08.023.
[87] C. Florindo, L.C. Branco, I.M. Marrucho, Quest for green-solvent design: From hydrophilic to hydrophobic (deep) eutectic solvents, ChemSusChem 12 (2019) 1549–1559, https://doi.org/10.1002/cssc.201900147.
[88] M. Zhang, X. Zhang, Y. Liu, K. Wu, Y. Zhu, H. Lu, B. Liang, Insights into the relationships between physicochemical properties, solvent performance, and applications of deep eutectic solvents, Environ. Sci. Pollut. Res. 28 (2021) 35537–35563, https://doi.org/10.1007/s11356-021-14485-2.
[89] D.J.G.P. Van Osch, L.F. Zubeir, A. Van Den Bruinhorst, M.A.A. Rocha, M. C. Kroon, Hydrophobic deep eutectic solvents as water-immiscible extractants, Green Chem. 17 (2015) 4518–4521, https://doi.org/10.1039/c5gc01451d.
[90] D.J.G.P. van Osch, D. Parmentier, C.H.J.T. Dietz, A. van den Bruinhorst, R. Tuinier, M.C. Kroon, Removal of alkali and transition metal ions from water with hydrophobic deep eutectic solvents, Chem. Commun. 52 (2016) 11987–11990, https://doi.org/10.1039/C6CC06105B.
[91] P. Makoś, E. Słupek, J. Gębicki, Hydrophobic deep eutectic solvents in microextraction techniques–A review, Microchem. J. 152 (2020) 104384, https://doi.org/10.1016/j.microc.2019.104384.
[92] V. Zakusilova, G. Zante, E.E. Tereshatov, C.M. Folden, M. Boltoeva, Extraction and separation of iridium(IV) and rhodium(III) from hydrochloric acid media by a quaternary ammonium-based hydrophobic eutectic solvent, Sep. Purif. Technol. 278 (2021) 118814, https://doi.org/10.1016/j.seppur.2021.118814.
[93] C. Shuping, Z. Zhihan, W. Dong, Z. Wenjing, Q. Tao, W. Zhi, X. Wanhai, L. Yong, L. Guobiao, Selective leaching and recovery of rare earth from NdFeB waste through a superior selective and stable deep eutectic solvent, Sep. Purif. Technol. 353 (2025) 128498, https://doi.org/10.1016/j.seppur.2024.128498.
[94] M. Francisco, A. van den Bruinhorst, M.C. Kroon, New natural and renewable low transition temperature mixtures (LTTMs): screening as solvents for lignocellulosic biomass processing, Green Chem. 14 (2012) 2153, https://doi.org/10.1039/c2gc35660k.
[95] A.L. Sazali, N. AlMasoud, S.K. Amran, T.S. Alomar, K.F. Pa'ee, Z.M. El-Bahy, T.L. K. Yong, D.J. Dailin, L.F. Chuah, Physicochemical and thermal characteristics of choline chloride-based deep eutectic solvents, Chemosphere 338 (2023) 139485. 10.1016/j.chemosphere.2023.139485.
[96] L.K. Savi, D. Carpiné, N. Waszczynskyj, R.H. Ribani, C.W.I. Haminiuk, Influence of temperature, water content and type of organic acid on the formation, stability and properties of functional natural deep eutectic solvents, Fluid Phase Equilib. 488 (2019) 40–47, https://doi.org/10.1016/j.fluid.2019.01.025.
[97] S. Riaño, M. Petranikova, B. Onghena, T. Vander Hoogerstraete, D. Banerjee, M.R. S. Foreman, C. Ekberg, K. Binnemans, Separation of rare earths and other valuable metals from deep-eutectic solvents: a new alternative for the recycling of used NdFeB magnets, RSC Adv. 7 (2017) 32100–32113, https://doi.org/10.1039/C7RA06540J.
[98] N. Delgado-Mellado, M. Larriba, P. Navarro, V. Rigual, M. Ayuso, J. García, F. Rodríguez, Thermal stability of choline chloride deep eutectic solvents by TGA/FTIR-ATR analysis, J. Mol. Liq. 260 (2018) 37–43, https://doi.org/10.1016/j.molliq.2018.03.076.
[99] N.F. Gajardo-Parra, M.J. Lubben, J.M. Winnert, Á. Leiva, J.F. Brennecke, R. I. Canales, Physicochemical properties of choline chloride-based deep eutectic

solvents and excess properties of their pseudo-binary mixtures with 1-butanol, J. Chem. Thermodyn. 133 (2019) 272–284, https://doi.org/10.1016/j.jct.2019.02.010.
[100] I.M. Pateli, A.P. Abbott, K. Binnemans, N. Rodriguez Rodriguez, Recovery of yttrium and europium from spent fluorescent lamps using pure levulinic acid and the deep eutectic solvent levulinic acid–choline chloride, RSC Adv. 10 (2020) 28879–28890, https://doi.org/10.1039/D0RA05508E.
[101] N. Rodriguez Rodriguez, L. Machiels, K. Binnemans, p-toluenesulfonic acid-based deep-eutectic solvents for solubilizing metal oxides, ACS Sustain. Chem. Eng. 7 (2019) 3940–3948. 10.1021/acssuschemeng.8b05072.
[102] R. Karan, T. Sreenivas, Recovery of rare earth values from micro-granite type hard rocks using deep eutectic solvents, Trans. Indian Inst. Met. (2023), https://doi.org/10.1007/s12666-023-02946-w.
[103] O. Lanaridi, S. Platzer, W. Nischkauer, J.H. Betanzos, A.U. Iturbe, C. Del Rio Gaztelurrutia, L. Sanchez-Cupido, A. Siriwardana, M. Schnürch, A. Limbeck, T. Konegger, K. Bica-Schröder, Benign recovery of platinum group metals from spent automotive catalysts using choline-based deep eutectic solvents, Green Chem. Lett. Rev. 15 (2022) 404–414, https://doi.org/10.1080/17518253.2022.2068973.
[104] S. Ni, J. Su, H. Zhang, Z. Zeng, H. Zhi, X. Sun, A cleaner strategy for comprehensive recovery of waste SmCo magnets based on deep eutectic solvents, Chem. Eng. J. 412 (2021) 128602, https://doi.org/10.1016/j.cej.2021.128602.
[105] G. Yu, S. Ni, Y. Gao, D. Mo, Z. Zeng, X. Sun, Recovery of rare earth metal oxides from NdFeB magnet leachate by hydrophobic deep eutectic solvent extraction, oxalate stripping and calcination, Hydrometallurgy 223 (2024) 106209, https://doi.org/10.1016/j.hydromet.2023.106209.
[106] E. Riveiro, B. González, Á. Domínguez, Extraction of adipic, levulinic and succinic acids from water using TOPO-based deep eutectic solvents, Sep. Purif. Technol. 241 (2020) 116692, https://doi.org/10.1016/j.seppur.2020.116692.
[107] S.J.R. Vargas, G. Pérez-Sánchez, N. Schaeffer, J.A.P. Coutinho, Solvent extraction in extended hydrogen bonded fluids – separation of Pt(IV) from Pd(II) using TOPO- based type V DES, Green Chem. 23 (2021) 4540–4550, https://doi.org/10.1039/D1GC00829C.
[108] D.J.G.P. van Osch, C.H.J.T. Dietz, J. van Spronsen, M.C. Kroon, F. Gallucci, M. van Sint Annaland, R. Tuinier, A search for natural hydrophobic deep eutectic solvents based on natural components, ACS Sustain, Chem. Eng. 7 (2019) 2933–2942, https://doi.org/10.1021/acssuschemeng.8b03520.
[109] R. Liu, J. Hao, Y. Wang, Y. Meng, Y. Yang, A separation strategy of Au(III), Pd(II) and Pt(IV) based on hydrophobic deep eutectic solvent from hydrochloric acid media, J. Mol. Liq. 365 (2022) 120200, https://doi.org/10.1016/j.molliq.2022.120200.
[110] P.D. Ola, M. Matsumoto, Extraction of Au(III), Pt(IV), and Pd(II) from aqueous media with deep eutectic solvent dissolved in n-heptane as extractant, Indones. J. Chem. 23 (2023) 1735–1741, https://doi.org/10.22146/ijc.80862.
[111] J. Cao, E. Su, Hydrophobic deep eutectic solvents: the new generation of green solvents for diversified and colorful applications in green chemistry, J. Clean. Prod. 314 (2021) 127965, https://doi.org/10.1016/j.jclepro.2021.127965.
[112] N. Schaeffer, J.H.F. Conceição, M.A.R. Martins, M.C. Neves, G. Pérez-Sánchez, J. R.B. Gomes, N. Papaiconomou, J.A.P. Coutinho, Non-ionic hydrophobic eutectics – versatile solvents for tailored metal separation and valorisation, Green Chem. 22 (2020) 2810–2820, https://doi.org/10.1039/D0GC00793E.
[113] C. Liu, Q. Yan, X. Zhang, L. Lei, C. Xiao, Efficient recovery of end-of-life NdFeB permanent magnets by selective leaching with deep eutectic solvents, Environ. Sci. Technol. 54 (2020) 10370–10379, https://doi.org/10.1021/acs.est.0c03278.
[114] Q. Yan, C. Liu, X. Zhang, L. Lei, C. Xiao, Selective dissolution and separation of rare earths using guanidine-based deep eutectic solvents, ACS Sustain. Chem. Eng. 9 (2021) 8507–8514, https://doi.org/10.1021/acssuschemeng.1c01616.
[115] S. Heo, R. Kim, H.-S. Yoon, C.-J. Kim, K.W. Chung, S. Lee, Effect of pretreatment methods on the selective leaching of rare earth elements from NdFeB permanent magnets using deep eutectic solvents, Hydrometallurgy 226 (2024) 106284, https://doi.org/10.1016/j.hydromet.2024.106284.
[116] T. Hanada, M. Goto, Synergistic deep eutectic solvents for lithium extraction, ACS Sustain. Chem. Eng. 9 (2021) 2152–2160, https://doi.org/10.1021/acssuschemeng.0c07606.
[117] H. Ghaedi, M. Ayoub, S. Sufian, B. Lal, Y. Uemura, Thermal stability and FT-IR analysis of Phosphonium-based deep eutectic solvents with different hydrogen bond donors, J. Mol. Liq. 242 (2017) 395–403, https://doi.org/10.1016/j.molliq.2017.07.016.
[118] I.M. Pateli, A.P. Abbott, G.R.T. Jenkin, J.M. Hartley, Electrochemical oxidation as alternative for dissolution of metal oxides in deep eutectic solvents, Green Chem. 22 (2020) 8360–8368, https://doi.org/10.1039/d0gc03491f.
[119] X. Wang, M. Liu, F. Peng, X. Ding, Hydrophobic magnetic deep eutectic solvent: Synthesis, properties, and application in DNA separation, J. Chromatogr. A 1659 (2021) 462626, https://doi.org/10.1016/j.chroma.2021.462626.
[120] E.S. Morais, M.G. Freire, C.S.R. Freire, J.A.P. Coutinho, A.J.D. Silvestre, Enhanced conversion of xylan into furfural using acidic deep eutectic solvents with dual solvent and catalyst behavior, ChemSusChem 13 (2020) 784–790, https://doi.org/10.1002/cssc.201902848.
[121] O.S. Hammond, D.T. Bowron, K.J. Edler, The effect of water upon deep eutectic solvent nanostructure: An unusual transition from ionic mixture to aqueous solution, Angew, Chemie 129 (2017) 9914–9917, https://doi.org/10.1002/ange.201702486.
[122] L. Weng, M. Toner, Janus-faced role of water in defining nanostructure of choline chloride/glycerol deep eutectic solvent, Phys. Chem. Chem. Phys. 20 (2018) 22455–22462, https://doi.org/10.1039/C8CP03882A.
[123] O.S. Hammond, D.T. Bowron, K.J. Edler, Liquid structure of the choline chloride-urea deep eutectic solvent (reline) from neutron diffraction and atomistic modelling, Green Chem. 18 (2016) 2736–2744, https://doi.org/10.1039/c5gc02914g.
[124] M. Marchel, M.P. Rayaroth, C. Wang, L. Kong, J.A. Khan, G. Boczkaj, Hydrophobic (deep) eutectic solvents (HDESs) as extractants for removal of pollutants from water and wastewater – A review, Chem. Eng. J. 475 (2023) 144971, https://doi.org/10.1016/j.cej.2023.144971.
[125] C. Florindo, L.C. Branco, I.M. Marrucho, Development of hydrophobic deep eutectic solvents for extraction of pesticides from aqueous environments, Fluid Phase Equilib. 448 (2017) 135–142, https://doi.org/10.1016/j.fluid.2017.04.002.
[126] K. Binnemans, P.T. Jones, Ionic liquids and deep-eutectic solvents in extractive metallurgy: mismatch between academic research and industrial applicability, J. Sustain. Metall. 9 (2023) 423–438, https://doi.org/10.1007/s40831-023-00681-6.
[127] K. Shahbaz, F.S. Mjalli, M.A. Hashim, I.M. Alnashef, Prediction of deep eutectic solvents densities at different temperatures, Thermochim. Acta 515 (2011) 67–72, https://doi.org/10.1016/j.tca.2010.12.022.
[128] H.S. Salehi, O.A. Moultos, T.J.H. Vlugt, Interfacial properties of hydrophobic deep eutectic solvents with water, J. Phys. Chem. B 125 (2021) 12303–12314, https://doi.org/10.1021/acs.jpcb.1c07796.
[129] A. Entezari-Zarandi, F. Larachi, Selective dissolution of rare-earth element carbonates in deep eutectic solvents, J. Rare Earths 37 (2019) 528–533, https://doi.org/10.1016/j.jre.2018.07.015.
[130] H. Shekaari, M.T. Zafarani-Moattar, B. Mohammadi, Thermophysical characterization of aqueous deep eutectic solvent (choline chloride/urea) solutions in full ranges of concentration at T= (293.15–323.15) K, J. Mol. Liq. (2017) 451–461, https://doi.org/10.1016/j.molliq.2017.08.051.
[131] M.-L. Doche, A. Mandroyan, M. Mourad-Mahmoud, V. Moutarlier, J.-Y. Hihn, An ultrasonic-assisted process for copper recovery in a des solvent: Leaching and re-deposition, Chem. Eng. Process. Process Intensif. 121 (2017) 90–96, https://doi.org/10.1016/j.cep.2017.08.006.
[132] A.R.R. Teles, E.V. Capela, R.S. Carmo, J.A.P. Coutinho, A.J.D. Silvestre, M. G. Freire, Solvatochromic parameters of deep eutectic solvents formed by ammonium-based salts and carboxylic acids, Fluid Phase Equilib. 448 (2017) 15–21, https://doi.org/10.1016/j.fluid.2017.04.020.
[133] C. Florindo, A.J.S. McIntosh, T. Welton, L.C. Branco, I.M. Marrucho, A closer look into deep eutectic solvents: exploring intermolecular interactions using solvatochromic probes, Phys. Chem. Chem. Phys. 20 (2018) 206–213, https://doi.org/10.1039/C7CP06471C.
[134] C.Y. Foong, M.F. Mohd Zulkifli, M.D.H. Wirzal, M.A. Bustam, L.H.M. Nor, M. S. Saad, N.S. Abd Halim, COSMO-RS prediction and experimental investigation of amino acid ionic liquid-based deep eutectic solvents for copper removal, J. Mol. Liq. 333 (2021) 115884, https://doi.org/10.1016/j.molliq.2021.115884.
[135] F. Eckert, A. Klamt, Fast solvent screening via quantum chemistry: COSMO-RS approach, AIChE J. 48 (2002) 369–385, https://doi.org/10.1002/aic.690480220.
[136] J. Otárola-Sepúlveda, E. Cea-Klapp, P. Aravena, S. Ormazábal-Latorre, R. I. Canales, J.M. Garrido, O. Valerio, Assessment of Hansen solubility parameters in deep eutectic solvents for solubility predictions, J. Mol. Liq. 388 (2023) 122669, https://doi.org/10.1016/j.molliq.2023.122669.
[137] M. Kamisono, T. Hanada, M. Goto, Green leaching of metallic platinum using an ionic liquid with synergistic organic acid–chlorinating agent additives, J. Chem. Eng. Japan 56 (2023) 2228363, https://doi.org/10.1080/00219592.2023.2228363.
[138] V.T. Nguyen, J. Lee, A. Chagnes, M. Kim, J. Jeong, G. Cote, Highly selective separation of individual platinum group metals (Pd, Pt, Rh) from acidic chloride media using phosphonium-based ionic liquid in aromatic diluent, RSC Adv. 6 (2016) 62717–62728, https://doi.org/10.1039/C6RA09328K.
[139] D. Panias, M. Taxiarchou, I. Paspaliaris, A. Kontopoulos, Mechanisms of dissolution of iron oxides in aqueous oxalic acid solutions, Hydrometallurgy 42 (1996) 257–265, https://doi.org/10.1016/0304-386X(95)00104-O.
[140] M. Kamisono, T. Hanada, M. Goto, Platinum group metal recycling from spent automotive catalysts using reusable hydrophobic deep eutectic solvent, ACS Sustain. Resour. Manag. 1 (2024) 1021–1028, https://doi.org/10.1021/acssusresmgt.4c00100.
[141] J.T.M. Amphlett, Y. Lee, W. Yang, D. Kang, N.-E. Sung, J. Park, E.C. Jung, S. Choi, Spectroscopic study into lanthanide speciation in deep eutectic solvents, ACS Omega 7 (2022) 921–932, https://doi.org/10.1021/acsomega.1c05386.
[142] S. Sanchez-Segado, S. Stodd, V. Chipakwe, E. Loye, M. Smith, F. Wall, A.P. Abbott, A. Jha, Influence of the Alkali-promoted phase transformation in monazite for selective recovery of rare-oxides using deep eutectic solvents, Miner. Eng. 182 (2022) 107564, https://doi.org/10.1016/j.mineng.2022.107564.
[143] R. Karan, T. Sreenivas, M.A. Kumar, D.K. Singh, Recovery of rare earth elements from coal flyash using deep eutectic solvents as leachants and precipitating as oxalate or fluoride, Hydrometallurgy 214 (2022) 105952, https://doi.org/10.1016/j.hydromet.2022.105952.
[144] Z. Liu, F. Yang, Z. Sun, Q. Chi, Y. Li, Efficient selective leaching of ytterbium and lutetium oxides by new hydrophobic deep eutectic solvents, Sep. Purif. Technol. 343 (2024) 127097, https://doi.org/10.1016/j.seppur.2024.127097.
[145] X. Li, W. Li, Y. Gao, G. Tian, Effect of mechanical activation on the leaching process of rare earth metal yttrium in deep eutectic solvents, Appl. Sci. 12 (2022) 8253, https://doi.org/10.3390/app12168253.
[146] P.L. Rozelle, A.B. Khadilkar, N. Pulati, N. Soundarrajan, M.S. Klima, M.M. Mosser, C.E. Miller, S.V. Pisupati, A study on removal of rare earth elements from U.S.

coal byproducts by ion exchange, Metall. Mater. Trans. E 3 (2016) 6–17, https://doi.org/10.1007/s40553-015-0064-7.
[147] M. Kaya, An overview of NdFeB magnets recycling technologies, Curr. Opin. Green Sustain. Chem. 46 (2024) 100884, https://doi.org/10.1016/j.cogsc.2024.100884.
[148] F.-L. Fan, Z. Qin, S.-W. Cao, C.-M. Tan, Q.-G. Huang, D.-S. Chen, J. Wang, X. Yin, C. Xu, X. Feng, Highly efficient and selective dissolution separation of fission products by an ionic liquid [Hbet][Tf_2N]: A new approach to spent nuclear fuel recycling, Inorg. Chem. 58 (2019) 603–609, https://doi.org/10.1021/acs.inorgchem.8b02783.
[149] C. Du, S. Ma, M. Xie, F. Yang, Z. Zhao, Y. Chen, Y. Ma, Recovery of high-value rare earth elements from waste NdFeB by the water-soluble ammonium salt [Hbet]cl, Sep. Purif. Technol. 308 (2023) 122946, https://doi.org/10.1016/j.seppur.2022.122946.
[150] K. Habib, K. Parajuly, H. Wenzel, Tracking the flow of resources in electronic waste - the case of end-of-life computer hard disk drives, Environ. Sci. Technol. 49 (2015) 12441–12449, https://doi.org/10.1021/acs.est.5b02264.
[151] D.V. Kuzmin, N.V. Gudkova, M.N. Leskiv, A.A. Kuzmina, V.I. Kuzmin, Dephosphorization of nitric acid solutions from the leaching of monazite ferrous ores under hydrothermal conditions by selective precipitation of iron(III) hydroxyphosphate (giniite), Hydrometallurgy 217 (2023) 106042, https://doi.org/10.1016/j.hydromet.2023.106042.
[152] Y. Ni, J.M. Hughes, A.N. Mariano, Crystal chemistry of the monazite and xenotime structures, Am. Mineral. 80 (1995) 21–26, https://doi.org/10.2138/am-1995-1-203.
[153] S.K. Bhushan, O.P. Somani, Rare earth elements and yttrium potentials of neoproterozoic peralkaline siwana granite of Malani Igneous Suite, Barmer District, Rajasthan, J. Geol. Soc. India 94 (2019) 35–41, https://doi.org/10.1007/s12594-019-1263-0.
[154] K. Binnemans, P.T. Jones, B. Blanpain, T. Van Gerven, Y. Pontikes, Towards zero-waste valorisation of rare-earth-containing industrial process residues: a critical review, J. Clean. Prod. 99 (2015) 17–38, https://doi.org/10.1016/j.jclepro.2015.02.089.
[155] B.R. Reddy, B. Raju, J.Y. Lee, H.K. Park, Process for the separation and recovery of palladium and platinum from spent automobile catalyst leach liquor using LIX 84I and Alamine 336, J. Hazard. Mater. 180 (2010) 253–258, https://doi.org/10.1016/j.jhazmat.2010.04.022.
[156] F. Xie, T.A. Zhang, D. Dreisinger, F. Doyle, A critical review on solvent extraction of rare earths from aqueous solutions, Miner. Eng. 56 (2014) 10–28, https://doi.org/10.1016/j.mineng.2013.10.021.
[157] F.L. Bernardis, R.A. Grant, D.C. Sherrington, A review of methods of separation of the platinum-group metals through their chloro-complexes, React. Funct. Polym. 65 (2005) 205–217, https://doi.org/10.1016/j.reactfunctpolym.2005.05.011.
[158] M.K. Jha, D. Gupta, J. Lee, V. Kumar, J. Jeong, Solvent extraction of platinum using amine based extractants in different solutions: A review, Hydrometallurgy 142 (2014) 60–69, https://doi.org/10.1016/j.hydromet.2013.11.009.
[159] R.G. Pearson, Hard and soft acids and bases, J. Am. Chem. Soc. 85 (1963) 3533–3539.
[160] S.A. Wood, The aqueous geochemistry of the rare-earth elements and yttrium, Chem. Geol. 82 (1990) 159–186, https://doi.org/10.1016/0009-2541(90)90080-Q.
[161] A. Gradwohl, J. Windisch, M. Weissensteiner, B.K. Keppler, W. Kandioller, F. Jirsa, Extraction of rare earth elements from aqueous solutions using the ionic liquid trihexyltetradecylphosphonium 3-hydroxy-2-naphthoate, RSC Adv. 13 (2023) 24899–24908, https://doi.org/10.1039/D3RA03967F.
[162] E.E. Tereshatov, M.Y. Boltoeva, C.M. Folden, First evidence of metal transfer into hydrophobic deep eutectic and low-transition-temperature mixtures: indium extraction from hydrochloric and oxalic acids, Green Chem. 18 (2016) 4616–4622, https://doi.org/10.1039/C5GC03080C.
[163] N. Tang, L. Liu, C. Yin, G. Zhu, Q. Huang, J. Dong, X. Yang, S. Wang, Environmentally benign hydrophobic deep eutectic solvents for palladium(II) extraction from hydrochloric acid solution, J. Taiwan Inst. Chem. Eng. 121 (2021) 92–100, https://doi.org/10.1016/j.jtice.2021.04.010.
[164] J. Lee, K. Kurniawan, S. Kim, V.T. Nguyen, B.D. Pandey, Ionic liquids-assisted solvent extraction of precious metals from chloride solutions, Sep. Purif. Rev. 52 (2023) 242–261, https://doi.org/10.1080/15422119.2022.2091458.
[165] Y. Wang, Y. Song, Y. Li, J. Li, J. Bao, X. Zhang, B. Li, Study on the extraction and separation of precious metals from wastewater using a hydrophobic deep eutectic solvent, J. Environ. Chem. Eng. 11 (2023) 111102, https://doi.org/10.1016/j.jece.2023.111102.
[166] P.J. Griffin, T. Cosby, A.P. Holt, R.S. Benson, J.R. Sangoro, Charge transport and structural dynamics in carboxylic-acid-based deep eutectic mixtures, J. Phys. Chem. B 118 (2014) 9378–9385, https://doi.org/10.1021/jp503105g.
[167] S. Ni, G. Yu, Y. Gao, S. Zhang, H. Su, X. Sun, Tailored hydrophobic deep eutectic solvent for removing trace aluminum impurity to produce high-purity $GdCl_3$, Sep. Purif. Technol. 314 (2023) 123620, https://doi.org/10.1016/j.seppur.2023.123620.
[168] D. Pouillon, F.M. Doyle, Solvent extraction of metals with carboxylic acids — Theoretical analysis of extraction behaviour, Hydrometallurgy 19 (1988) 269–288, https://doi.org/10.1016/0304-386X(88)90035-7.
[169] P. Calandra, V. Turco Liveri, P. Riello, I. Freris, A. Mandanici, Self-assembly in surfactant-based liquid mixtures: Octanoic acid/Bis(2-ethylhexyl)amine systems, J. Colloid Interface Sci. 367 (2012) 280–285, https://doi.org/10.1016/j.jcis.2011.10.015.
[170] S. Ni, Y. Gao, G. Yu, S. Zhang, Z. Zeng, X. Sun, Tailored ternary hydrophobic deep eutectic solvents for synergistic separation of yttrium from heavy rare earth elements, Green Chem. 24 (2022) 7148–7161, https://doi.org/10.1039/D2GC02566C.
[171] E. Yilmaz, M. Soylak, Ultrasound assisted-deep eutectic solvent extraction of iron from sheep, bovine and chicken liver samples, Talanta 136 (2015) 170–173, https://doi.org/10.1016/j.talanta.2014.12.034.
[172] A.H. Panhwar, M. Tuzen, T.G. Kazi, Use of deep eutectic solvent-based air-assisted emulsification liquid-liquid microextraction of palladium and determination by flame atomic absorption spectrometry in water and environmental samples, At. Spectrosc. 40 (2019) 227–232. 10.46770/as.2019.06.005.
[173] Z.A. ALOthman, M.A. Habila, E. Yilmaz, E.A. Alabdullkarem, M. Soylak, A novel deep eutectic solvent microextraction procedure for enrichment, separation and atomic absorption spectrometric determination of palladium at ultra-trace levels in environmental samples, Measurement 153 (2020) 107394. 10.1016/j.measurement.2019.107394.
[174] K. Abdi, M. Ezoddin, N. Pirooznia, Temperature-controlled liquid–liquid microextraction using a biocompatible hydrophobic deep eutectic solvent for microextraction of palladium from catalytic converter and road dust samples prior to ETAAS determination, Microchem. J. 157 (2020) 104999, https://doi.org/10.1016/j.microc.2020.104999.
[175] O. Mokhodoeva, V. Maksimova, A. Shishov, V. Shkinev, Separation of platinum group metals using deep eutectic solvents based on quaternary ammonium salts, Sep. Purif. Technol. 305 (2023) 122427, https://doi.org/10.1016/j.seppur.2022.122427.
[176] N. Tang, Y. Wang, M. Liu, L. Liu, C. Yin, X. Yang, S. Wang, Ionic liquid as adjuvant in an aqueous biphasic system composed of polyethylene glycol for green separation of Pd(II) from hydrochloric solution, Sep. Purif. Technol. 246 (2020) 116898, https://doi.org/10.1016/j.seppur.2020.116898.
[177] R. Liu, Y. Geng, Z. Tian, N. Wang, M. Wang, G. Zhang, Y. Yang, Extraction of platinum(IV) by hydrophobic deep eutectic solvents based on trioctylphosphine oxide, Hydrometallurgy 199 (2021) 105521, https://doi.org/10.1016/j.hydromet.2020.105521.
[178] W. Meng, F. Xiaogui, C. Jing, Studies on stripping of actinides, and some fission and corrosion products from loaded TRPO by N,N,N′,N′- tetramethyl diglycolamide, Sep. Sci. Technol. 48 (2013) 741–748, https://doi.org/10.1080/01496395.2012.707732.
[179] M. Allan, L.S. Taylor, L.J. Mauer, Common-ion effects on the deliquescence lowering of crystalline ingredient blends, Food Chem. 195 (2016) 2–10, https://doi.org/10.1016/j.foodchem.2015.04.063.
[180] H. Fu, X. Wang, Y. Sun, L. Yan, J. Shen, J. Wang, S.-T. Yang, Z. Xiu, Effects of salting-out and salting-out extraction on the separation of butyric acid, Sep. Purif. Technol. 180 (2017) 44–50, https://doi.org/10.1016/j.seppur.2017.02.042.
[181] H.U. Haq, M. Balal, R. Castro-Muñoz, Z. Hussain, F. Safi, S. Ullah, G. Boczkaj, Deep eutectic solvents based assay for extraction and determination of zinc in fish and eel samples using FAAS, J. Mol. Liq. 333 (2021) 115930, https://doi.org/10.1016/j.molliq.2021.115930.
[182] F. Xie, W. Wang, Recovery of copper and cyanide from waste cyanide solutions using emulsion liquid membrane with LIX 7950 as the carrier, Environ. Technol. 38 (2017) 1961–1968, https://doi.org/10.1080/09593330.2016.1242657.
[183] T.H. Nguyen, C.H. Sonu, M.S. Lee, Separation of Ir(IV) and Rh(III) from strong hydrochloric acid solutions by solvent extraction with amines, J. Ind. Eng. Chem. 36 (2016) 245–250, https://doi.org/10.1016/j.jiec.2016.02.006.
[184] C.H. Desch, The Le Chatelier memorial lecture, J. Chem. Soc. (1938) 139, https://doi.org/10.1039/jr9380000139.
[185] M.N. Le, T.H. Nguyen, M.S. Lee, Comparison of separation behavior of Ir(IV) and Rh(III) between tin(II) chloride and ascorbic acid as a reducing agent in the extraction with Cyanex 921 and Cyanex 301, Solvent Extr. Ion Exch. 36 (2018) 272–285, https://doi.org/10.1080/07366299.2018.1478373.
[186] S. Prusty, S. Pradhan, S. Mishra, Extraction and separation studies of Nd/Fe and Sm/Co by deep eutectic solvent containing Aliquat 336 and glycerol, J. Chem. Technol. Biotechnol. 98 (2023) 1631–1641, https://doi.org/10.1002/jctb.7381.
[187] T. Cheisson, E.J. Schelter, Rare earth elements: Mendeleev's bane, modern marvels, Science (80-.). 363 (2019) 489–493. 10.1126/science.aau7628.
[188] U.G. Favero, N. Schaeffer, H. Passos, K.A.M.L. Cruz, D. Ananias, S. Dourdain, M. C. Hespanhol, Solvent extraction in non-ideal eutectic solvents – Application towards lanthanide separation, Sep. Purif. Technol. 314 (2023) 123592, https://doi.org/10.1016/j.seppur.2023.123592.
[189] D. Li, Development course of separating rare earths with acid phosphorus extractants: A critical review, J. Rare Earths 37 (2019) 468–486, https://doi.org/10.1016/j.jre.2018.07.016.
[190] A.Y. Ku, C. Dosch, T.R. Grossman, J.L. Herzog, A.F. Maricocchi, D. Polli, D. M. Lipkin, Addressing rare-earth element criticality: an example from the aviation industry, JOM 66 (2014) 2355–2359, https://doi.org/10.1007/s11837-014-1159-9.
[191] A.P.S. Crema, N. Schaeffer, H. Bastos, L.P. Silva, D.O. Abranches, H. Passos, M. C. Hespanhol, J.A.P. Coutinho, New family of Type V eutectic solvents based on 1,10-phenanthroline and their application in metal extraction, Hydrometallurgy 215 (2023) 105971, https://doi.org/10.1016/j.hydromet.2022.105971.
[192] L.F. Guidugli, T. Reza, Extraction of rare earth elements from water by trioctylphosphine oxide-based hydrophobic deep eutectic solvents, Ind. Eng. Chem. Res. 63 (2024) 12582–12590, https://doi.org/10.1021/acs.iecr.4c00597.
[193] S. Ushizaki, S. Kanemaru, K. Sugamoto, Y. Baba, Selective extraction equilibria of Sc(III), Y(III), Fe(III) and Al(III) from acidic media with toluene mixture of deep eutectic solvent (DES) composed of TOPO and isostearic acid, Anal. Sci. 39 (2023) 473–481, https://doi.org/10.1007/s44211-022-00234-z.
[194] A.I. Stankiewicz, J.A. Moulijn, Process intensification: Transforming chemical engineering, Chem. Eng. Prog. 96 (2000) 22–34.

[195] T. Suoranta, O. Zugazua, M. Niemelä, P. Perämäki, Recovery of palladium, platinum, rhodium and ruthenium from catalyst materials using microwave-assisted leaching and cloud point extraction, Hydrometallurgy 154 (2015) 56–62, https://doi.org/10.1016/j.hydromet.2015.03.014.
[196] T. Abo Atia, W. Wouters, G. Monforte, J. Spooren, Microwave chloride leaching of valuable elements from spent automotive catalysts: Understanding the role of hydrogen peroxide, Resour. Conserv. Recycl. 166 (2021) 105349, https://doi.org/10.1016/j.resconrec.2020.105349.
[197] R. Marin Rivera, C.E. Elgar, B. Jacobson, A. Feeney, P. Prentice, K. Ryder, A. P. Abbott, Ultra-fast extraction of metals from a printed circuit board using high power ultrasound in a calcium chloride-based deep eutectic solvent, RSC Sustain. 2 (2024) 403–415, https://doi.org/10.1039/D3SU00147D.
[198] B. Pesic, T. Zhou, Application of ultrasound in extractive metallurgy: Sonochemical extraction of nickel, Metall. Trans. B 23 (1992) 13–22, https://doi.org/10.1007/BF02654031.
[199] G. Nicol, E. Goosey, D.Ş. Yıldız, E. Loving, V.T. Nguyen, S. Riaño, I. Yakoumis, A. M. Martinez, A. Siriwardana, A. Unzurrunzaga, J. Spooren, T.A. Atia, B. Michielsen, X. Dominguez-Benetton, O. Lanaridi, Platinum group metals recovery using secondary raw materials (PLATIRUS): project overview with a focus on processing spent autocatalyst, Johnson Matthey, Technol. Rev. 65 (2021) 127–147, https://doi.org/10.1595/205651321X16057842276133.
[200] D. Jafarifar, M.R. Daryanavard, S. Sheibani, Ultra fast microwave-assisted leaching for recovery of platinum from spent catalyst, Hydrometallurgy 78 (2005) 166–171, https://doi.org/10.1016/j.hydromet.2005.02.006.
[201] W. Zhang, Z. Lei, Y. Wang, J. Wei, S. Ren, Y. Hou, W. Wu, Molecular mechanism and process of efficient separation of benzene and cyclohexane using a low-cost deep eutectic solvent, Chem. Eng. Sci. 279 (2023) 118963, https://doi.org/10.1016/j.ces.2023.118963.
[202] A. Martínez-Lomovskoi, A.G. Romero-García, E. Sánchez-Ramírez, J.G. Segovia-Hernández, Design and multi-objective optimization of a CO_2 capture plant using deep eutectic solvents, Chem. Eng. Res. Des. 192 (2023) 570–581, https://doi.org/10.1016/j.cherd.2023.03.006.
[203] J. Luo, H. Yang, Energy, exergy, exergoeconomic and enviroeconomic (4E) assessment on a liquid desiccant air-conditioning system using green deep eutectic solvent of ethaline, Energy Convers. Manag. 277 (2023) 116685, https://doi.org/10.1016/j.enconman.2023.116685.
[204] A. Azzouz, M. Hayyan, Techno-economic feasibility analysis: The missing piece in the puzzle of deep eutectic solvents, Sustain. Mater. Technol. 39 (2024) e00795.
[205] C. Ma, C. Liu, X. Lu, X. Ji, Techno-economic analysis and performance comparison of aqueous deep eutectic solvent and other physical absorbents for biogas upgrading, Appl. Energy 225 (2018) 437–447, https://doi.org/10.1016/j.apenergy.2018.04.112.